National Research Council Canada
Conseil national de recherches Canada

LEVEL II 6

THEORETICAL ANALYSIS OF THE TRANSIENT RESPONSE OF A WING TO NON-STATIONARY BUFFETS LOADS

by
B.H.K. Lee
National Aeronautical Establishment

OTTAWA
APRIL 1979

NRC NO. 17465

AERONAUTICAL REPORT
LR-597

(6)

THEORETICAL ANALYSIS OF THE TRANSIENT RESPONSE OF A WING TO NON-STATIONARY BUFFET LOADS

(ANALYSE THÉORIQUE DE LA RÉACTION TRANSITOIRE D'UNE AILE SOUMISE AU BUFFETING NON-STATIONNAIRE)

by/par

(10) B.H.K. Lee

(11) Apr. 79

(13) 88 p.

(14) NRC-LR-597

(15) NRC

(19) 17465

L.H. Ohman, Head/Chef
High Speed Aerodynamics Laboratory/
Laboratoire d'aérodynamique à hautes vitesses

F.R. Thurston
Director/Directeur

240 00

SUMMARY

A method for predicting the response of a wing to non-stationary buffet loads is presented. The wing is treated as a cantilever beam with known mass distribution. Using generalized co-ordinates, the vibration of the wing is governed by the second order mass-spring-damper oscillator equation. The buffet load on the wing is expressed as an integral of the sectional force, which is a function of the spanwise location and time. The non-stationary load is represented by the product of a deterministic time function and a statistically stationary random function. The time history of the applied load is segmented into a number of time intervals. Analytical expressions for the mean square response of the wing displacement are derived using a power spectral density for the random part of the applied load, similar to that used in the theory of isotropic turbulence. The effects of damping, ratio of the undamped natural frequency of the system to the half power frequency of the power spectral density, length of time segment, and duration of applied load on the response of the wing have been investigated for three examples of the load versus time histories.

RÉSUMÉ

La présente communication porte sur une méthode de prévoire la réaction d'une aile soumise à une charge non-stationnaire de buffeting. On considère que l'aile est une poutre en porte-à-faux dont la répartition de la masse est connue. En faisant usage à des coordonnées généralisées, la vibration de l'aile est gouvernée par l'équation de l'oscillateur masse-resort amortie du deuxième ordre. La charge du buffeting sur l'aile est exprimée comme une intégrale de la force par unité de surface de la section et qui est une fonction du temps et de la position suivant l'envergure. La charge instationnaire est représentée par le produit d'une fonction déterminé du temps et une fonction stationnaire statistiquement aléatoire. L'évolution chronologique de la charge appliquée est fractionnée en un certain nombre d'intervalles de temps. On dérive des expressions analytiques de la réponse efficace du déplacement de l'aile en utilisant, comme dans la théorie de la turbulence isotropique, une densité spectrale développée en puissances pour la partie aléatoire de la charge appliquée. On a étudié pour trois exemples de la charge en fonction de l'évolution chronologique les effets sur la réponse de l'aile de l'amortissement, du rapport de la fréquence propre non amortie du système sur la fréquence à demi-puissance de la densité spectrale développée en puissances, de la longueur de l'intervalle de temps et de la durée d'application de la charge.

CONTENTS

ILLUSTRATIONS

ILLUSTRATIONS (Cont'd)

ILLUSTRATIONS (Cont'd)

SYMBOLS

Symbols	Definition
b	wing span
$\bar{c}$	mean chord
$c(y)$	wing chord
$c_n(y,t)$	fluctuating sectional normal force coefficient
$c_{l_\alpha}(y)$	effective slope of sectional lift curve
C	generalized damping coefficient
$C_{zz}(t_1,t_2)$	covariance function
E	Young's modulus
$E[z^2(t)]$	expected value of z(t)
$\mathfrak{E}[z^2(t)]$	defined in Equation (55)
$f(t)$	stationary function
$F(y,t)$	sectional fluctuating force
$\bar{F}(y,t)$	force
$H(\omega)$	frequency response function
I	sectional moment of inertia
$I(t,\omega)$	time dependent frequency response function
K	generalized stiffness
$L(t)$	generalized force
$m(y)$	mass distribution
M	generalized mass
q	dynamic pressure
$R_L(\tau)$	auto-correlation function of input load
S_0	constant in expression for power spectral density
$S_{LL}(\omega_1,\omega_2)$	power spectral density of applied load
t,T	time

SYMBOLS (Cont'd)

Symbols	Definition
T_B	duration aircraft spent in buffet régime or duration of applied load
T_n	undamped natural period
Δt_r	duration of time segment
$u(t)$	unit step function
V	aircraft velocity
$w_1(y)$	mode shape function
y	distance along span direction
z	displacement
$\beta_r(t)$	$u(t-t_{r-1}) - u(t-t_r)$
$\gamma(t)$	deterministic function
δ	spatial decay coefficient; also amplitude function
ϵ	intensity of applied load
λ	correlation length
ζ	damping ratio
ξ	$y_2 - y_1$
$\rho(y_1, y_2, \tau)$	cross correlation coefficient
τ	delay; also $t_1 - t_2$
ω	frequency
ω_n	undamped natural frequency
ω_d	damped natural frequency
ω_f	half power frequency
Subscripts: '1'	denotes first fundamental bending mode
'r'	denotes rth time segment
'L'	denotes applied load
Superscript: '	denotes nondimensional time with respect to T_n

THEORETICAL ANALYSIS OF THE TRANSIENT RESPONSE OF A WING TO NON-STATIONARY BUFFET LOADS

1.0 INTRODUCTION

In recent years, increased attention has been given to the investigation of buffet characteristics in order to meet the design requirements of future aircraft. This arises from the demand for greater maneuverability and gust requirements in the transonic flight régime. Furthermore, the advent of the supercritical wing held promise for expanding the buffet onset boundary at transonic speeds.

Historically, the term buffeting was first introduced in connection with the structural failure that occurred to the tail of a Junkers monoplane in 1930. This led to wind tunnel testing of tail vibrations excited by the separated flow of the wing. The complexities of the buffet phenomenon, which involves the solutions of the vibrations of the wing surface and the unsteady aerodynamics around it, made the problem not easily amenable to theoretical analysis. Most of the earlier investigations involved wind tunnel tests to predict buffet onset and to provide some indications of buffet intensities. A complete account of the earlier work on the study of buffeting is given by Pearcy (Ref. 1).

The use of statistical theory in the investigation of buffeting was pioneered by Liepman (Ref. 2) who examined the problem of the lift force exerted on a two-dimensional thin airfoil moving in turbulent air. Later, he extended the method to wings of finite span (Ref. 3). The analysis was generalized by Ribner (Ref. 4) using a model of turbulence represented by the superposition of plane sinusoidal shear waves of all orientations and wavelengths. These analyses assumed the exciting force to be statistically stationary, so that well known statistical concepts developed in other branches of science could be applied. Experimental studies involving model testings in wind tunnels and flight tests were carried out mainly by NACA using strain gages developed for measuring the wing root bending moment. These investigations were reported in detail by Huston and Skopinski (Refs. 5, 6), Huston (Ref. 7), and Skopinski and Huston (Ref. 8). After this period of intense studies in the fifties, research in this subject was continued into the sixties at a slower pace. Aside from wing buffeting, work on dynamic response of launch vehicles to transonic buffeting was carried out by Cole (Ref. 9), Cole, Robinson and Gambucci (Ref. 10), and Coe (Refs. 11, 12). In the seventies, the rapid advances in transonic aerodynamics generated numerous studies on the transonic buffet characteristics of wind tunnel models as well as of actual aircraft. Hollingsworth and Cohen (Ref. 13) reported comparisons of flight tests with wind tunnel data for the F-4 aircraft. Mayes, Lores and Barnard (Ref. 14) studied the transonic buffet characteristics of a 60 degrees swept wing fighter aircraft. The flight and wind tunnel tests on the F-8D aircraft was carried out by Damstrom and Mayes (Ref. 15), and the buffet studies of the F-8 supercritical wing aircraft was reported by DeAngelis and Monaghan (Ref. 16). Detailed investigations of the Northrop F-5A using an extensively instrumented aircraft to study the dynamic buffet pressure distributions on the wing surfaces and the responses during a series of transonic maneuvers were reported in References 17 and 18 by Hwang and Pi. A first generation method for predicting the buffet loads and responses was described by Mullans and Lemley (Ref. 19), while Cunningham et al (Ref. 20) used fluctuating pressure data obtained for a rigid wind tunnel model as the forcing function to calculate the aircraft dynamic response and presented results for the F-111A. In general, methods employing wing fluctuating pressure data are found expensive due to the work and time involved in model construction. Butler and Spavins (Ref. 21) used a more direct approach in predicting buffet response in flight. The technique was based on a method proposed by Jones (Ref. 22) who suggested using a nondimensional representation of the overall aerodynamic excitation and damping parameters determined from model testing in a wind tunnel. Preliminary results for a combat trainer aircraft showed good agreement between predicted and measured response data.

All the prediction methods for the dynamic response of a wing to buffet loads assume the exciting force to be statistically stationary. This assumption is valid if at a certain buffet condition, the aircraft flight path is unchanged within a long analysis time. In wind tunnel testing, statistical stationarity requires running time to be very long compared to some characteristic time, for example, the natural period of the first bending mode, assuming the first bending mode to be the dominant one.

However, in actual flight during buffet maneuvers, the condition of stationarity may not be met, or in wind tunnel testing, transients have to be considered if the running time is very short or the model is pitched during a test. To analyse the response of a wing under such conditions, nonstationary techniques to predict the dynamic response has to be developed. A theory of non-stationary response of a linear dynamic system has been given by Caughey (Ref. 23) and extended by Barnoski and Maurer (Ref. 24), and Holman and Hart (Ref. 25). Using some of the concepts developed in these earlier studies a method is given in this report to compute the non-stationary response of a wing for specified power spectral density and time history of the exciting force. With this method, it is possible to investigate the continuous excursion of an aircraft into the buffet régime. Information such as the maximum rms response and the time delay between the maximum response and the applied force can be computed for known structural and inertial properties of the wing as a function of the duration the aircraft spent in the buffet régime.

2.0 ANALYSIS

2.1 Differential Equation of Wing Vibration

Figure 1 shows a schematic of the wing which is treated as a cantilever beam fixed at y = 0. The differential equation of beam bending relates the time and space derivatives of the displacement z to the load distribution on the beam which may include inertia forces, external or applied components, as well as internal components. The equation can be written as:

$$\frac{\partial^2}{\partial y^2}\left(EI\,\frac{\partial^2 z(y,t)}{\partial y^2}\right) = -\,m(y)\,\frac{\partial^2 z(y,t)}{\partial t^2} + \bar{F}(y,t) \tag{1}$$

Let

$$z(y,t) = w_1(y)z_1(t) \tag{2}$$

where $w_1(y)$ is the mode shape function. Here $z(y,t)$ is confined to a single normal mode appropriate to vibration in the first fundamental bending mode, and the subscript "1" is used to denote this mode. Normally, Equation (2) is written as a summation of all the possible modes, but in almost all wing buffeting tests, most of the energy in the power spectrum of the buffet bending moment is concentrated in the vicinity of the natural frequency of the first mode. Usually, the first mode is well separated from the higher modes, and as a result, the response due to the higher mode is small and Equation (2) suffices in describing the vibrating system. To find $z(y,t)$ at any point on the wing, it is necessary to determine $z_1(t)$ first. When the wing is subjected to a time dependent load, $z_1(t)$ is governed by the usual simple second order mass-spring-damper oscillator equation in generalized co-ordinates. Equation (1) can now be written as:

$$M\ddot{z}_1 + C\dot{z}_1 + Kz_1 = L(t) \tag{3}$$

where the dots denote differentiation with respect to time.

The generalized mass M and stiffness K are defined as:

$$M = \int_0^b m(y)w_1^2(y)dy \tag{4}$$

$$K = \int_0^b EI \left(\frac{d^2 w_1(y)}{dy^2} \right)^2 dy \tag{5}$$

Included in the term $\bar{F}(y,t)$ in Equation (1) are two aerodynamic forces, namely, a fluctuating lift force and a damping force associated with the fluctuating angle of attack ($\dot{z}/V$) induced by the relative velocity of the wing. If the fluctuating sectional normal force coefficient $c_n(y,t)$ is known, the generalized force L(t) can be evaluated as:

$$L(t) = q \int_0^b c(y) w_1(y) c_n(y,t) dy \tag{6}$$

while the generalized damping coefficient C is

$$C = \frac{q}{V} \int_0^b c_{l_\alpha}(y) c(y) w_1^2(y) dy \tag{7}$$

In the above equation, $c_{l_\alpha}(y)$ is the effective slope of the sectional lift curve. Define the undamped natural frequency ω_n as:

$$\omega_n^2 = \frac{K}{M} \tag{8}$$

and let

$$\zeta = \frac{C}{2\sqrt{MK}} \tag{9}$$

Using the above two equations, Equation (3) can be written as

$$\ddot{z}_1 + 2\zeta\omega_n \dot{z}_1 + \omega_n{}^2 z_1 = \frac{1}{M} L(t) \tag{10}$$

Equation (7) gives the aerodynamic damping coefficient. When structural damping is to be included, it can be added directly to C to give the total damping coefficient (Refs. 22, 26). Another approach of introducing structural damping is discussed by Scalan and Rosenbaum (Ref. 27) and Davies and Wornom (Ref. 28). The damping is assumed to be proportional to the displacement but in phase with the velocity of a harmonically oscillating system. The method applies strictly to harmonic motion and to the complex exponential form of solution. For random motion, great caution has to be exercised in using such a form of damping. Let the fluctuating sectional force be written as:

$$F(y,t) = q\, c(y)\, c_n(y,t)\, w_1(y) \tag{11}$$

and from Equation (6),

$$L(t) = \int_0^b F(y,t)dy \tag{12}$$

In the above equation, the buffet load L(t) on the wing is expressed as an integral of the sectional force expressed as a function of the spanwise location and time. If the sectional force is assumed to be independent of position along the span, the overall load is obtained by multiplying it by the wing span. However, the exciting force thus obtained will be overestimated since fluctuations at one chord station will not be in phase with fluctuations at another station.

Assume the time average value of F(y,t) to vanish, that is, $\overline{F(y,t)} = 0$. The auto-correlation function of L(t) is defined as:

$$R_L(\tau) = \lim_{T\to\infty} \frac{1}{2T} \int_{-T}^{T} L(t)L(t+\tau)dt \tag{13}$$

Substituting Equations (11) and (12) into (13), $R_L(\tau)$ can now be expressed as:

$$R_L(\tau) = \int_0^b \int_0^b R_F(y_1,y_2;\tau)dy_1 dy_2 \tag{14}$$

where $R_F(y_1,y_2;\tau)$ is the space-time correlation function of the sectional force, whose mean is taken to be zero. Define a cross-correlation coefficient $\rho(y_1,y_2;\tau)$ such that

$$R_F(y_1,y_2;\tau) = \left[\overline{F^2(y_1,t)}\ \overline{F^2(y_2,t)}\right]^{1/2} \rho(y_1,y_2;\tau) \tag{15}$$

where $\overline{F^2(y_1,t)}$, $\overline{F^2(y_2,t)}$ are the mean square values of $F(y_1,t)$ and $F(y_2,t)$ respectively. Once $R_F(y_1,y_2;\tau)$ is known, then from Equation (14) the mean square value of the load L(t) can be obtained since

$$\overline{L^2(t)} = R_L(0) \tag{16}$$

For some special types of flow, $R_F(y_1,y_2;\tau)$ has the same shape at different values of y and depends only on $\xi = y_2 - y_1$. From Equations (14) to (16),

$$\overline{L^2(t)} = \overline{F^2(y,t)} \int_0^b dy \int_{-y}^{b-y} \rho(\xi)d\xi \tag{17}$$

If $\rho(\xi)$ is equal to a constant and has a value unity over the interval $0 \leq y \leq b$, then Equation (17) becomes

$$\overline{L^2(t)} = \overline{F^2(y,t)} \cdot b^2 \tag{18}$$

which gives the mean square value of the load for perfect correlation. If $\rho(\xi)$ drops rapidly, then $\int_{-y}^{b-y} \rho(\xi)d\xi$ hardly depends on y. Since this has the dimension of length, it can be termed as the correlation length λ. From Equation (17),

$$\overline{L^2(t)} = \overline{F^2(y,t)}\,\lambda \cdot b \tag{19}$$

Since the sectional force is correlated only for a short distance, then λ is small and hence $\overline{L^2(t)}$ is smaller than that obtained from Equation (18) for perfect correlation. In actual cases, the form of the correlation function $R_F(y_1,y_2;\tau)$ depends on the wing geometry (swept or unswept), presence of leading edge flaps and other special characteristics in the design of the wing. However, in the preliminary stage of design, it is helpful to obtain a rough estimate of the buffet load. In order to do so, some approximate form of the correlation function is needed since the exact form will not be known for the wing until it has been constructed and tested experimentally. Although it is not within the scope of this report to discuss this subject in great detail, two other forms of $R_F(y_1,y_2;\tau)$ are briefly considered and the resulting values of $\overline{L^2(t)}$ are evaluated to give some idea of the form of the fluctuating load on the wing.

For a straight wing with large aspect ratio, the influence of tip vortices on the fluctuating load is unimportant. The buffet load will be predominantly determined by the fluctuating pressure in the separated flow region. In Reference 2, Liepman considered isotropic turbulence to illustrate the random excitation on a thin wing moving through turbulent air. If it is assumed that the buffet load has a similar form of power spectrum, the correlation function can be expressed as:

$$R_F(\xi,0) = \overline{F^2(t)}\, e^{-\xi/\bar{c}} \left(1 - \frac{\xi}{2\bar{c}}\right) \tag{20}$$

where $\bar{c}$ is the mean chord and $\overline{F^2(t)}$ is constant and independent of y. Substituting into Equation (17) gives

$$\overline{L^2(t)} = \overline{F^2(t)} \cdot (1 - e^{-b/\bar{c}})b\bar{c} \tag{21}$$

Another form of the correlation function that is of some interest is given by

$$R_F(\xi,0) = \overline{F^2(t)}\, e^{-\delta\xi/\bar{c}} \tag{22}$$

where δ is the spatial decay constant which is determined empirically. This form of the correlation function is similar to that given by Mullan and Lemley (Ref. 19) based on data obtained from wind tunnel tests of a 10% scale model of the F-4E aircraft. For highly swept wings, they found that wing tip vortices and snag vortices have an important influence on the fluctuating pressure on the wing. The buffet load for this correlation function, after substituting Equation (22) into Equation (17) and performing the integration, is

$$\overline{L^2(t)} = \overline{F^2(t)} \cdot \frac{2\bar{c}^2}{\delta} \left\{ \frac{b}{\bar{c}} - \frac{1}{\delta} (1 - e^{-\delta b/\bar{c}}) \right\} \tag{23}$$

2.2 Response to Non-Stationary Input

For a given buffet maneuver, the mean square loading on the wing versus time may be represented schematically as in Figure 2. The points A and B correspond to the onset and exit of buffeting respectively. The duration of time the aircraft spends in the buffet régime is denoted by T_B. The load is non-stationary and time varying properties, such as the mean square of the response, can only be determined by instantaneous averaging over an ensemble.

The load L(t) can be represented as:

$$L(t) = \gamma(t) \cdot f(t) \tag{24}$$

where $\gamma(t)$ is a deterministic function of time and f(t) is stationary (Ref. 29). Furthermore, it is assumed that f(t) is Gaussian such that the response is Gaussian as well. The non-stationary input can be represented by a time segmentation technique whereby the time T_B the aircraft experiences buffeting is divided into a number of time segments. At any segment, L(t) is expressed as:

$$L(t) = \sum_{r=1}^{m} \gamma_r(t) \cdot f_r(t) \tag{25}$$

where the subscript r denotes the rth time segment and the deterministic function $\gamma_r(t)$ may be considered as a shaping function written in the following form:

$$\gamma_r(t) = \epsilon_r \beta_r(t) \tag{26}$$

where $\beta_r(t) = u(t-t_{r-1}) - u(t-t_r)$. Here u(t) is a unit step function. ϵ_r is a constant at each time segment and represents the intensity of the generalized input load. Figure 3 illustrates the variation of ϵ with time and hence represents the load intensity as a function of time. The formulation as described in the above manner gives an approximate description of a continuously varying load. However, such a representation can be exact in practice, for example, in wind tunnel testings where the model angle of incidence advances in steps with time so that the buffet load can be represented by Equation (25).

To determine $z_1(t)$, the response $z_{1_r}(t)$ due to the rth time segment is first evaluated since

$$E\left[z_1^2(t)\right] = \sum_{r=1}^{m} E\left[z_{1_r}^2(t)\right] \tag{27}$$

where m is the time segment where t is located, that is, $t_{m-1} \leq t \leq t_m$ and E denotes the expected value. Knowing the load L(t), Equation (10) may be solved for $z_{1_r}(t)$. Introduce a frequency response function $H(\omega)$ as

$$H(\omega) = \frac{1}{M[\omega_n^2 - \omega^2 + i2\zeta\omega\omega_n]} \tag{28}$$

and

$$|H(\omega)|^2 = \frac{1}{M^2[(\omega_n{}^2 - \omega^2)^2 + 4\zeta^2\omega^2\omega_n{}^2]} \tag{29}$$

The covariance $C_{z_1z_1}(t_1,t_2)$ can be expressed in terms of the power spectral density of the applied load $S_{LL}(\omega_1,\omega_2)$ as:

$$C_{z_1z_1}(t_1,t_2) = \int_{-\infty}^{\infty}\int_{-\infty}^{\infty} S_{LL}(\omega_1,\omega_2)H(\omega_1)H^*(\omega_2)\, e^{i(\omega_1t_1-\omega_2t_2)}\, d\omega_1 d\omega_2 \tag{30}$$

where $H^*(\omega_2)$ is the conjugate of $H(\omega_2)$. If $z_1(t)$ has zero mean, then

$$C_{z_1z_1}(t_1,t_2) = R_{z_1z_1}(t_1,t_2) \tag{31}$$

where $R_{z_1z_1}(t_1,t_2)$ is the auto-correlation function. The mean square response can simply be obtained by setting $t_1=t_2=t$, that is,

$$E[z_1{}^2(t)] = R_{z_1z_1}(t,t) \tag{32}$$

In Equation (25), let $\overline{f_r(t)} = 0$. Since $R_{LL}(t_1,t_2) = E[L(t_1)L(t_2)]$, it may be expressed in the following form after using Equation (25) for $L(t_1)$ and $L(t_2)$:

$$R_{LL}(t_1,t_2) = \sum_{r=1}^{m}\sum_{s=1}^{m} \gamma_r(t_1)\gamma_s(t_2)E[f_r(t_1)f_s(t_2)] \tag{33}$$

Expressing $E[f_r(t_1)f_s(t_2)] = R_{f_rf_s}(t_1,t_2)$, Equation (33) can be rewritten as

$$R_{LL}(t_1,t_2) = \sum_{r=1}^{m}\sum_{s=1}^{m} \gamma_r(t_1)\gamma_s(t_2)R_{f_rf_s}(t_1,t_2) \tag{34}$$

If $R_{LL}(t_1,t_2)$ is known, then from the generalized Wiener-Khinchine relations (Ref. 29),

$$S_{LL}(\omega_1,\omega_2) = \frac{1}{4\pi^2}\int_{-\infty}^{\infty}\int_{-\infty}^{\infty} R_{LL}(t_1,t_2)\, e^{-i(\omega_1t_1 - \omega_2t_2)}\, dt_1 dt_2 \tag{35}$$

Combining Equations (34) and (35) yields:

$$S_{LL}(\omega_1,\omega_2) = \frac{1}{4\pi^2}\sum_{r=1}^{m}\sum_{s=1}^{m}\int_{-\infty}^{\infty}\int_{-\infty}^{\infty}\gamma_r(t_1)\gamma_s(t_2)R_{f_rf_s}(t_1,t_2)\,e^{-i(\omega_1 t_1-\omega_2 t_2)}\,dt_1 dt_2 \tag{36}$$

If $f_r(t)$ and $f_s(t)$ are stationary, then $R_{f_rf_s}(t_1,t_2) = R_{f_rf_s}(t_1-t_2) = R_{f_rf_s}(\tau)$, that is, the correlation depends only on $\tau = t_1 - t_2$. Since

$$R_{f_rf_s}(\tau) = \int_{-\infty}^{\infty} S_{f_rf_s}(\omega)\, e^{i\omega\tau}\,d\omega \tag{37}$$

and substituting into Equation (36) gives

$$S_{LL}(\omega_1,\omega_2) = \sum_{r=1}^{m}\sum_{s=1}^{m}\int_{-\infty}^{\infty} S_{f_rf_s}(\omega)\, A_r(\omega-\omega_1)\, A_s^*(\omega-\omega_2)\,d\omega \tag{38}$$

where

$$A_r(\omega-\omega_1) = \frac{1}{2\pi}\int_{-\infty}^{\infty}\gamma_r(t_1)\,e^{i(\omega-\omega_1)t_1}\,dt_1 \tag{39}$$

and

$$A_s^*(\omega-\omega_2) = \frac{1}{2\pi}\int_{-\infty}^{\infty}\gamma_s(t_2)\,e^{-i(\omega-\omega_2)t_2}\,dt_2 \tag{40}$$

From Equation (30), the mean square value of $z_1(t)$ is given as:

$$E\left[z_1^2(t)\right] = \int_{-\infty}^{\infty}\int_{-\infty}^{\infty} S_{LL}(\omega_1,\omega_2)\, H(\omega_1)\, H^*(\omega_2)\, e^{i(\omega_1-\omega_2)t}\,d\omega_1 d\omega_2 \tag{41}$$

Substituting Equation (38) into Equation (41) yields

$$E\left[z_1^2(t)\right] = \sum_{r=1}^{m} E\left[z_{1_r}^2(t)\right] = \sum_{r=1}^{m}\sum_{s=1}^{m}\int_{-\infty}^{\infty} S_{f_rf_s}(\omega)\, I_r(t,\omega)\, I_s^*(t,\omega)\,d\omega \tag{42}$$

where

$$I_r(t,\omega) = \int_{-\infty}^{\infty} A_r(\omega-\omega_1)\, H(\omega_1)\, e^{i\omega_1 t}\,d\omega_1 \tag{43}$$

and

$$I_s^*(t,\omega) = \int_{-\infty}^{\infty} A_s^*(\omega-\omega_2)\, H^*(\omega_2)\, e^{-i\omega_2 t}\, d\omega_2 \tag{44}$$

$I(t,\omega)$ is the time dependent frequency response function. Equation (42) gives the general formulation for amplitude modulated stationary inputs and is a function of the spectral density $S_{f_r f_r}(\omega)$ and cross spectral density $S_{f_r f_s}(\omega)$.

To evaluate $I(t,\omega)$, consider the time segment denoted by $t_{r-1} \leq t \leq t_r$ (Figure 3). It can be shown that in Equation (39)

$$A_r(\omega-\omega_1) = \frac{\epsilon_r}{2\pi}\left\{\pi\delta(\omega_1-\omega) + \frac{1}{i(\omega_1-\omega)}\right\}\left\{e^{i(\omega-\omega_1)t_{r-1}} - e^{i(\omega-\omega_1)t_r}\right\} \tag{45}$$

Substituting this expression into Equation (43) gives

$$I_r(t,\omega) = \frac{\epsilon_r}{2\pi}\left\{e^{i\omega t_r}\int_{-\infty}^{\infty}\frac{H(\omega_1)}{i(\omega-\omega_1)}\, e^{i\omega_1(t-t_r)}\, d\omega_1 - e^{i\omega t_{r-1}}\int_{-\infty}^{\infty}\frac{H(\omega_1)}{i(\omega-\omega_1)}\, e^{i\omega_1(t-t_{r-1})}\, d\omega_1\right\} \tag{46}$$

The integrals $\int_{-\infty}^{\infty}\frac{H(\omega_1)}{i(\omega-\omega_1)}\, e^{i\omega_1(t-t_r)}\, d\omega_1$ and $\int_{-\infty}^{\infty}\frac{H(\omega_1)}{i(\omega-\omega_1)}\, e^{i\omega_1(t-t_{r-1})}\, d\omega_1$ can be evaluated by contour integration. The function $H(\omega_1)\,(\omega-\omega_1)^{-1}$ has poles at $\sigma_1 = \omega$, $\sigma_2 = \omega_d + i\,\zeta\,\omega_n$ and $\sigma_3 = -\,\omega_d + i\,\zeta\,\omega_n$, where ω_d is the damped natural frequency and is defined as:

$$\omega_d = \sqrt{1-\zeta^2}\;\omega_n \tag{47}$$

Considering the first integral, the integration path for $t > t_r$ is taken above the real axis as depicted in Figure 4a, while for $t < t_r$, the integration is below the real axis. Similar paths of integration are taken for the second integral. Upon substitution of these integrals into Equation (46), the final form becomes:

$$I_r(t,\omega) = \epsilon_r H(\omega)\cdot\left\{u(t-t_{r-1})\left[e^{i\omega t} - e^{i\omega t_{r-1}}\left(\psi(t-t_{r-1}) + \frac{i\omega}{\omega_d}\,\phi(t-t_{r-1})\right)\right]\right.$$

$$\left. - u(t-t_r)\left[e^{i\omega t} - e^{i\omega t_r}\left(\psi(t-t_r) + \frac{i\omega}{\omega_d}\,\phi(t-t_r)\right)\right]\right\} \tag{48}$$

where

$$\psi(t) = e^{-\zeta\omega_n t}\left(\cos\omega_d t + \zeta\frac{\omega_n}{\omega_d}\sin\omega_d t\right) \tag{49}$$

and

$$\phi(t) = e^{-\zeta\omega_n t}\sin\omega_d t \tag{50}$$

In buffet maneuvers or in wind tunnel testing of a pitched model whose incidence changes with time like a step function, the loading on the wing can be approximated by Equation (25) with $f_r(t)$ being the same in all time segments. The only changes in L(t) being the intensity. This may be a fair approximation since buffeting is primarily due to the fluctuating pressure forces of the separated flow on the upper wing surface. The frequency structure of the separated flow may not change by a large extent as the incidence varies. If it is assumed that there is no correlation between different segments, then from Equation (42),

$$E\left[z_{l_r}^2(t)\right] = \int_{-\infty}^{\infty} S_{f_r f_r}(\omega)|I_r(t,\omega)|^2\,d\omega \tag{51}$$

where after some algebra, $|I_r(t,\omega)|^2$ is given as follows:

for $t_{r-1} \leqslant t \leqslant t_r$,

$$|I_r(t,\omega)|^2 = \epsilon_r^2|H(\omega)|^2 \cdot \left\{1 - 2\psi(t-t_{r-1})\cos\omega(t-t_{r-1})\right.$$

$$- 2\frac{\omega}{\omega_d}\phi(t-t_{r-1})\sin\omega(t-t_{r-1})$$

$$\left. + \psi^2(t-t_{r-1}) + \frac{\omega^2}{\omega_d^2}\phi^2(t-t_{r-1})\right\} \tag{52}$$

for $t > t_r$,

$$|I_r(t,\omega)|^2 = \epsilon_r^2|H(\omega)|^2 \cdot \left\{\psi^2(t-t_{r-1}) + \psi^2(t-t_r)\right.$$

$$\left. + \frac{\omega^2}{\omega_d^2}\phi^2(t-t_{r-1}) + \frac{\omega^2}{\omega_d^2}\phi^2(t-t_r)\right. \tag{53}$$

$$- 2\cos\omega(t_r - t_{r-1})\left[\psi(t-t_{r-1})\psi(t-t_r) + \frac{\omega^2}{\omega_d{}^2}\phi(t-t_{r-1})\phi(t-t_r)\right]$$

$$+ 2\frac{\omega}{\omega_d}\sin\omega(t_r - t_{r-1})\left[\psi(t-t_{r-1})\phi(t-t_r) - \phi(t-t_{r-1})\psi(t-t_r)\right]\Bigg\} \tag{53}$$

2.3 Evaluation of Mean Square Response for a Given Power Spectral Density of the Input

Equation (51) can be integrated to give the mean square response, provided the form of the power spectral density $S_{f_r f_r}(\omega)$ of the input is specified. Cole (Ref. 26) gives a form of the spectral density which has been found to adequately describe the buffeting input to launch vehicles. In the present notations, this can be written as

$$S_{f_r f_r}(\omega) = \frac{S_o}{1 + \left(\frac{\omega}{\omega_f}\right)^2} \tag{54}$$

where ω_f is the half power frequency and S_o is a constant. In Figure 5, $\frac{S_{f_r f_r}(\omega)}{S_o}$ is plotted versus $\frac{\omega}{\omega_n}$ for different values of $\frac{\omega_n}{\omega_f}$. For $\frac{\omega_n}{\omega_f} = 0$, $S_{f_r f_r}(\omega) = \text{constant} = S_o$, which is the power spectral density for white noise. As $\frac{\omega_n}{\omega_f}$ increases, the energy of the exciting force near the natural frequency ω_n diminishes and this will have an appreciable effect on the response of the system.

Consider the rth time segment and using Equation (52) or (53) for $|I_r(t,\omega)|^2$ together with the expression for $|H(\omega)|^2$ given in Equation (29), the mean square value $E[z_{1_r}{}^2(t)]$ can be evaluated analytically since the form of the power spectral density is known. Let

$$\mathcal{E}[z_{1_r}{}^2(t)] = \frac{2\zeta M^2 \omega_n{}^3}{\pi S_o} E[z_{1_r}{}^2(t)] \tag{55}$$

Using contour integration and after much algebra the final expression for $\mathcal{E}[z_{1_r}{}^2(t)]$ are as follows:

where for $t_{r-1} \leq t \leq t_r$,

$$\mathcal{E}[z_{1_r}^2(t)] = \frac{\epsilon_r^2}{G} \cdot \Bigg\{ K[1+\psi^2(t-t_{r-1})] - 2\psi(t-t_{r-1}) \cdot \left[F(t-t_{r-1}) + 2\zeta \left(\frac{\omega_n}{\omega_f}\right)^3 e^{-\omega_f(t-t_{r-1})} \right]$$

$$- 2\phi(t-t_{r-1}) \left[\frac{H(t-t_{r-1})}{1-\zeta^2} + \frac{2\zeta}{\sqrt{1-\zeta^2}} \left(\frac{\omega_n}{\omega_f}\right)^2 e^{-\omega_f(t-t_{r-1})} \right]$$

$$+ \phi^2(t-t_{r-1}) \left[\frac{1 + \frac{\omega_n^2}{\omega_f^2} - 2\zeta\frac{\omega_n}{\omega_f}}{1-\zeta^2} \right] \Bigg\} \qquad (56)$$

and for $t > t_r$,

$$\mathcal{E}[z_{1_r}^2(t)] = \frac{\epsilon_r^2}{G} \cdot \Bigg\{ K[\psi^2(t-t_{r-1}) + \psi^2(t-t_r)]$$

$$+ [\phi^2(t-t_{r-1}) + \phi^2(t-t_r)] \left[\frac{1 + \frac{\omega_n^2}{\omega_f} - 2\zeta\frac{\omega_n}{\omega_f}}{1-\zeta^2} \right]$$

$$- [\psi(t-t_{r-1})\psi(t-t_r)] \left[2F(t_r-t_{r-1}) + 4\zeta\frac{\omega_n^3}{\omega_f^3} e^{-\omega_f(t_r-t_{r-1})} \right]$$

$$- [\phi(t-t_{r-1})\phi(t-t_r)] \left[\frac{2Q(t_r-t_{r-1}) - 4\zeta\frac{\omega_n}{\omega_f} e^{-\omega_f(t_r-t_{r-1})}}{1-\zeta^2} \right]$$

$$+ [\psi(t-t_{r-1})\phi(t-t_r) - \phi(t-t_{r-1})\psi(t-t_r)]$$

$$\cdot \left[\frac{2H(t_r-t_{r-1})}{1-\zeta^2} + \frac{4\zeta}{\sqrt{1-\zeta^2}} \frac{\omega_n^2}{\omega_f^2} e^{-\omega_f(t_r-t_{r-1})} \right] \Bigg\} \qquad (57)$$

with

$$F(t) = \left\{1 + (1 - 4\zeta^2)\frac{\omega_n^2}{\omega_f^2}\right\}\psi(t) + \frac{2\zeta}{\sqrt{1-\zeta^2}}\frac{\omega_n^2}{\omega_f^2}\phi(t) \tag{58}$$

$$G = \left(1 + \frac{\omega_n^2}{\omega_f^2}\right)^2 - 4\zeta\frac{\omega_n^2}{\omega_f^2} \tag{59}$$

$$H(t) = \left(1 + \frac{\omega_n^2}{\omega_f^2}\right)\phi(t) - 2\zeta\frac{\omega_n^2}{\omega_f^2}\sqrt{1-\zeta^2}\,\psi(t) \tag{60}$$

$$K = 1 + (1-4\zeta^2)\frac{\omega_n^2}{\omega_f^2} + 2\zeta\frac{\omega_n^3}{\omega_f^3} \tag{61}$$

$$Q(t) = \left(1 + \frac{\omega_n^2}{\omega_f^2}\right)\psi(t) - \frac{2\zeta}{\sqrt{1-\zeta^2}}\phi(t) \tag{62}$$

Equations (58) to (62) can be simplified considerably for $\frac{\omega_n}{\omega_f} \to 0$, namely,

$$F(t) \to \psi(t)$$

$$G \to 1$$

$$H(t) \to \phi(t)$$

$$K \to 1$$

$$Q(t) \to \psi(t) - \frac{2\zeta}{\sqrt{1-\zeta^2}}\phi(t)$$

Substituting these functions into Equations (56) and (57) gives:

for $t_{r-1} \leq t \leq t_r$,

$$\mathcal{E}\left[z_{1_r}^2(t)\right] \to e_r^2\left[1 - \psi^2(t-t_{r-1}) - \frac{\phi^2(t-t_{r-1})}{1-\zeta^2}\right] \tag{63}$$

and for $t > t_r$,

$$\mathcal{E}[z_{1_r}^2(t)] \to \epsilon_r^2 \left\{ \psi^2(t-t_{r-1}) + \psi^2(t-t_r) \right.$$

$$+ \frac{1}{1-\zeta^2}[\phi^2(t-t_{r-1}) + \phi^2(t-t_r)]$$

$$- 2\psi(t-t_r)\left[\psi(t-t_{r-1})\psi(t_r-t_{r-1}) + \frac{\phi(t-t_{r-1})\phi(t_r-t_{r-1})}{1-\zeta^2}\right]$$

$$+ \frac{2\phi(t-t_r)}{1-\zeta^2}\left[\frac{2\zeta}{\sqrt{1-\zeta^2}}\phi(t-t_{r-1})\phi(t_r-t_{r-1}) - \phi(t-t_{r-1})\psi(t_r-t_{r-1})\right.$$

$$\left.\left. + \psi(t-t_{r-1})\phi(t_r-t_{r-1})\right]\right\} \qquad (64)$$

In the limit for $\frac{\omega_n}{\omega_f} = 0$, these two expressions give the response to white noise.

2.4 Computational Procedure

The steps involved in computing the mean square response is fairly simple and straightforward. For a given value of $\frac{\omega_n}{\omega_f}$, $\mathcal{E}[z_{1_r}^2(t)]$ can be evaluated from Equations (56) and (57) (or Equations (63) and (64) for white noise) once the ϵ_r's are given as functions of time. Referring to Figure 3, at any specified time t, the procedure is to establish the time segment where t lies. If it falls between t_{m-1} and t_m, then $\mathcal{E}[z_1^2(t)]$ is obtained as follows:

$$\mathcal{E}[z_1^2(t)] = \mathcal{E}[z_{1_m}^2(t)] + \sum_{r=1}^{m-1} \mathcal{E}[z_{1_r}^2(t)] \qquad (65)$$

where the first term on the right hand side of the equation is determined from Equation (56) while the second term from Equation (57).

Three cases are considered where ϵ varies with time in the form of the following functions:

Case I: : Sinusoidal

Case II: Ramp

Case III: Triangular.

These functions are shown schematically in Figure 6 and shall be referred to the case number in the future. For convenience, the maximum value of ϵ is taken to be unity and this does not affect the

generality of the solutions. The number of time segments in T_B will be specified later on after the effect of varying the segment duration $(t_r - t_{r-1})$ has been investigated. The variables involved in the analysis are $\frac{\omega_n}{\omega_f}$, ζ, and T_B, and their influence on the mean square response are studied in some detail.

3.0 RESULTS AND DISCUSSIONS

Since Equations (56) and (57) are the principle expressions to be used to compute the mean square value of $z_1(t)$ for specified non-stationary loads, their characteristics are first investigated in some detail. Equation (56) determines the response or rise to a step modulated stationary exciting force, while Equation (57) governs the decay when the applied force is withdrawn. Taking ϵ_r to be unity, Equation (56) is plotted in Figures 7 to 10 as a function of time $t' - t'_{r-1}$ for three values of the damping ratio (ζ = 0.02, 0.04 and 0.08) and four values of $\frac{\omega_n}{\omega_f}$, namely, $\frac{\omega_n}{\omega_f}$ = 0, 0.5, 1 and 2. The superscript $'$ is used to denote that time is non-dimensionalized with respect to the undamped natural period $T_n = 2\pi/\omega_n$. From these figures, it can be seen that for larger values of ζ, the mean square of $z_1(t')$ reaches an asymptotic value for $t' - t'_{r-1} \to \infty$ sooner than that with smaller values of ζ. Increasing the value of ω_n/ω_f tends to diminish the asymptotic value. This can be explained from Figure 5 where the normalized power spectral density is plotted versus ω/ω_n. The energy in the exciting force near the natural frequency ω_n diminishes for increasing ω_n/ω_f, and hence it can be expected that the value of the mean square response will decrease as ω_n/ω_f increases. From Equations (49) and (50), it is seen that as $t' - t'_{r-1} \to \infty, \psi(t' - t'_{r-1}) \to 0$ and $\phi(t' - t'_{r-1}) \to 0$. Hence Equation (56) can be written as (taking $\epsilon_r = 1$):

$$\mathcal{E}[z_{1_r}^2(t')] \to \frac{1 + (1-4\zeta^2)\frac{\omega_n^2}{\omega_f^2} + 2\zeta\frac{\omega_n^3}{\omega_f^3}}{\left(1 + \frac{\omega_n^2}{\omega_f^2}\right)^2 - 4\zeta^2\frac{\omega_n^2}{\omega_f^2}} \tag{66}$$

$\mathcal{E}[z_{1_r}^2(t')]$ decreases as ω_n/ω_f increases. For $\omega_n/\omega_f \gg 1$,

$$\mathcal{E}[z_{1_r}^2(t')] \to \frac{2\zeta}{\frac{\omega_n}{\omega_f}} \tag{67}$$

In the limit $\omega_n/\omega_f \to \infty$, $\mathcal{E}[z_{1_r}^2(t')] \to 0$.

In the computations, no significant changes in $\mathcal{E}[z_{1_r}^2(t')]$ compared to that at $\omega_n/\omega_f = 0$ are detected for values of ω_n/ω_f less than 0.1. These curves are replotted in Figures 11 to 13 for fixed ζ with ω_n/ω_f as the variable. The oscillations observed are due to the sine and cosine terms in the expressions for $\psi(t' - t'_{r-1})$ and $\phi(t' - t'_{r-1})$, but they are rapidly damped out for increasing $t' - t'_{r-1}$.

Equation (57) is used to compute the decay of the mean square of $z_{1_r}(t')$ after the exciting force has been withdrawn at time t'_r. Using the same values of ζ and ω_n/ω_f as before, the decay to a pulse modulated stationary exciting force are shown in Figures 14 to 25 for different values of the

pulse duration ($t'_r - t'_{r-1}$ = 0.5, 1, 2, 4 and 8). Since the curves are plotted with $t' - t'_{r-1}$ as the absicca, then $t'_r - t'_{r-1}$ is simply measured from 0 along the axis to the time $t' - t'_{r-1}$ when the decay curve starts.

For large values of the pulse duration, Equations (49) and (50) give

$$\psi(t'_r - t'_{r-1}) \to 0$$

$$\phi(t'_r - t'_{r-1}) \to 0$$

as $t'_r - t'_{r-1} \to \infty$.

Also from Equations (58), (60) and (62),

$$F(t'_r - t'_{r-1}) \to 0$$

$$H(t'_r - t'_{r-1}) \to 0$$

$$Q(t'_r - t'_{r-1}) \to 0$$

Equation (57) can be written as (taking $\epsilon_r = 1$)

$$\mathcal{E}[z_{1_r}^2(t')] = \frac{1}{G}\left\{K\psi^2(t'-t'_r) + \phi^2(t'-t'_r)\,\frac{\left(1 + \frac{\omega_n^2}{\omega_f^2} - 2\zeta\frac{\omega_n}{\omega_f}\right)}{1-\zeta^2}\right\} \tag{68}$$

which is independent of $t'_r - t'_{r-1}$. In other words, the decay is independent of the step duration for large values of $t'_r - t'_{r-1}$. From the figures, it is also observed that for constant ζ, the decay is more rapid as ω_n/ω_f decreases, especially for cases with the larger values of $t'_r - t'_{r-1}$. This can be shown from Equation (68).

For $\omega_n/\omega_f \ll 1$,

$$\mathcal{E}[z_{1_r}^2(t')] \to \psi^2(t'-t'_r) + \frac{\phi^2(t'-t'_r)}{1-\zeta^2}$$

while for $\omega_n/\omega_f \gg 1$,

$$\mathcal{E}[z_{1_r}^2(t')] \to \frac{2\zeta}{\frac{\omega_n}{\omega_f}} \cdot \psi^2(t'-t'_r)$$

Also of interest in those figures are the oscillations in the decay curves. For small damping, the oscillations are very clearly shown. The amplitudes increase with ω_n/ω_f while the decay is less rapid. This is even more significant for smaller values of $t'_r - t'_{r-1}$ and will be shown later to have quite an effect on non-stationary loads.

For an input load with sinusoidal variation of ϵ with time (Case I in Figure 6), $\mathcal{E}[z_1^2(t')]$ has been computed using Equation (65). The duration of the applied load T'_B is forty times the natural period, and it is divided into eighty equal time segments giving a value $\Delta t'_r = t'_r - t'_{r-1}$ of 0.5. Figure 26 shows the response for $\zeta = 0.02$, 0.04 and 0.08 with $\omega_n/\omega_f = 0$. Also plotted in the same figure is the ϵ versus time curve for comparison purposes. Similar to Figures 7 to 10, the rise time is seen to be smaller for the larger values of ζ. Shown in the figure is the delay τ, which is the time where the maximum value of $\mathcal{E}[z_1^2(t')]$ lags behind the applied force, and the amplitude function δ defined as

$$\delta = 1 - \mathcal{E}[z_1^2(t')]_{max}.$$

The effect of changing the number of time segments has been studied, and it is found that if $\Delta t'_r < 1$, the differences in the computed results are not very significant. Figure 27 shows the response curves for three values of $\Delta t'_r$ and it is seen that the curves with $\Delta t'_r = 2$ and 0.5 are quite close. In all subsequent computations, $\Delta t'_r$ is taken to be 0.5.

The effect of ω_n/ω_f on $\mathcal{E}[z_1^2(t')]$ are shown in Figures 28 to 31 for $\omega_n/\omega_f = 0.1$, 0.5, 1 and 2 with $\zeta = 0.2$. The oscillations in the response curves increase with ω_n/ω_f, and the peak to peak values reach a maximum at $\omega_n/\omega_f = 1$. These oscillations arise mainly from the second term of Equation (65) where previous results (Figures 14 to 25) show that for increasing values of ω_n/ω_f, the decay to a pulse modulated input has fairly large amplitude oscillations and diminishes rather slowly with time. The summation in Equation (65) for a large number of segments help to accentuate this effect, thus resulting in large regular oscillations.

To illustrate the effect of the duration of the applied force, results with $T'_B = 10$ are presented keeping all other variables the same as before. Figure 32 shows $\mathcal{E}[z_1^2(t')]$ versus t' for $\omega_n/\omega_f = 0$, $\zeta = 0.02$, 0.04 and 0.08. Comparison with Figure 26 shows that the delay τ is shorter while δ increases. Comparing Figures 33 to 36 with Figures 28 to 31 gives the effect of T'_B on the mean square response. Decreasing the value of T'_B results not only in a smaller peak value of $\mathcal{E}[z_1^2(t')]$, but also decreases the peak to peak value of the oscillations.

The delay τ is a function of ζ and T'_B. Its variations with T'_B for $\zeta = 0.02$, 0.04 and 0.1 are shown in Figure 37. The delay increases with T'_B in steps of half the natural period. For $\zeta = 0.04$, and 0.1, computations up to $T'_B = 60$ show that τ does not change from the values 1 and 2 which correspond to those reached at $T'_B = 10$ and 18 respectively. It thus appears that τ has reached the maximum for these two values of ζ. For $\zeta = 0.02$, computations have not proceeded for sufficiently large values of T'_B to determine the maximum τ. Figures 38 to 42 show the variations of δ with T'_B for $\omega_n/\omega_f = 0$, 0.1, 0.5, 1 and 2 with ζ as the parameter. The results indicate that δ increases with decreasing ζ for any fixed ω_n/ω_f while increasing T'_B results in smaller δ. For large values of T'_B, δ tends to an asymptotic value and the approach to this value is more rapid as ζ increases. By increasing ω_n/ω_f, δ is also increased as shown in Figures 43 to 46 where δ is plotted against T'_B for fixed ζ with ω_n/ω_f as the parameter. These curves again indicate that for larger values of ζ, δ approaches its asymptotic value more rapidly.

Similar to Figure 27, the effect of $\Delta t'_r$ on $\mathcal{E}[z_1^2(t')]$ is plotted in Figure 47 for Case II with $\zeta = 0.08$ and three values of $\Delta t'_r$ (0.5, 2 and 4) are considered. The same conclusions are arrived at as before, that is, for $\Delta t'_r < 1$, the differences in the response curves are very small for different $\Delta t'_r$, and hence a value of 0.5 is again used throughout the computations.

The results for Case II ($T'_B = 20$) and Case III ($T'_B = 40$) are shown in Figure 48 which serves to illustrate the effect of ζ at $\omega_n/\omega_f = 0$. Figures 49 to 52 give the response curves for these

two cases. The value of ζ is 0.02 and ω_n/ω_f = 0.1, 0.5, 1 and 2. The effect of T'_B is demonstrated in Figures 53 to 57 where T'_B = 5 for Case II and T'_B = 10 for Case III. These results are very similar to those for Case I. The most significant differences between Case I and Case III are the smaller values of the $\mathcal{E}[z_1^2(t')]_{max}$ for the latter case. This is to be expected since ϵ reaches its maximum and decreases at a much faster rate than in Case I.

4.0 CONCLUSIONS

A method for predicting the response of a wing to non-stationary buffet loads has been developed and applied successfully to a number of hypothetical examples. For buffet maneuvers in an aircraft, the fluctuating loads change continuously and hence the analysis presented herein which models the load by a time segmentation technique, is to be treated as an approximation. However, this approximation has been found to be fairly good since a study of the effect of the duration of time segments shows that if it is below a certain value, there is little change in the results when smaller time segments are taken. In wind tunnel buffet tests, it is possible to control the incidence of the model by pitching it in a prescribed manner. The buffet load can be made to vary with time in the form of a step function. In this case, the method of representing the load described in this report can be considered to be exact.

The form of the power spectral density of the input load used in this study is similar to that encountered in the theory of isotropic turbulence, and analytical expressions for the mean square response of the wing displacement has been derived. The effect of varying the ratio of the undamped natural frequency to the half power frequency ω_n/ω_f on the response of the system has been investigated and it is shown that if ω_n/ω_f is small, the maximum value of the response is greater than that obtained for larger values of ω_n/ω_f. This is due to the distribution of energy in the input load since a large value of ω_n/ω_f implies that little energy is distributed near the undamped natural frequency. It should be noted that for white noise, equal energy is distributed at all frequencies, and ω_n/ω_f in this case is equal to zero.

The duration of the applied load T'_B and the form of the time history of the load have also been studied. Detail results are presented for a sinusoidal variation of the force with time. Computations have been carried out showing the effect of damping and ω_n/ω_f on the delay τ and amplitude function δ of the response curve. It is found that for larger values of ζ, τ reaches a constant value less than those obtained for smaller ζ. Also, the time T'_B it takes to reach this constant value is much shorter for larger values of ζ. For fixed ω_n/ω_f, decreasing ζ increases δ, while for fixed ζ, increasing ω_n/ω_f increases δ. Results for input loads expressed as ramp and triangular functions are also presented. For the triangular input, the results are quite similar to those for the sinusoidal case; the most significant difference being the smaller values obtained in the response curves.

5.0 REFERENCES

1. Pearcey, H.H. — *A Method for the Prediction of the Onset of Buffeting and Other Separation Effects from Wind Tunnel Tests on Rigid Models.* North Atlantic Treaty Organization, Advisory Group for Aeronautical Research and Development Report 223, October, 1958.

2. Liepman, H.W. — *On the Application of Statistical Concepts to the Buffeting Problem.* Journal Aeronautical Sciences, Vol. 19, No. 12, December, 1952, pp. 793-800.

3. Liepman, H.W. — *Extension of the Statistical Approach to Buffeting and Gust Response of Wings of Finite Span.* Journal Aeronautical Sciences, Vol. 22, No. 3, March, 1955, pp. 197-200.

4. Ribner, H.S. — *Spectral Theory of Buffeting and Gust Response: Unification and Extension.* Journal Aeronautical Sciences, Vol. 23, No. 12, December, 1956, pp. 1075-1077.

5. Huston, W.B. Skopinski, T.H. — *Measurement and Analysis of Wing and Tail Buffeting Loads on a Fighter Airplane.* National Advisory Committee for Aeronautics, Report 1219, 1955.

6. Huston, W.B. Skopinski, T.H. — *Probability and Frequency Characteristics of Some Flight Buffet Loads.* National Advisory Committee for Aeronautics, Technical Note 3733, August, 1956.

7. Huston, W.B. — *A Study of the Correlation Between Flight and Wind Tunnel Buffet Loads.* North Atlantic Treaty Organization Advisory Group for Aeronautical Research and Development, Report 111, April-May, 1957.

8. Skopinski, T.H. Huston, W.B. — *A Semi-Empirical Procedure for Estimating Wing Buffet Loads in the Transonic Region.* National Advisory Committee for Aeronautics, RM L56E01, September, 1956.

9. Cole, Jr. H.A. — *Dynamic Response of Hammerhead Launch Vehicles to Transonic Buffeting.* National Aeronautics and Space Administration, TN D-1982, October 1963.

10. Cole, Jr. H.A. Robinson, R.C. Gambucci, B.J. — *Detection of Flow-Field Instability in the Presence of Buffeting by the Partial-Mode Technique.* National Aeronautics and Space Administration, TN D-2689, February, 1965.

11. Coe, C.F. — *Steady and Fluctuating Pressures at Transonic Speeds on Two Space-Vehicle Payload Shapes.* National Aeronautics and Space Administration, TM X-503, 1961.

12. Coe, C.F. — *The Effects of Some Variations in Launch-Vehicle Nose Shape on Steady and Fluctuating Pressures at Transonic Speeds.* National Aeronautics and Space Administration, TM X-646, 1962.

13. Hollingsworth, E.G. Cohen, M. — *Determination of F-4 Aircraft Transonic Buffet Characteristics.* Journal of Aircraft, Vol. 8, No. 10, 1971, pp. 757-763.

14. Mayes, J.F. Lores, M.E. Barnard, H.R. — *Transonic Buffet Characteristics of a 60° Swept Wing with Design Variations.* Journal of Aircraft, Vol. 7, No. 6, 1970, pp. 524-530.

15. Damstrom, E.K. Mayes, J.F. — *Transonic Flight and Wind-Tunnel Buffet Onset Investigation of the F-8D Aircraft.* Journal of Aircraft, Vol. 8, No. 4, 1971, pp. 263-270.

16. DeAngelis, V.M. Monaghan, R.C. — *Buffet Characteristics of the F-8 Supercritical Wing Airplane.* National Aeronautics and Space Administration, TM 56049, 1977.

17. Hwang, C.
Pi, W.S.
Investigation of Northrop F-5A Wing Buffet Intensity in Transonic Flight.
National Aeronautics and Space Administration, CR-2484, November, 1974.

18. Hwang, C.
Pi, W.S.
Transonic Buffet Behavior of Northrop F-5A Aircraft.
American Institute of Aeronautics and Astronautics, Paper 75-70, January, 1975.

19. Mullans, R.E.
Lemley, C.E.
Buffet Dynamic Loads During Transonic Maneuvers.
Air Force Flight Dynamics Laboratory, Technical Report AFFDL-TR-72-46, September, 1972.

20. Cunningham, A.E.
Waner, Jr. P.G.
Watts, J.D.
Benepe, D.B.
Riddle, D.W.
Development and Evaluation of a New Method for Predicting Aircraft Buffet Response.
American Institute of Aeronautics and Astronautics, Paper 75-69, January, 1975.

21. Butler, G.F.
Spavins, G.R.
Preliminary Evaluation of a Technique for Predicting Buffet Loads in Flight from Wind-Tunnel Measurements on Models of Conventional Construction.
North Atlantic Treaty Organization, Advisory Group for Aerospace Research and Development, Paper 23 of AGARD CP-204, 1976.

22. Jones, J.G.
A Survey of the Dynamic Analysis of Buffeting and Related Phenomenon.
Royal Aircraft Establishment Technical Report 72197, February, 1973.

23. Caughey, T.K.
Nonstationary Random Inputs and Responses, in "Random Vibration".
Vol. 2 ed. Crandall, S.H., MIT Press, Cambridge, Massachusetts, 1963.

24. Barnoski, R.L.
Maurer, J.R.
Mean-Square Response of Simple Mechanical Systems to Non-stationary Random Excitation.
Transaction of the American Society of Mechanical Engineers, Series E; Journal of Applied Mechanics, Vol. 36, No. 12, June, 1969, pp. 221-227.

25. Holman, R.E.
Hart, G.C.
Nonstationary Response of Structural Systems.
ASCE Journal of Engineering Mechanics Division, Vol. 100, No. EM2, April, 1974, pp. 415-431.

26. Cole, Jr. H.A.
On-The-Line Analysis of Random Vibrations.
American Institute of Aeronautics and Astronautics, Paper 68-288, April, 1968.

27. Scanlan, R.H.
Rosenbaum, R.
Introduction to the Study of Aircraft Vibration and Flutter.
Dover Publications Inc., New York, 1968.

28. Davis, D.D.
Wornom, D.E.
Buffet Tests of an Attack-Airplane Model with Emphasis on Analysis of Data from Wind-Tunnel Tests.
National Advisory Committee for Aeronautics, RM L57H13, February, 1958.

29. Bendat, J.S.
Piersol, A.G.
Random Data: Analysis and Measurement Procedures.
Wiley-Interscience 1971.

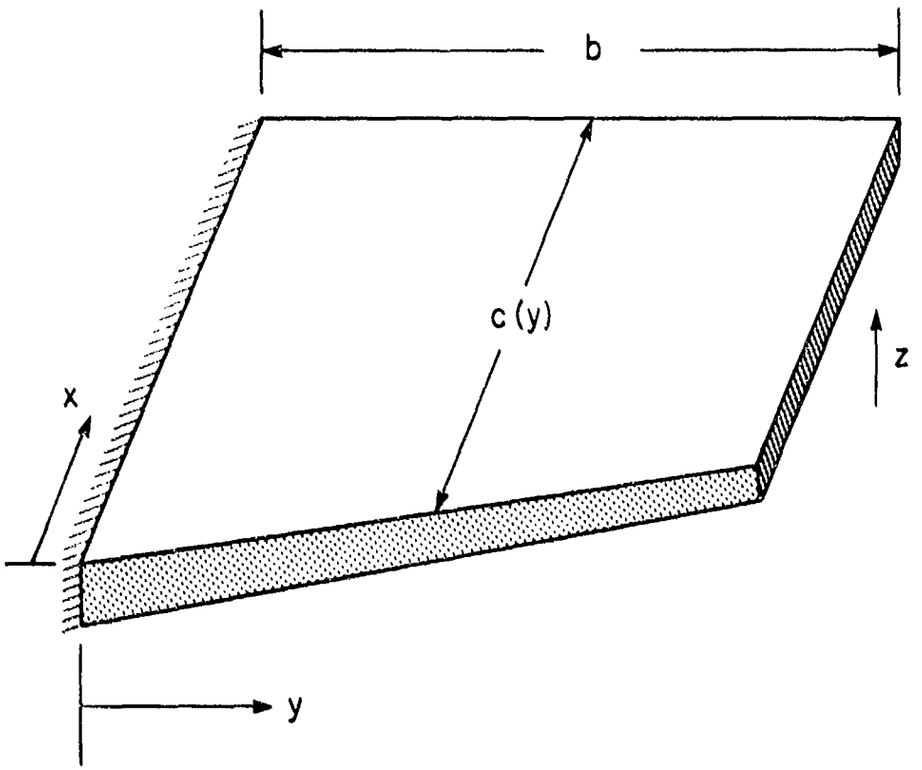

FIG. 1: SCHEMATIC OF WING

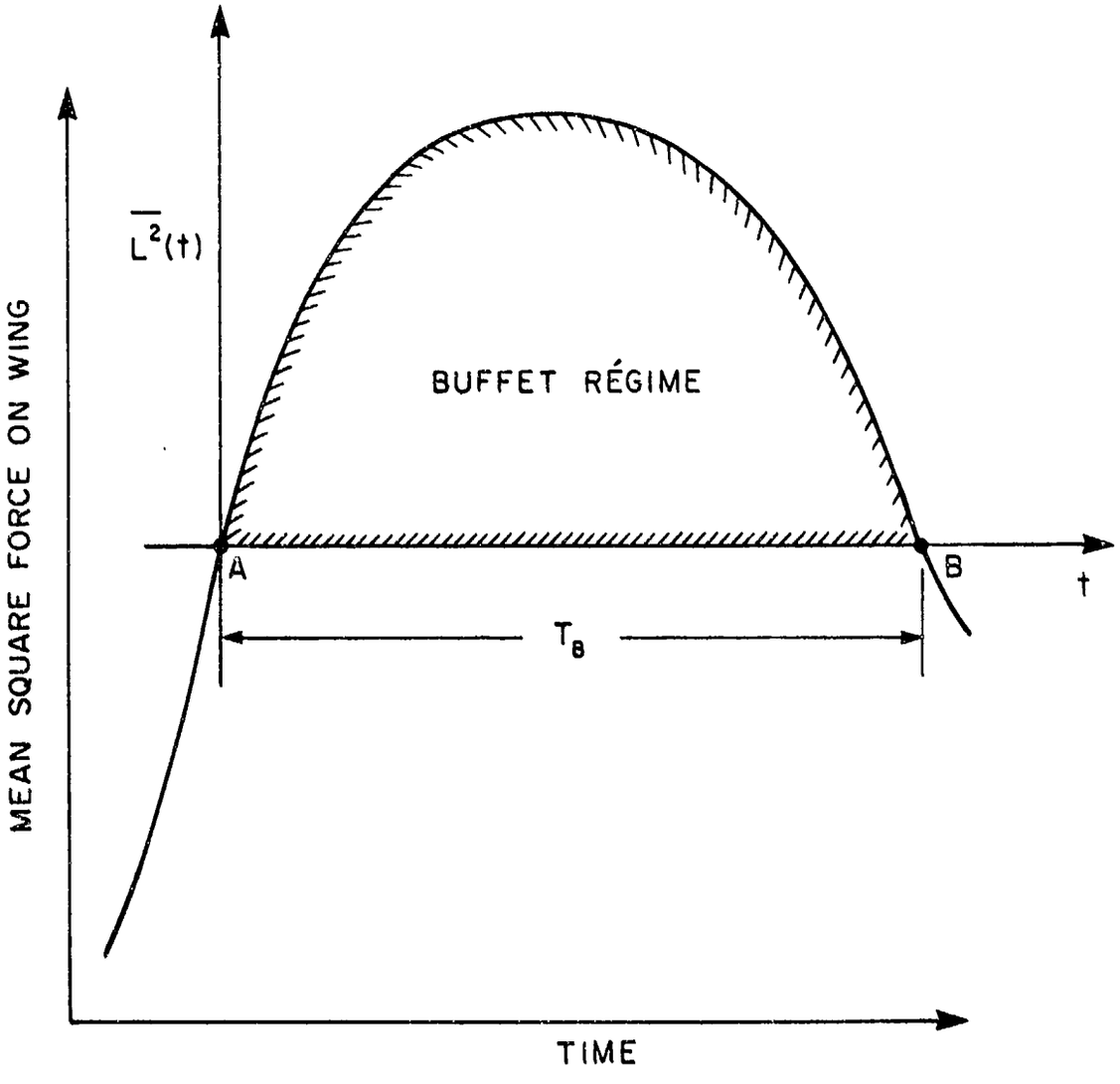

FIG. 2: SCHEMATIC ILLUSTRATING MEAN SQUARE LOADING ON WING VERSUS TIME

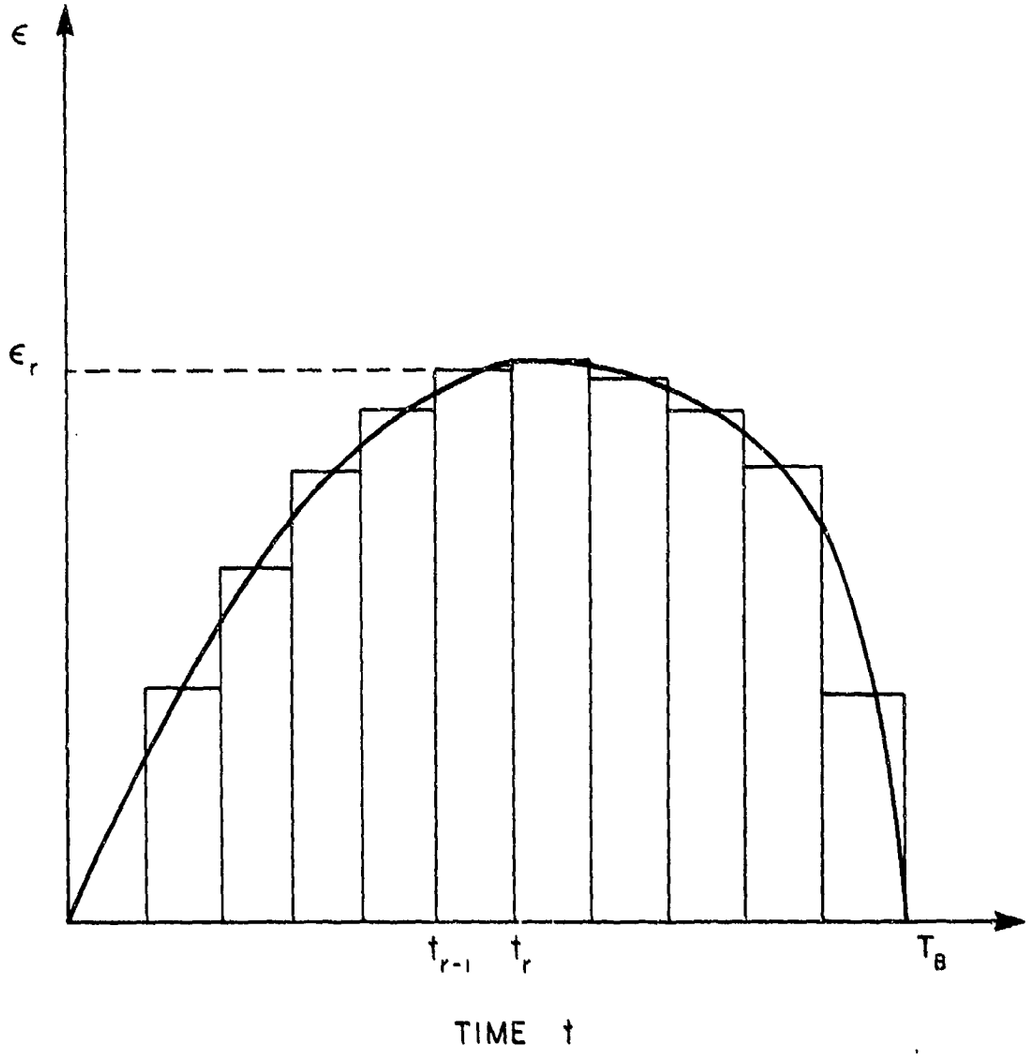

FIG. 3: SCHEMATIC SHOWING VARIATION OF ϵ WITH TIME

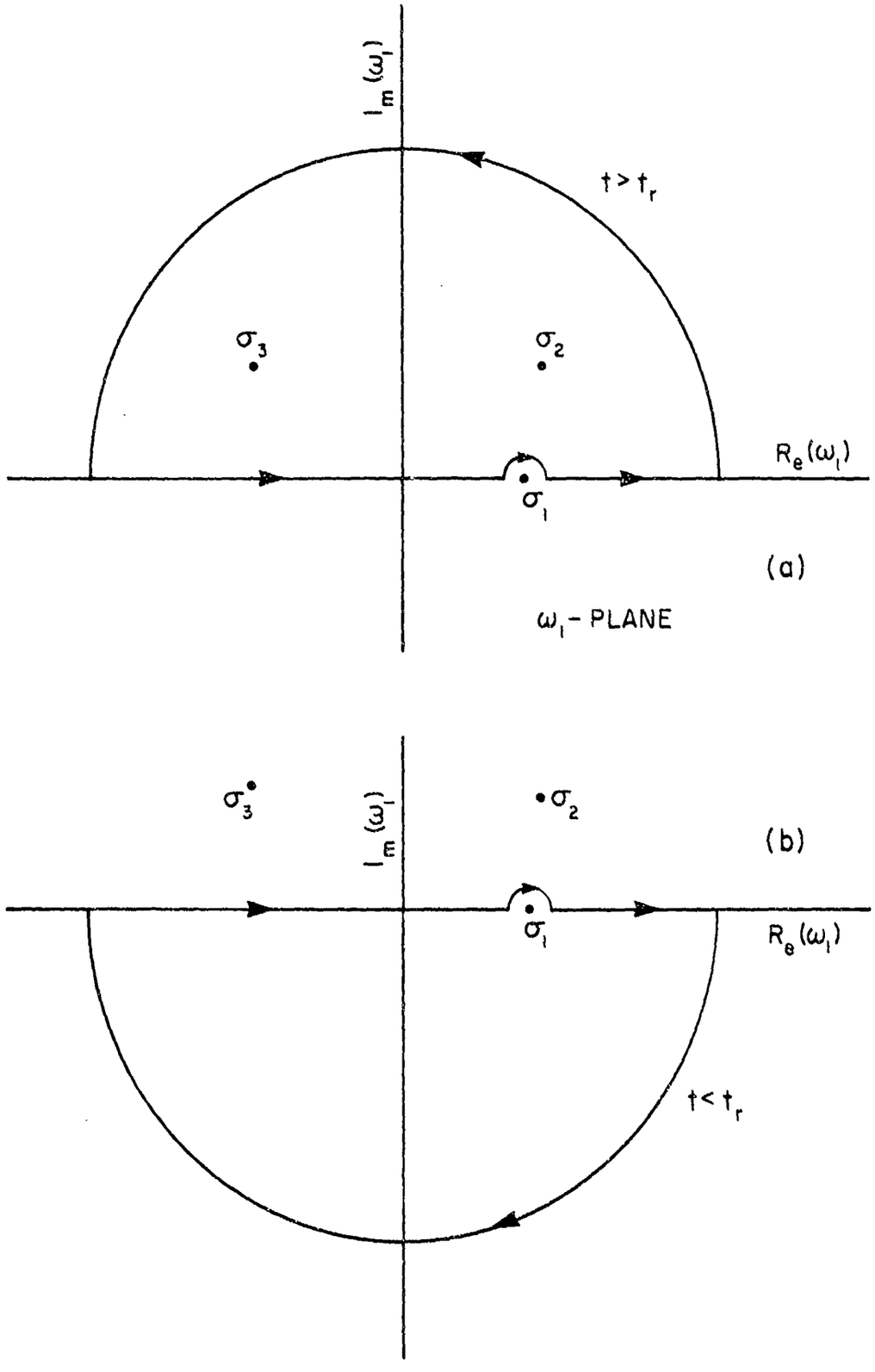

FIG. 4: CONTOUR INTEGRATION PATHS FOR $I_r(t,\omega)$

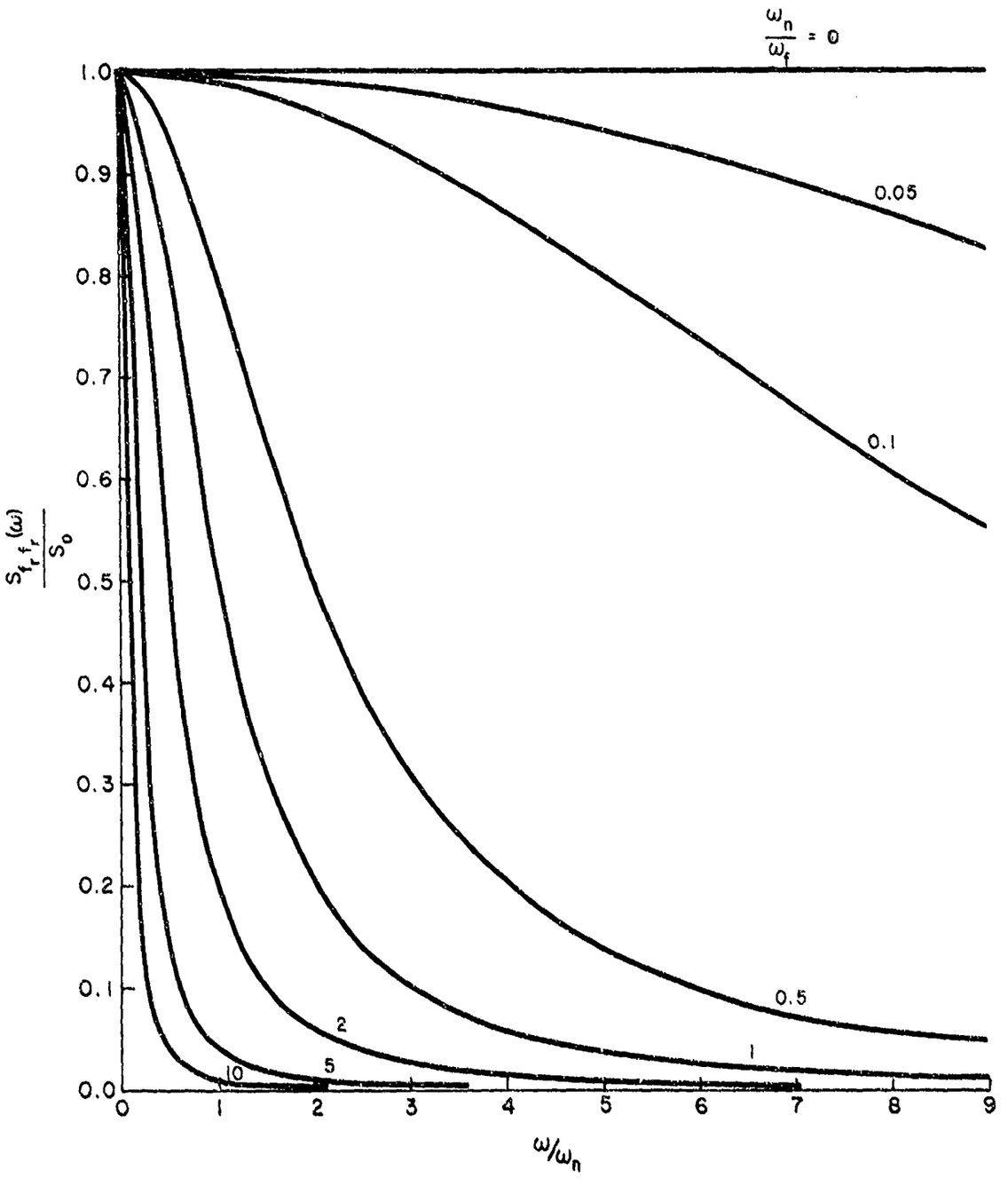

FIG. 5: NORMALIZED POWER SPECTRAL DENSITY

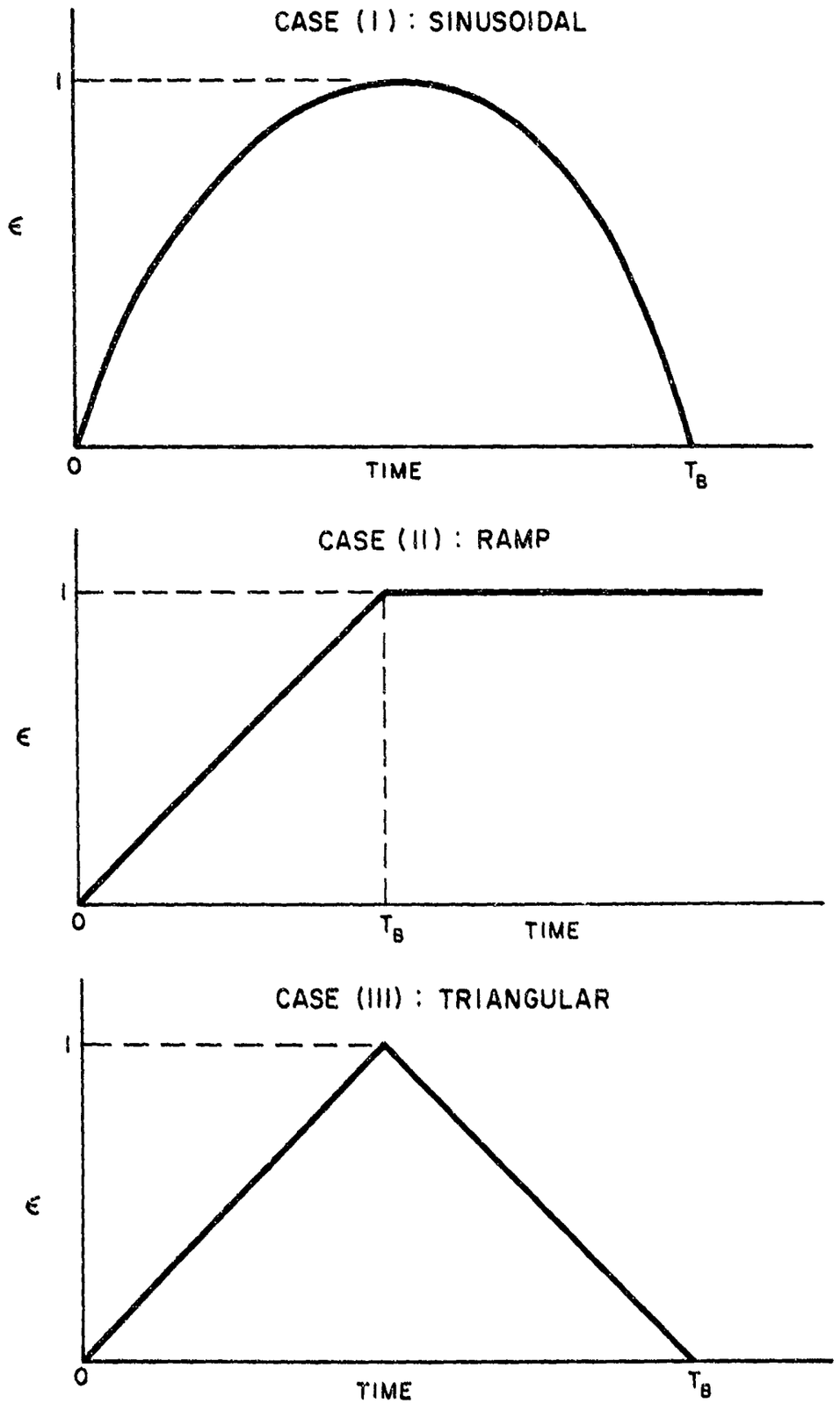

FIG. 6: ILLUSTRATION OF THE ε VERSUS TIME HISTORIES FOR THE THREE CASES STUDIED

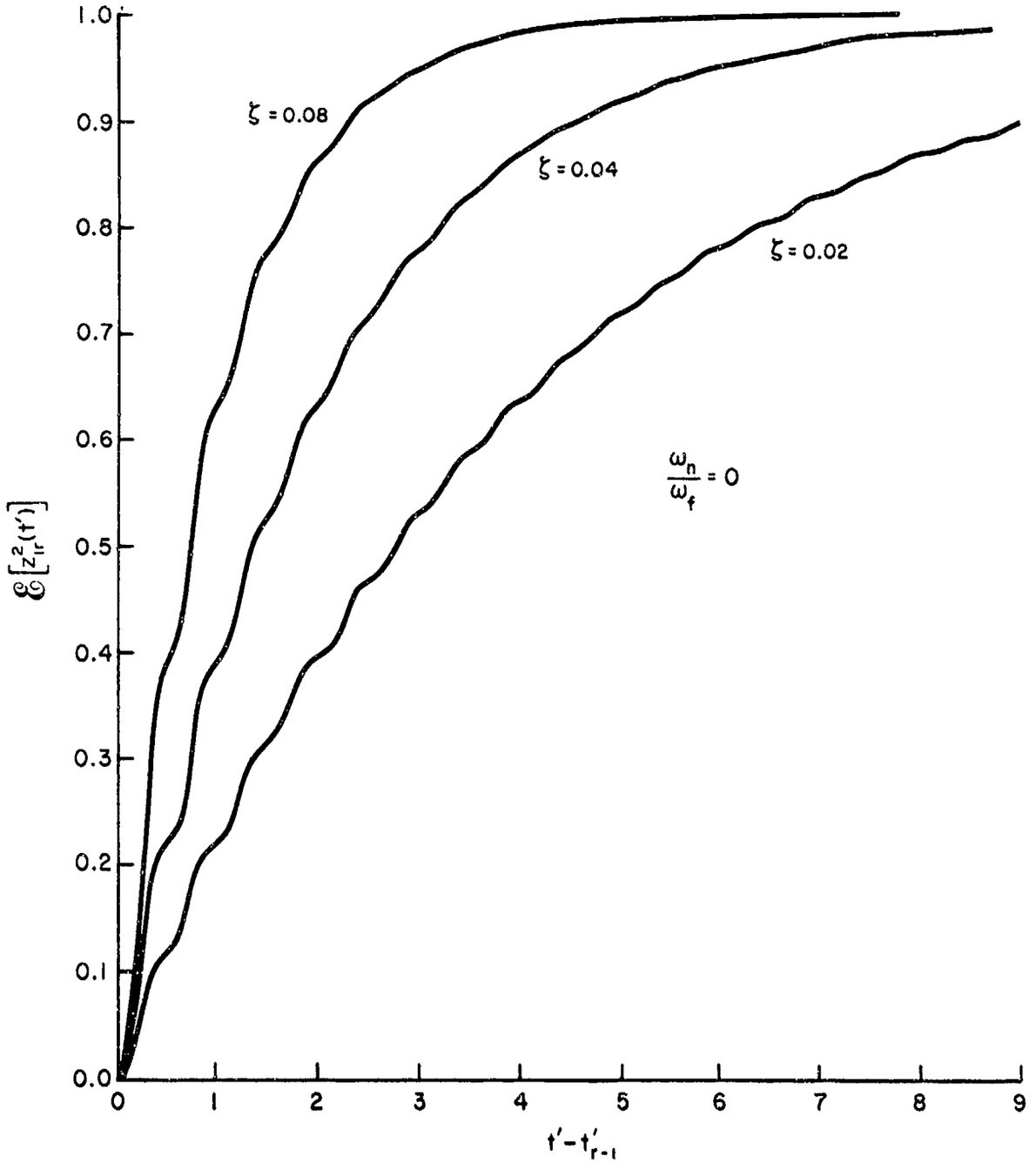

FIG. 7: RESPONSE TO A STEP MODULATED INPUT FOR $\omega_n/\omega_f = 0$

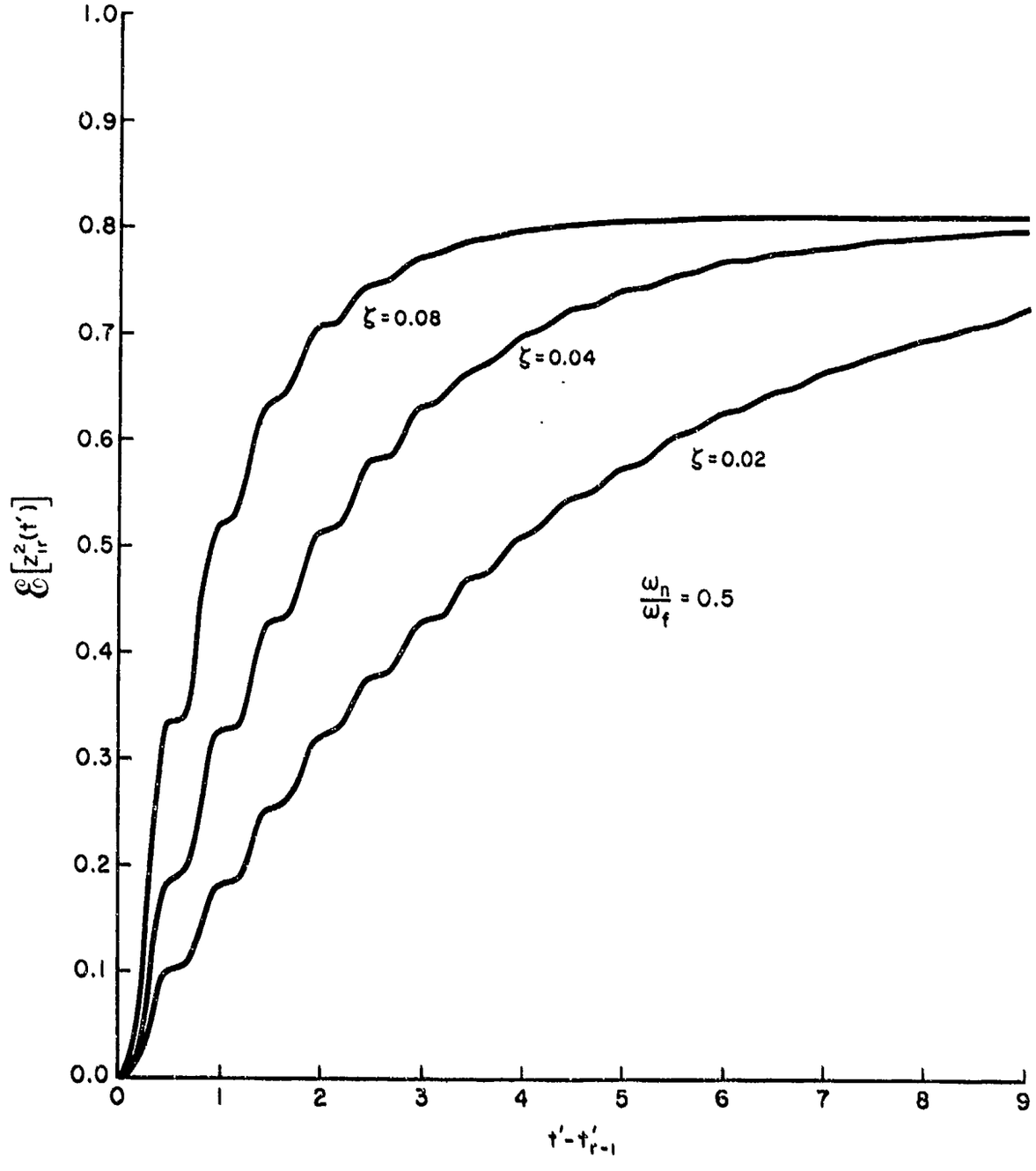

FIG. 8: RESPONSE TO A STEP MODULATED INPUT FOR $\omega_n/\omega_f = 0.5$

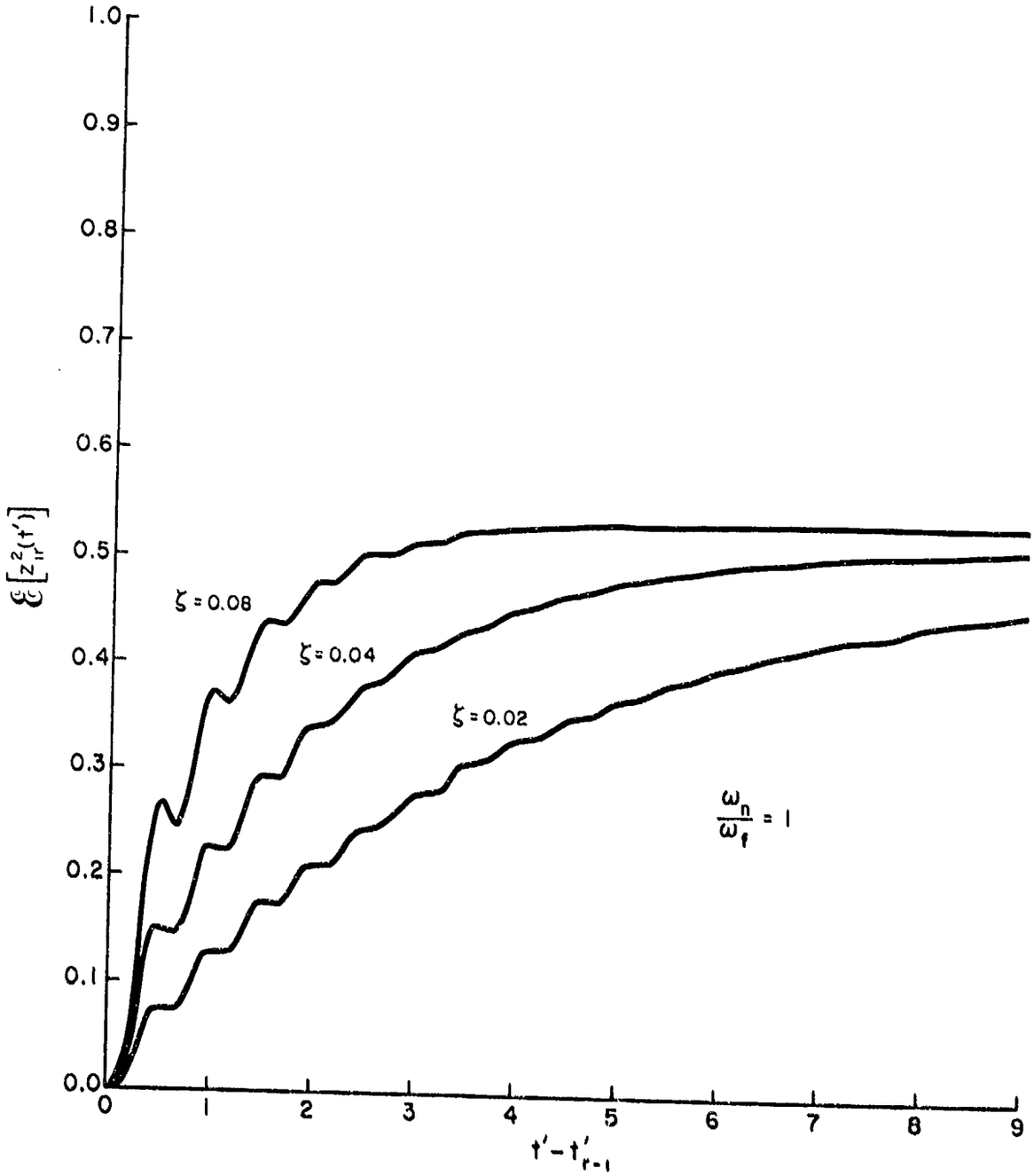

FIG. 9: RESPONSE TO A STEP MODULATED INPUT FOR $\omega_n/\omega_f = 1$

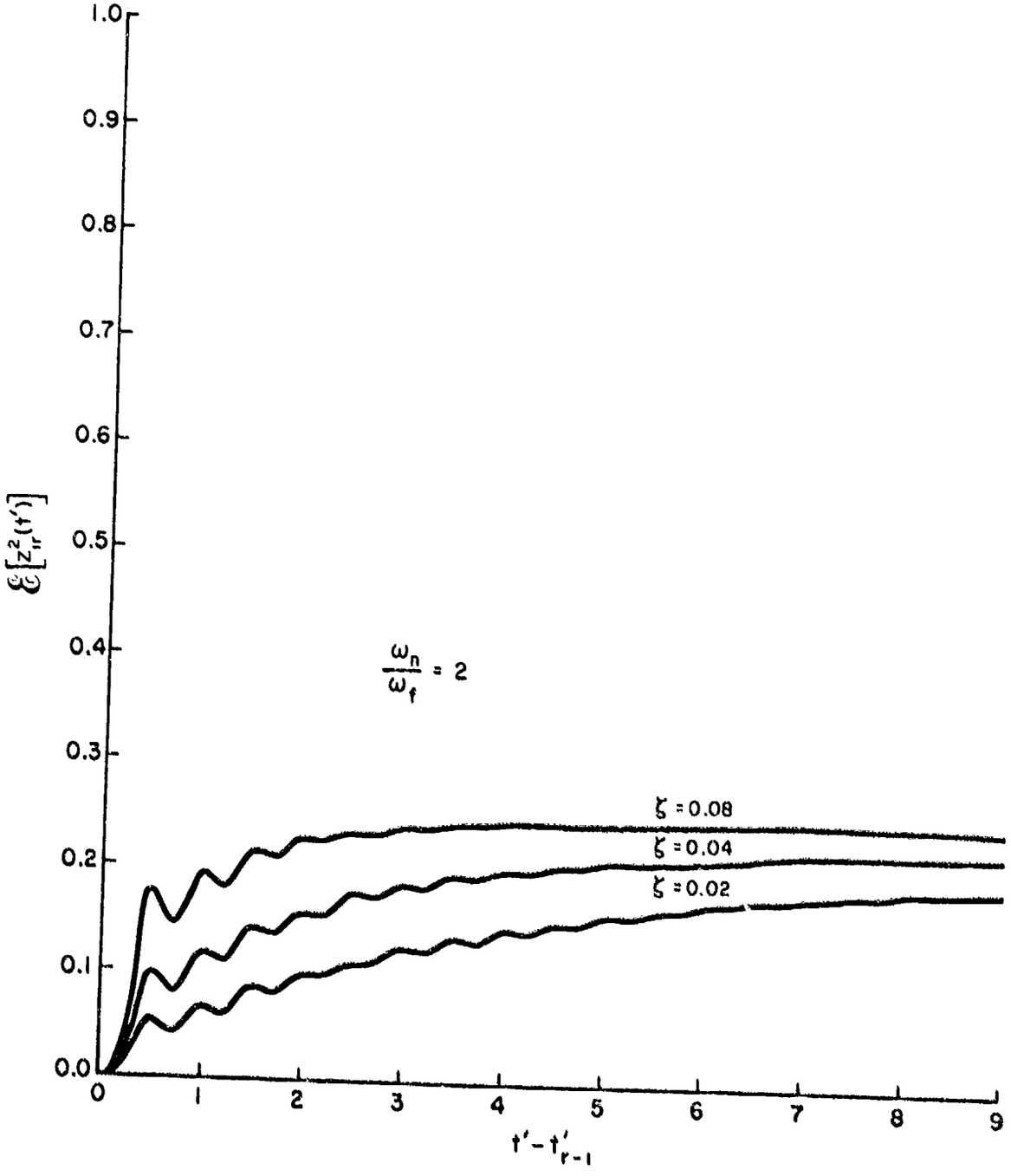

FIG. 10: RESPONSE TO A STEP MODULATED INPUT FOR $\omega_n/\omega_f = 2$

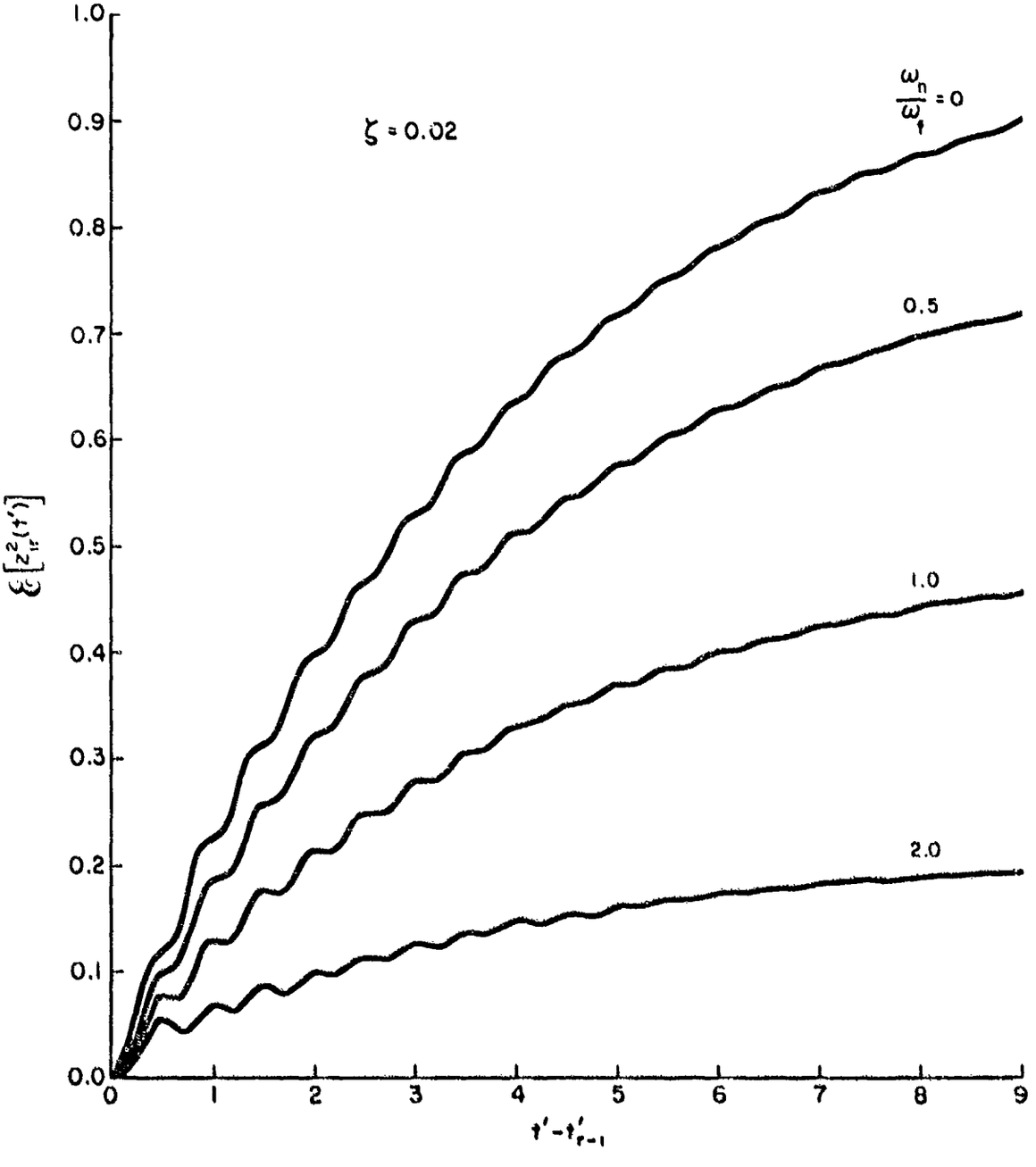

FIG. 11: RESPONSE TO A STEP MODULATED INPUT FOR $\zeta = 0.02$

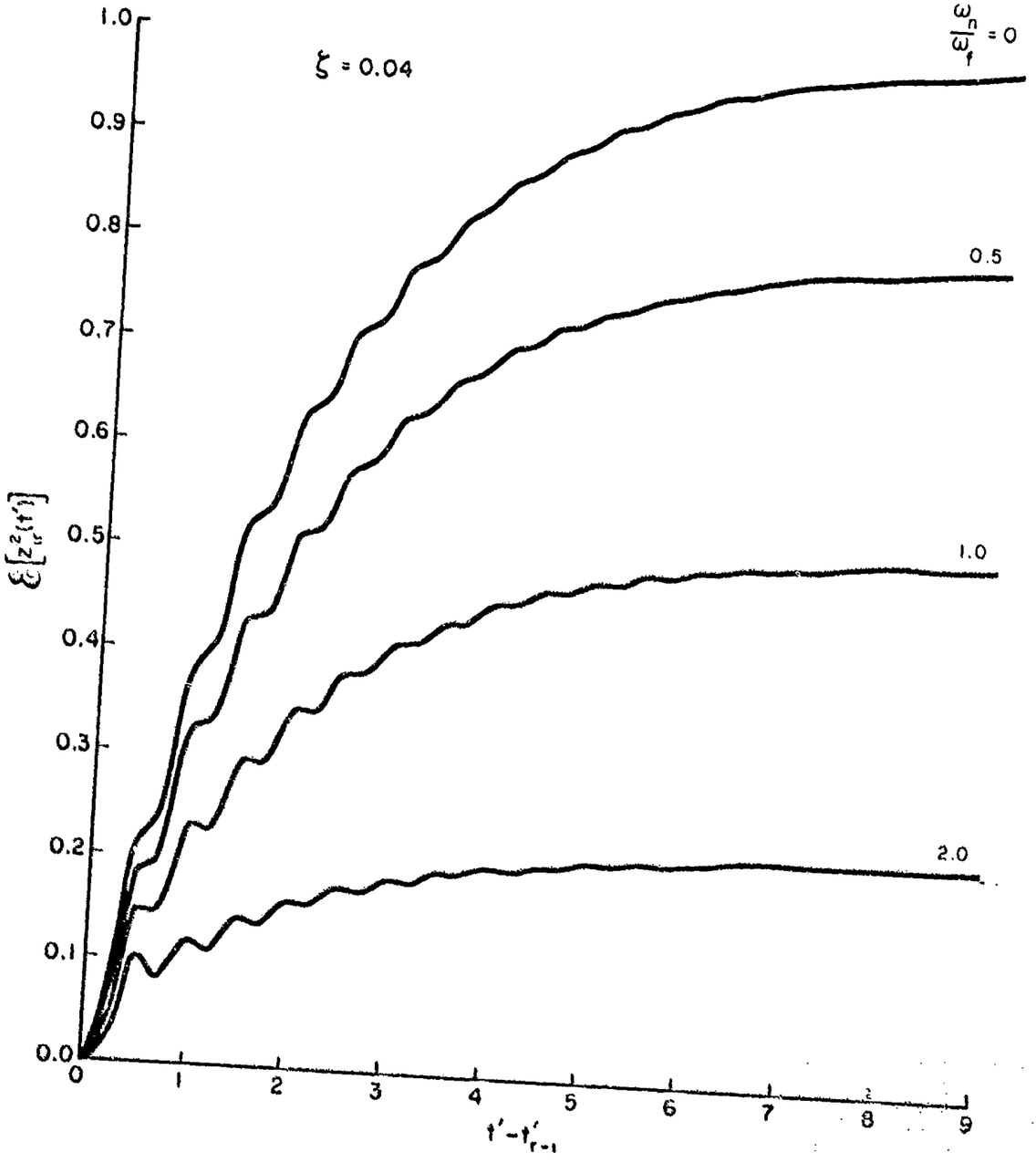

FIG. 12: RESPONSE TO A STEP MODULATED INPUT FOR ζ = 0.04

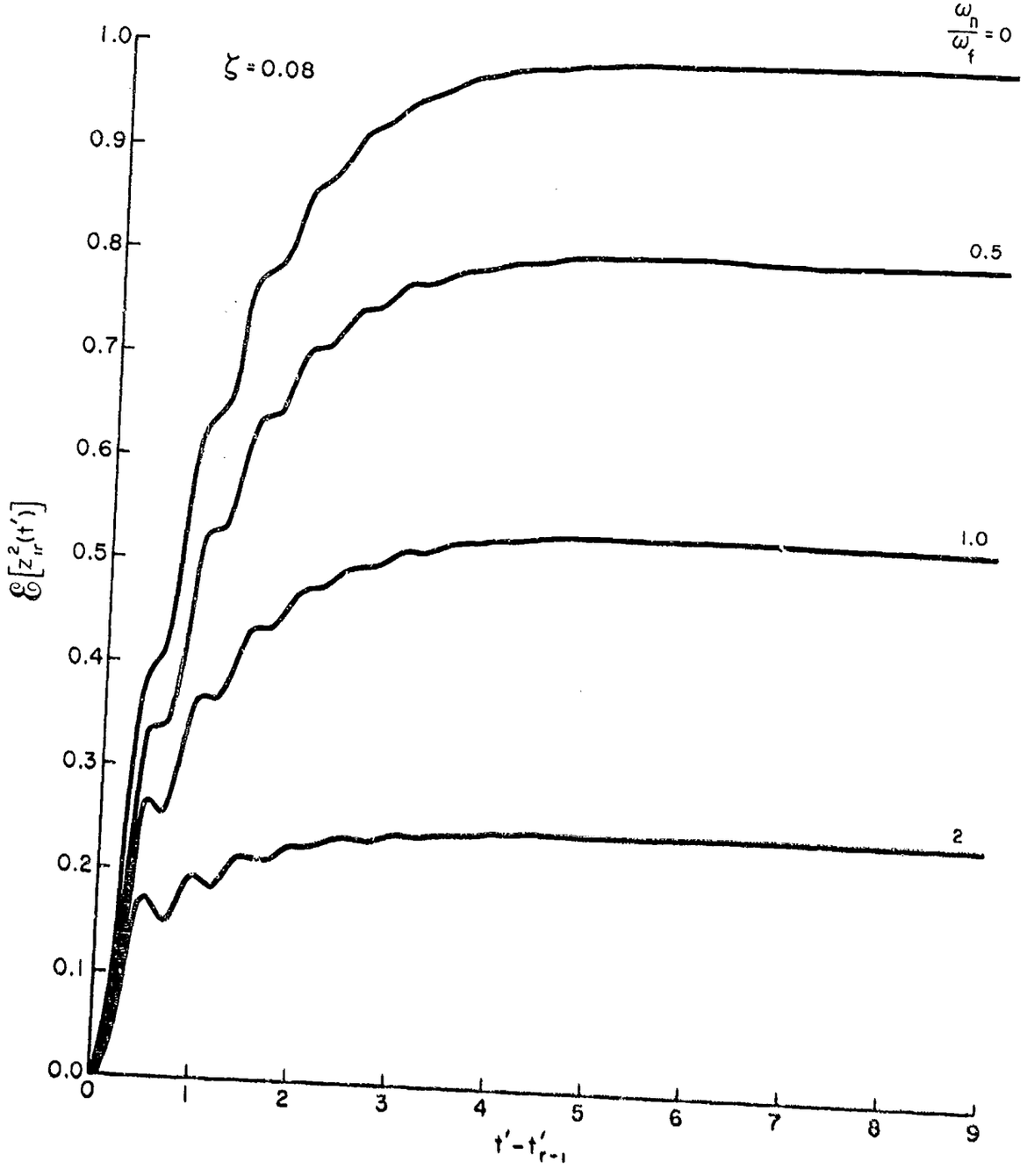

FIG. 13: RESPONSE TO A STEP MODULATED INPUT FOR $\zeta = 0.08$

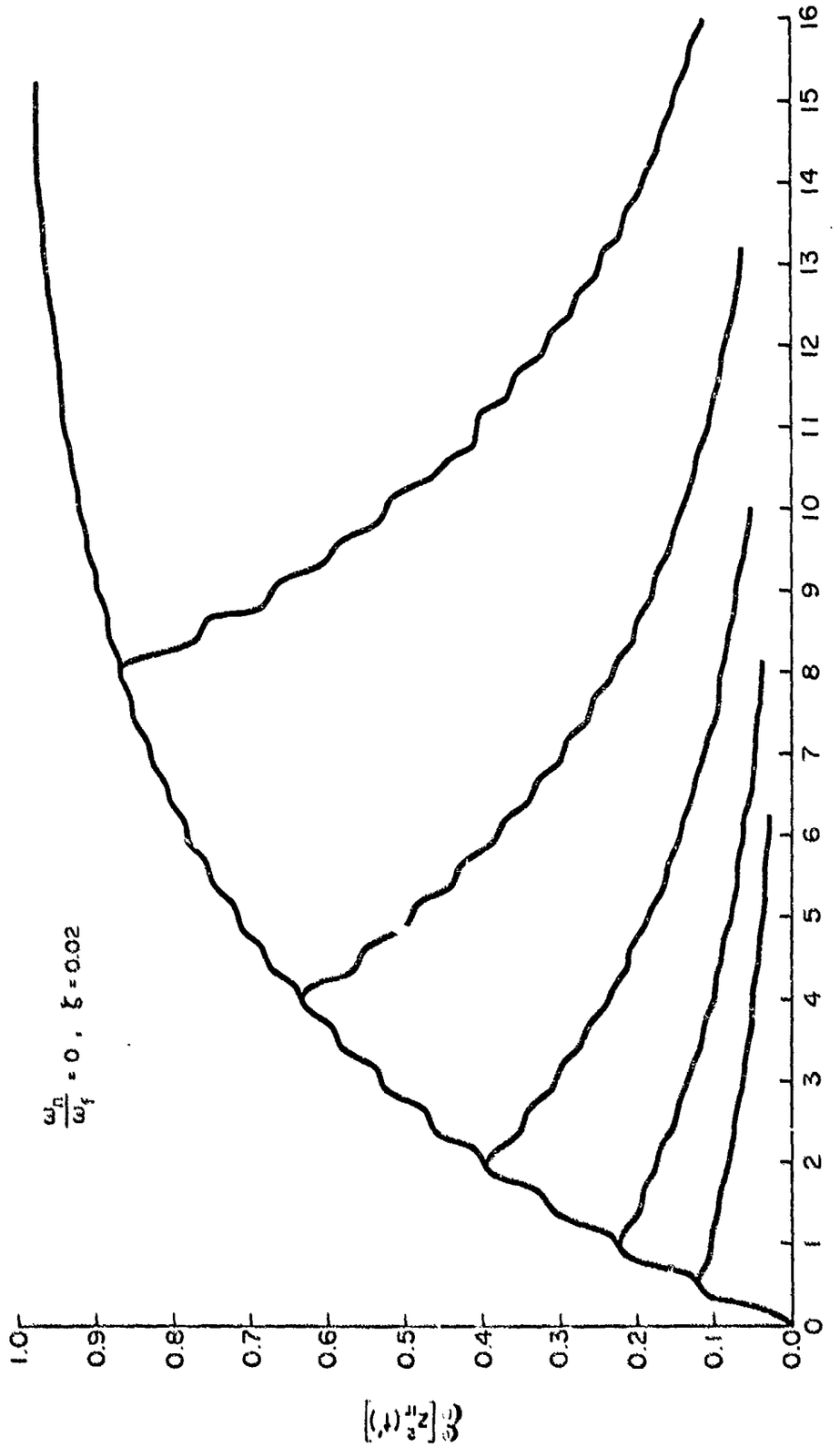

FIG. 14: DECAY TO A PULSE MODULATED INPUT FOR $\omega_n/\omega_f = 0$, $\zeta = 0.02$

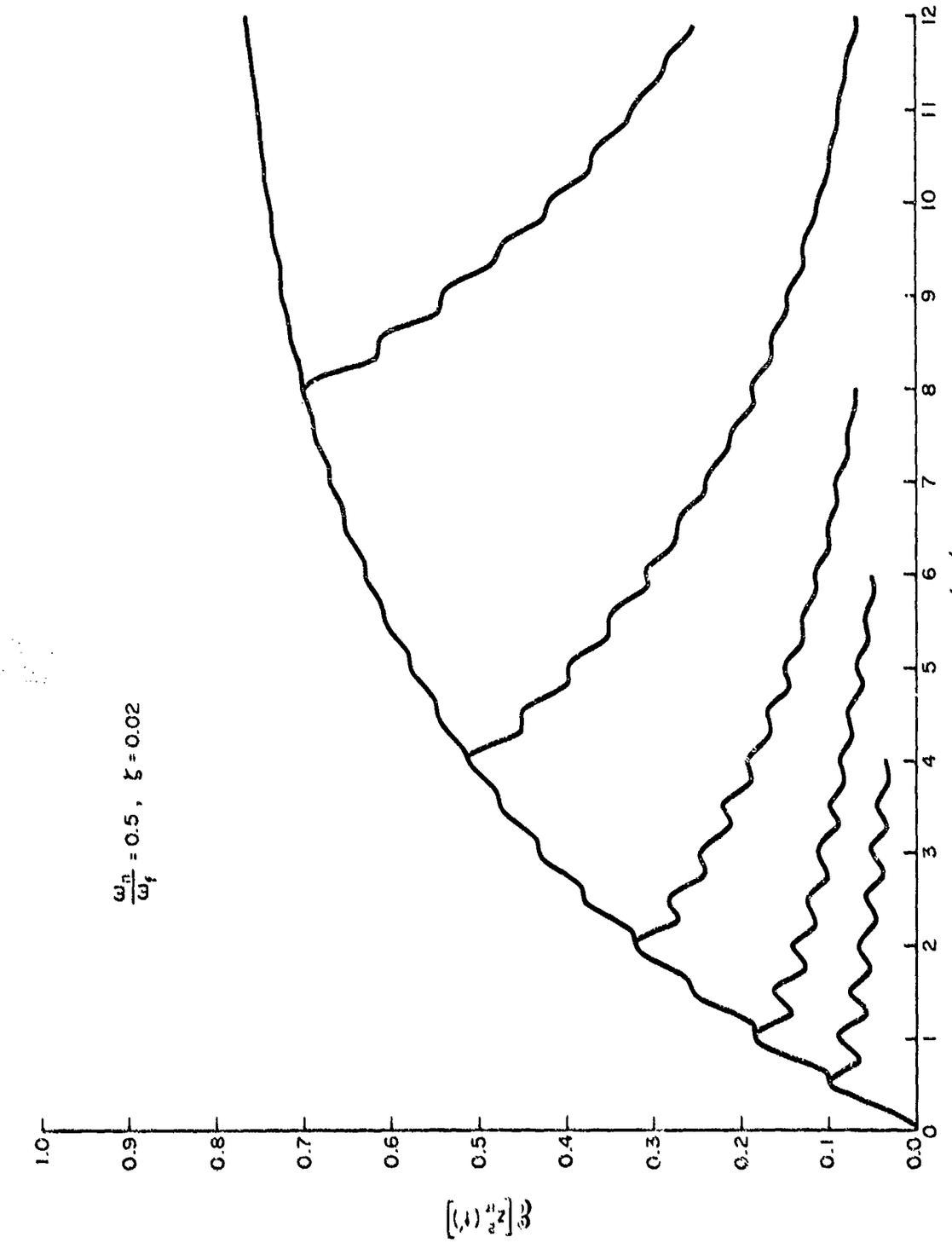

FIG. 15: DECAY TO A PULSE MODULATED INPUT FOR $\omega_n/\omega_f = 0.5$, $\zeta = 0.02$

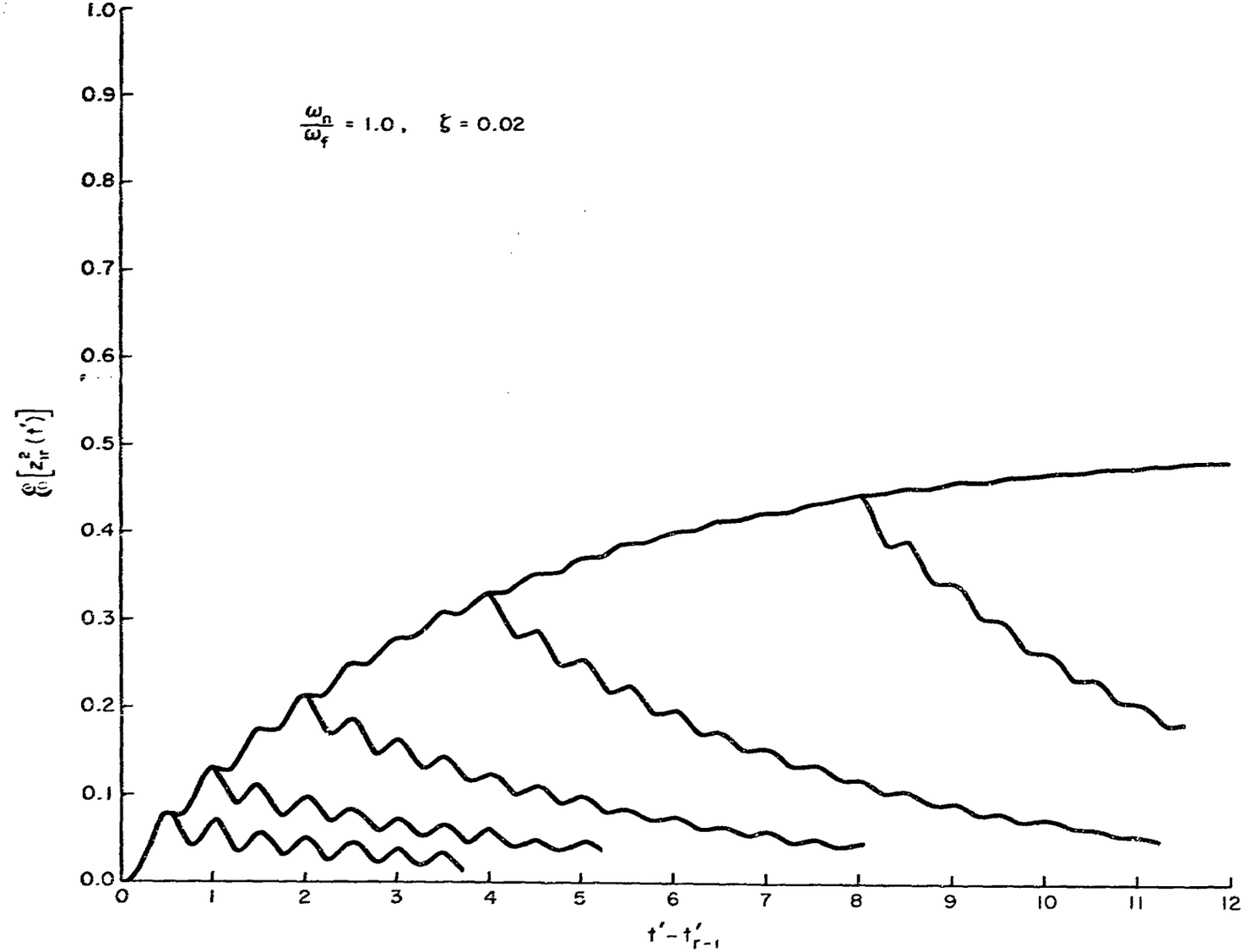

FIG. 16: DECAY TO A PULSE MODULATED INPUT FOR $\omega_n/\omega_f = 1$, $\zeta = 0.02$

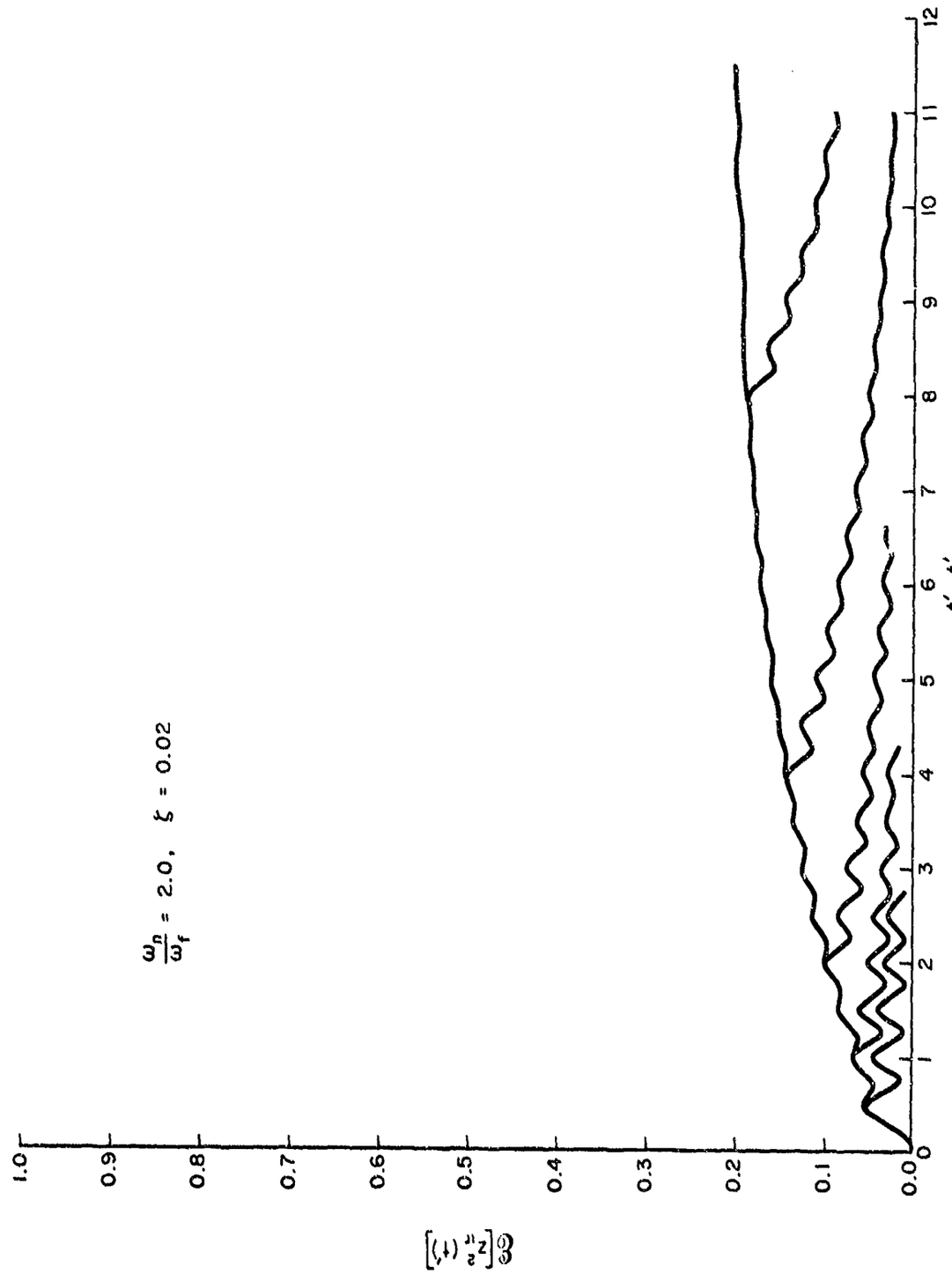

FIG. 17: DECAY TO A PULSE MODULATED INPUT FOR $\omega_n/\omega_f = 2$, $\zeta = 0.02$

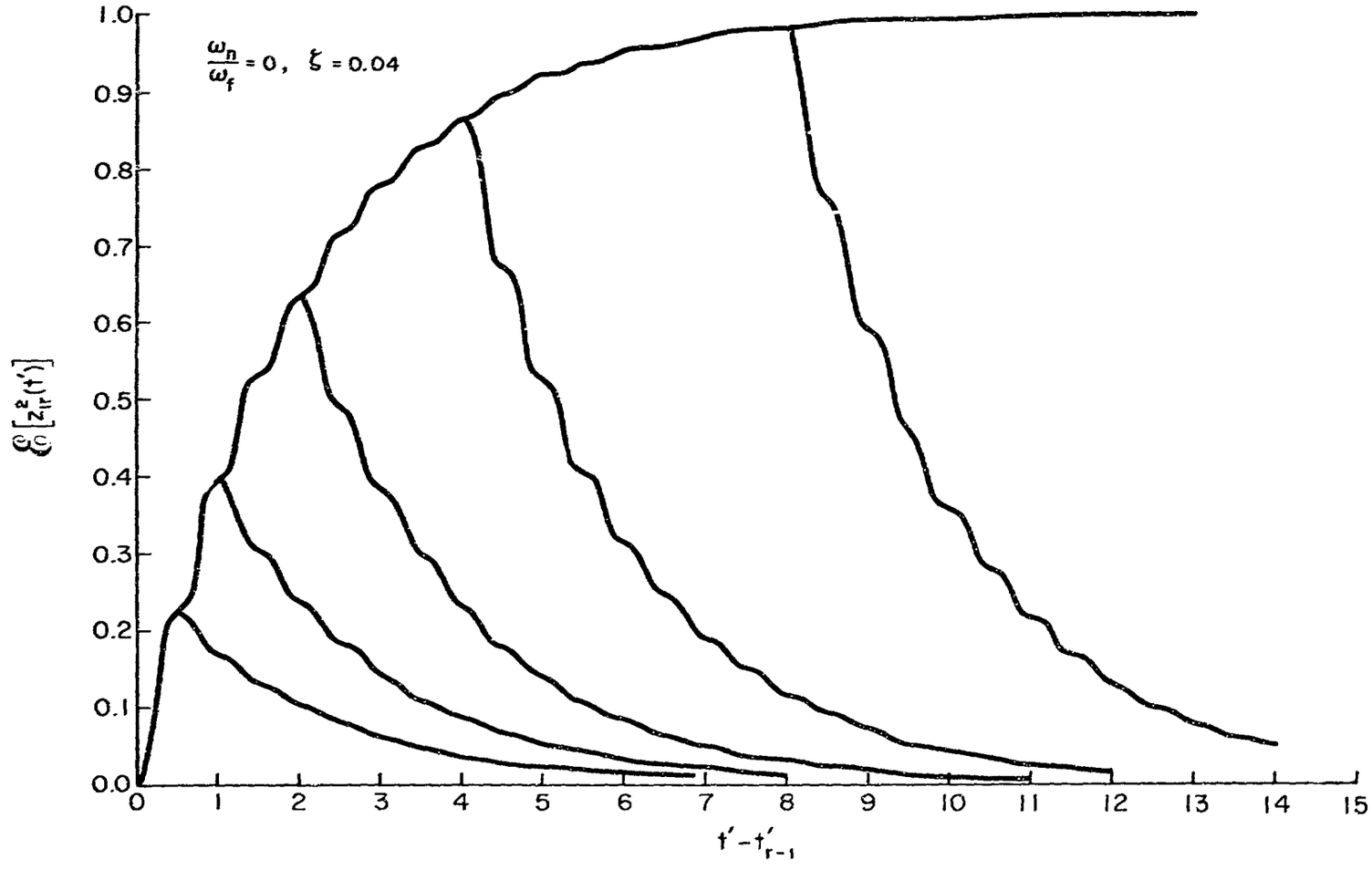

FIG. 18: DECAY TO A PULSE MODULATED INPUT FOR $\omega_n/\omega_f = 0, \ \zeta = 0.04$

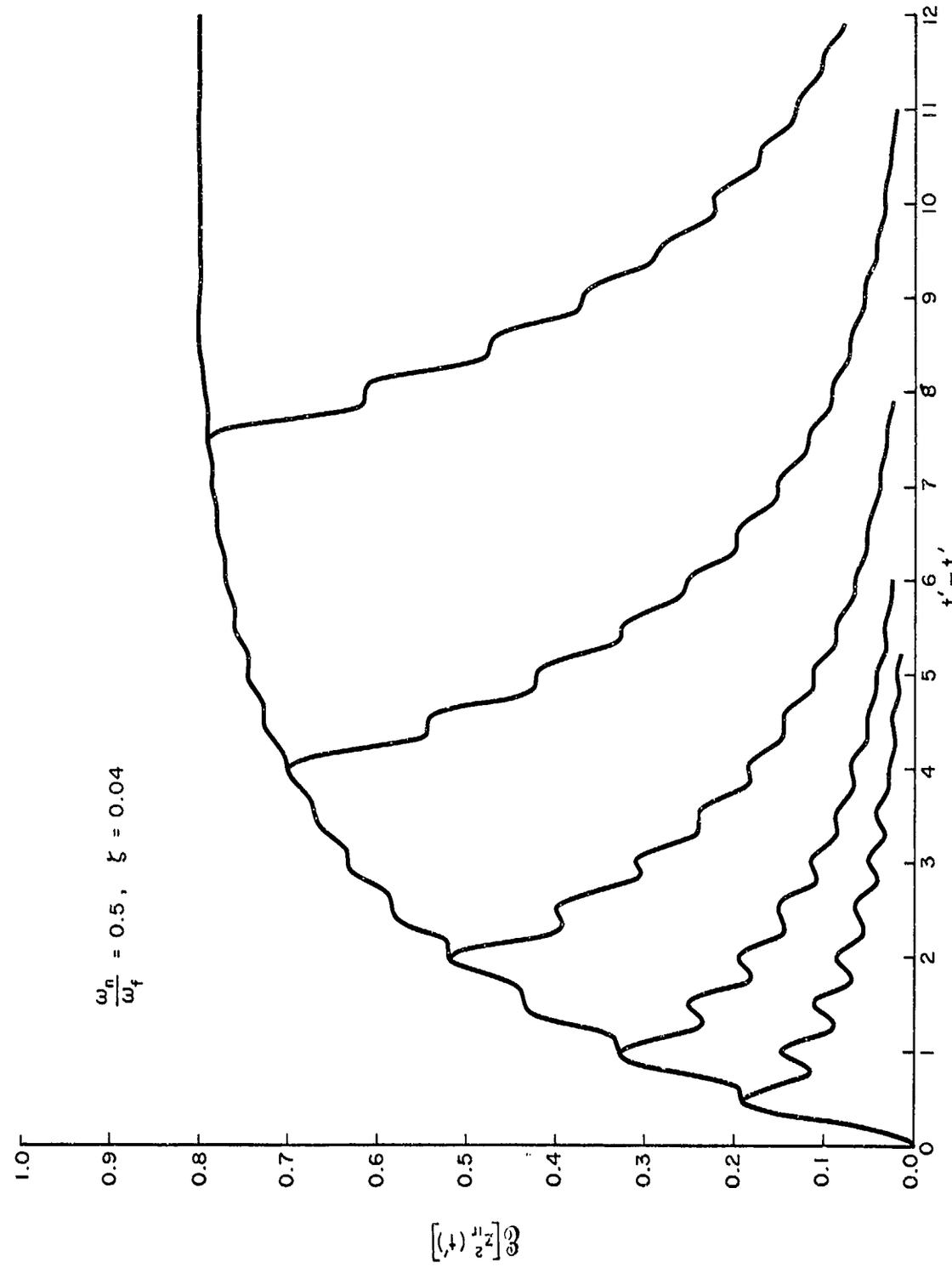

FIG. 19: DECAY TO A PULSE MODULATED INPUT FOR $\omega_n/\omega_f = 0.5$, $\zeta = 0.04$

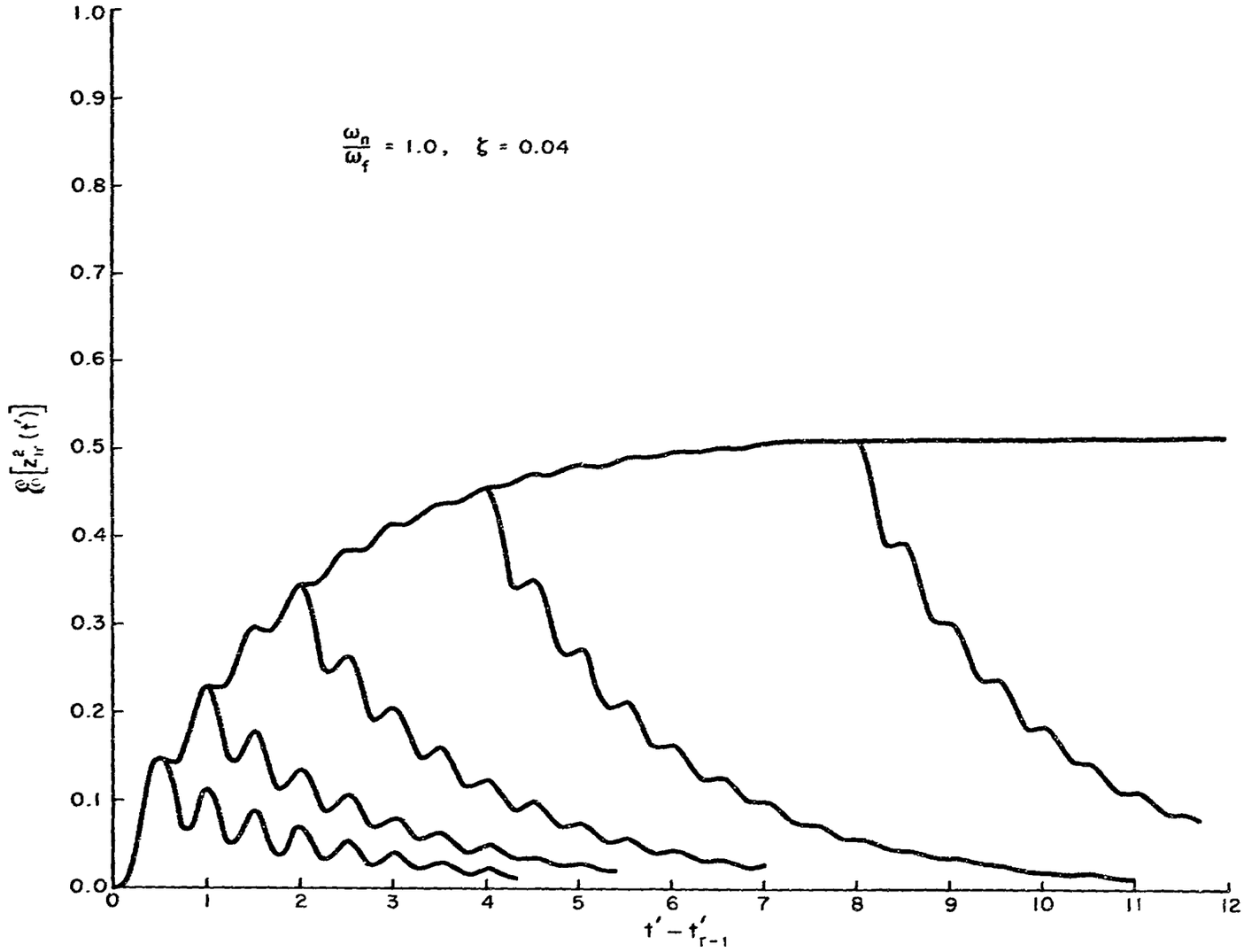

FIG. 20: DECAY TO A PULSE MODULATED INPUT FOR ω_n/ω_f = 1, ζ = 0.04

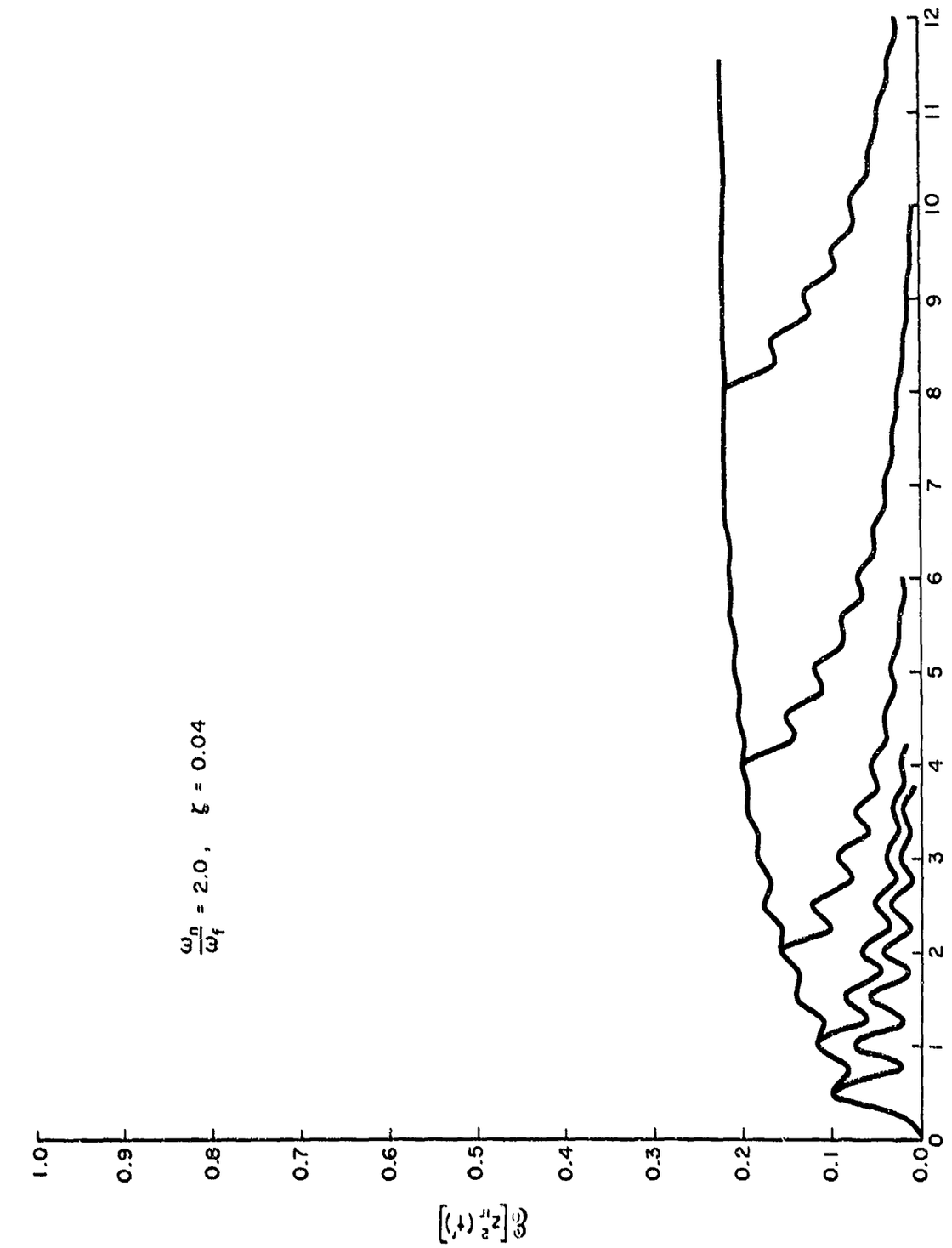

FIG. 21: DECAY TO A PULSE MODULATED INPUT FOR $\omega_n/\omega_f = 2$, $\zeta = 0.04$

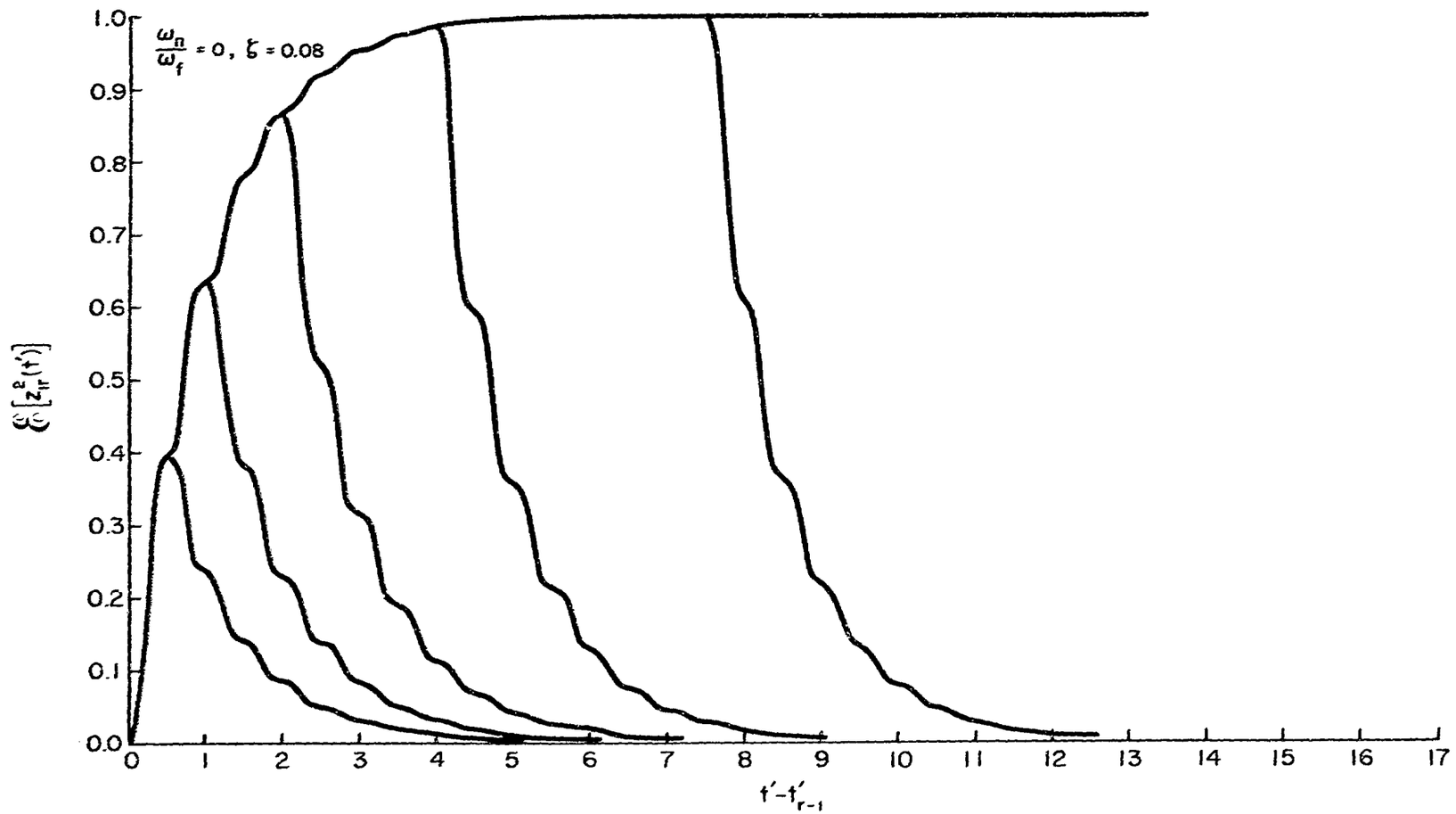

FIG. 22: DECAY TO A PULSE MODULATED INPUT FOR $\omega_n/\omega_f = 0,\ \zeta = 0.08$

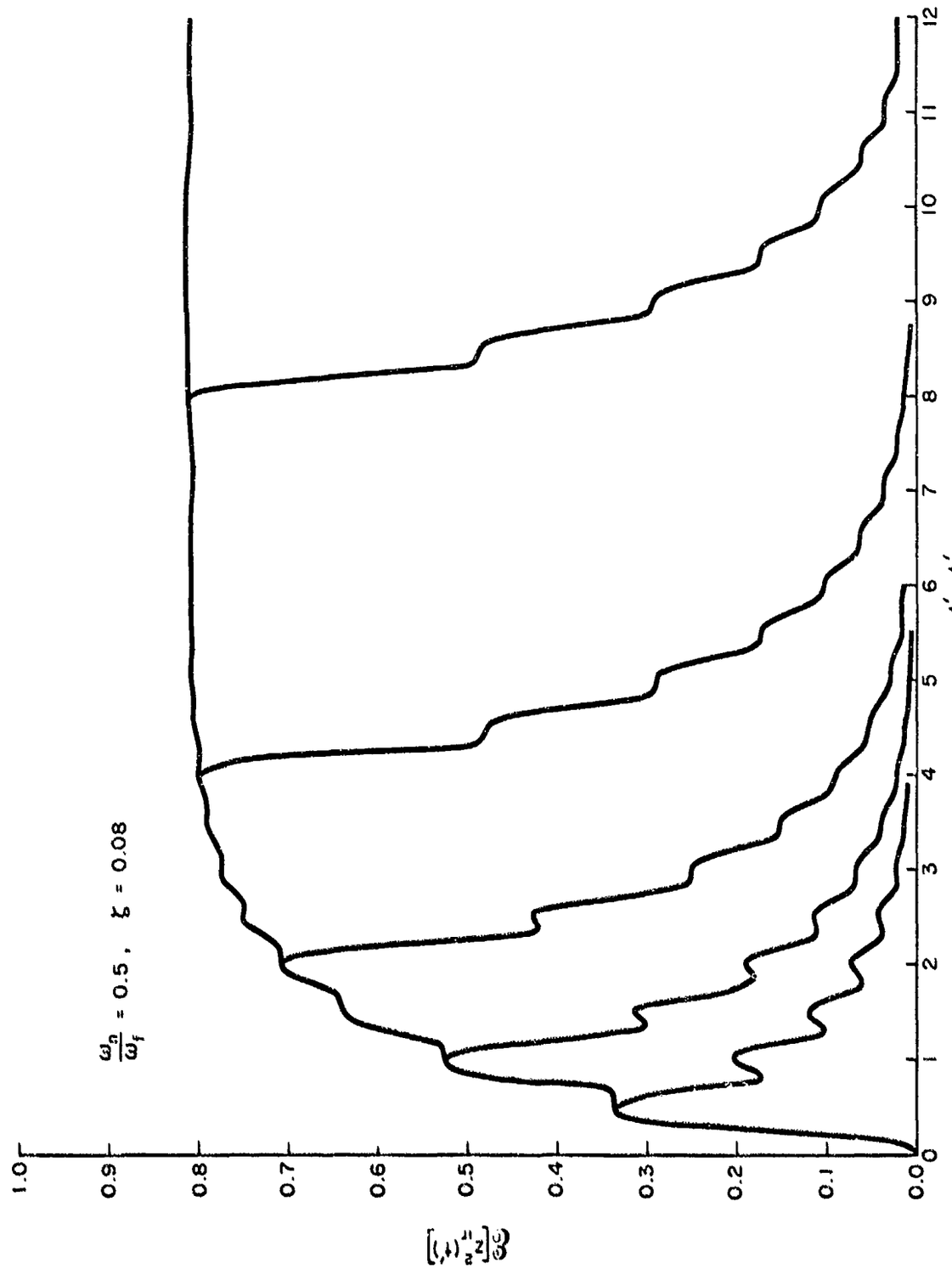

FIG. 23: DECAY TO A PULSE MODULATED INPUT FOR $\omega_n/\omega_f = 0.5$, $\zeta = 0.08$

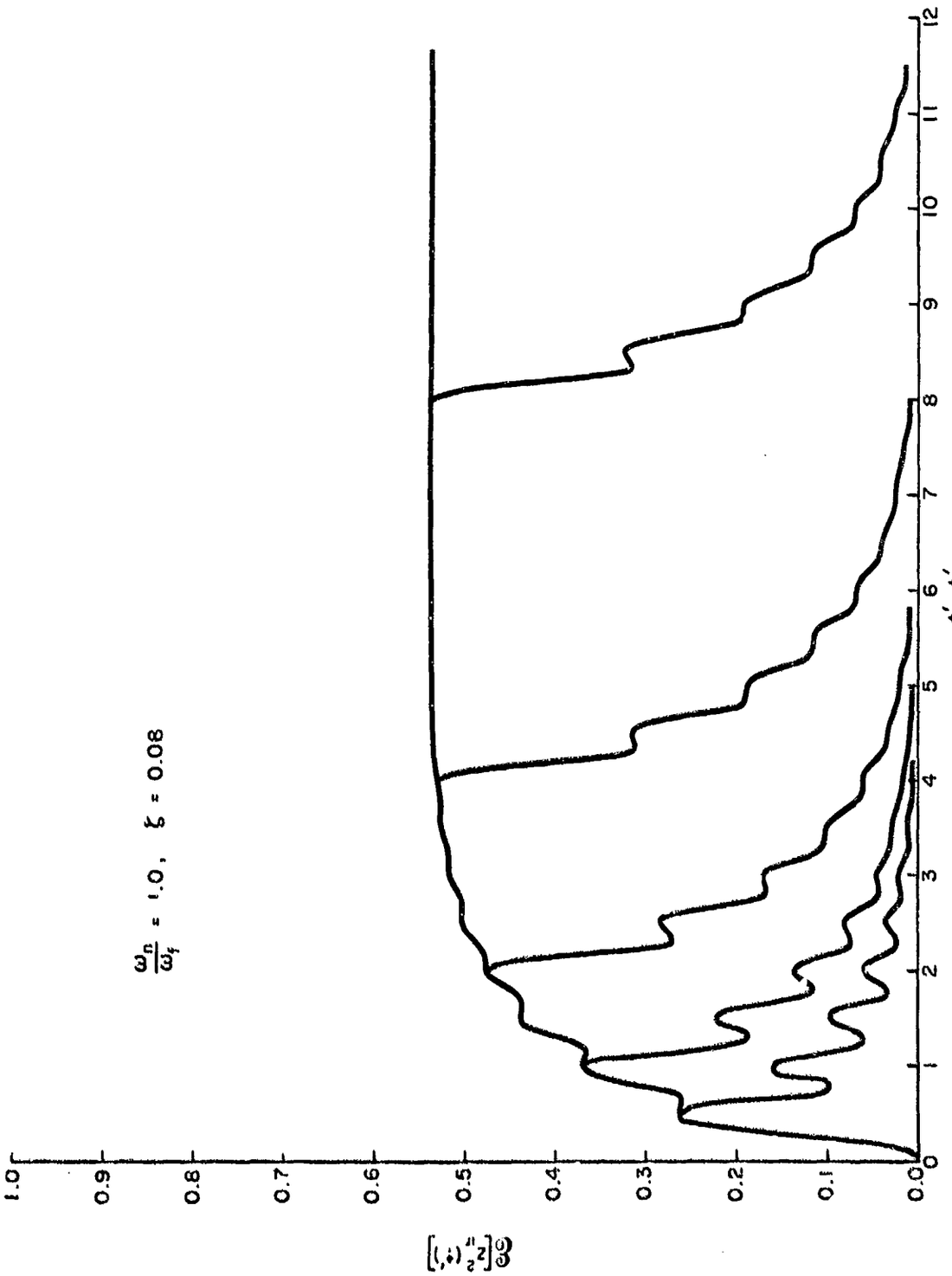

FIG. 24: DECAY TO A PULSE MODULATED INPUT FOR $\omega_n/\omega_f = 1$, $\zeta = 0.08$

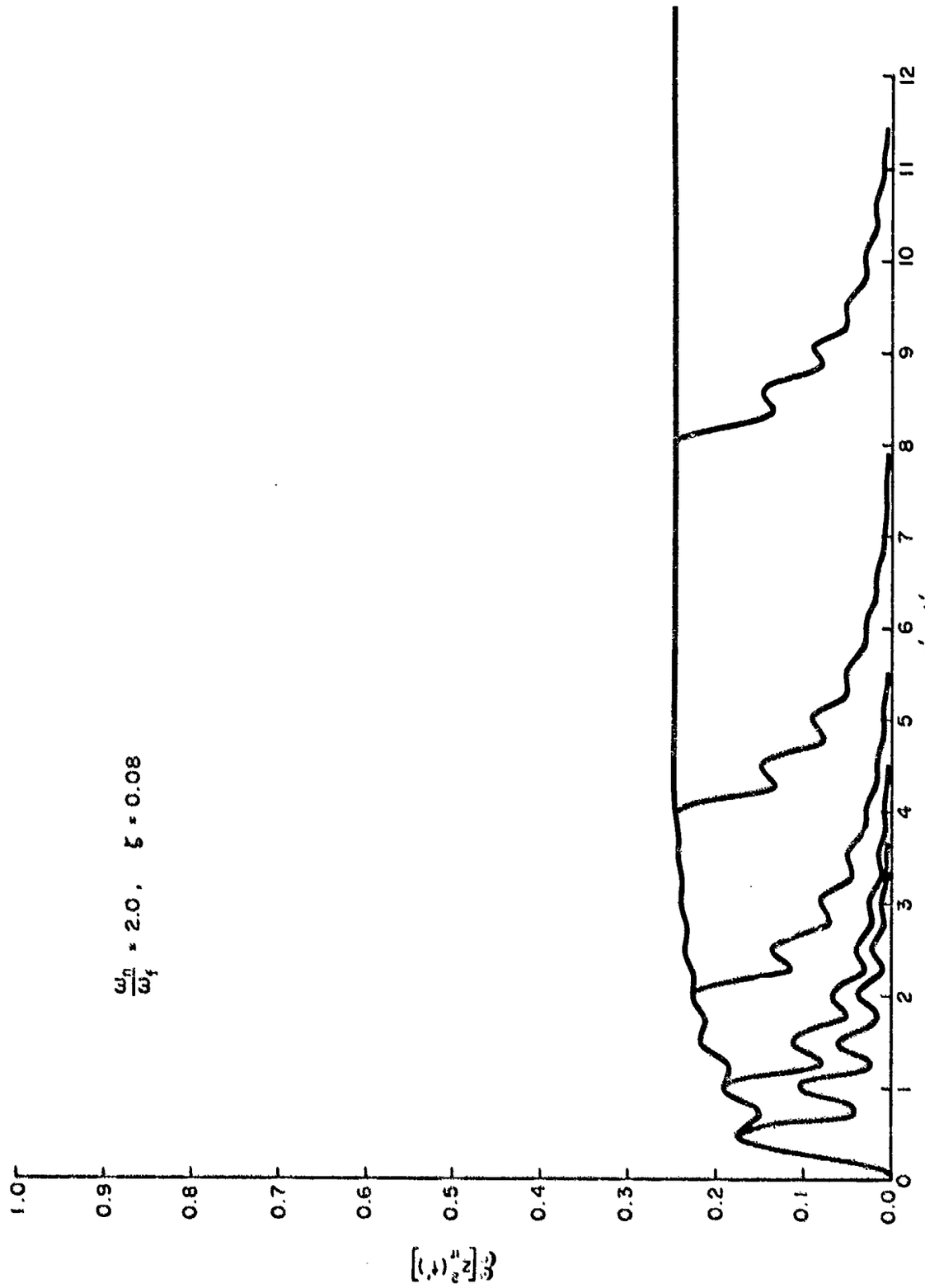

FIG. 25: DECAY TO A PULSE MODULATED INPUT FOR $\omega_n/\omega_f = 2$, $\zeta = 0.08$

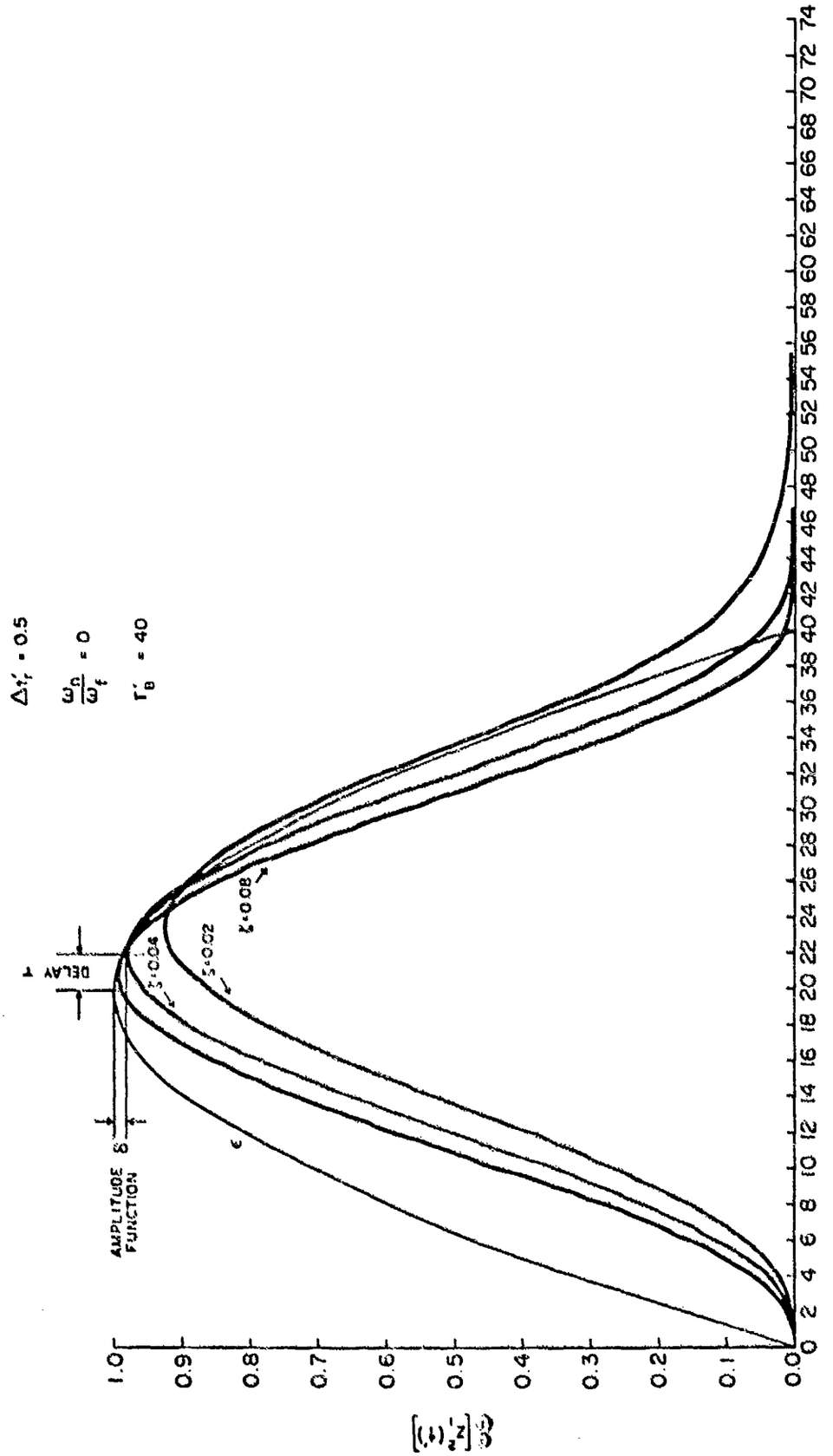

FIG. 26: MEAN SQUARE RESPONSE FOR CASE I: $T_B' = 40$, $\omega_n/\omega_f = 0$

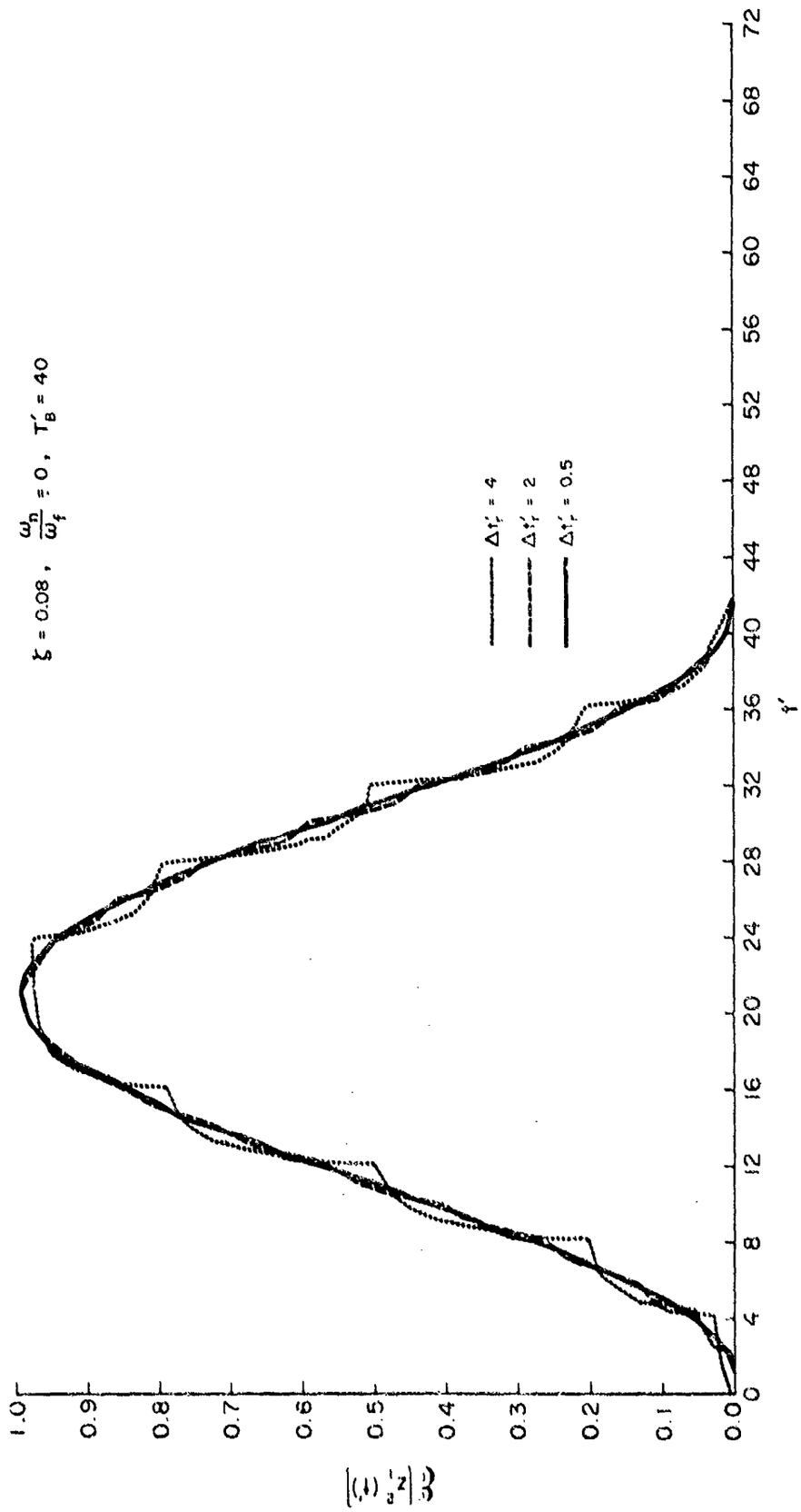

FIG. 27: EFFECT OF $\Delta t'_f$ ON MEAN SQUARE RESPONSE FOR CASE I

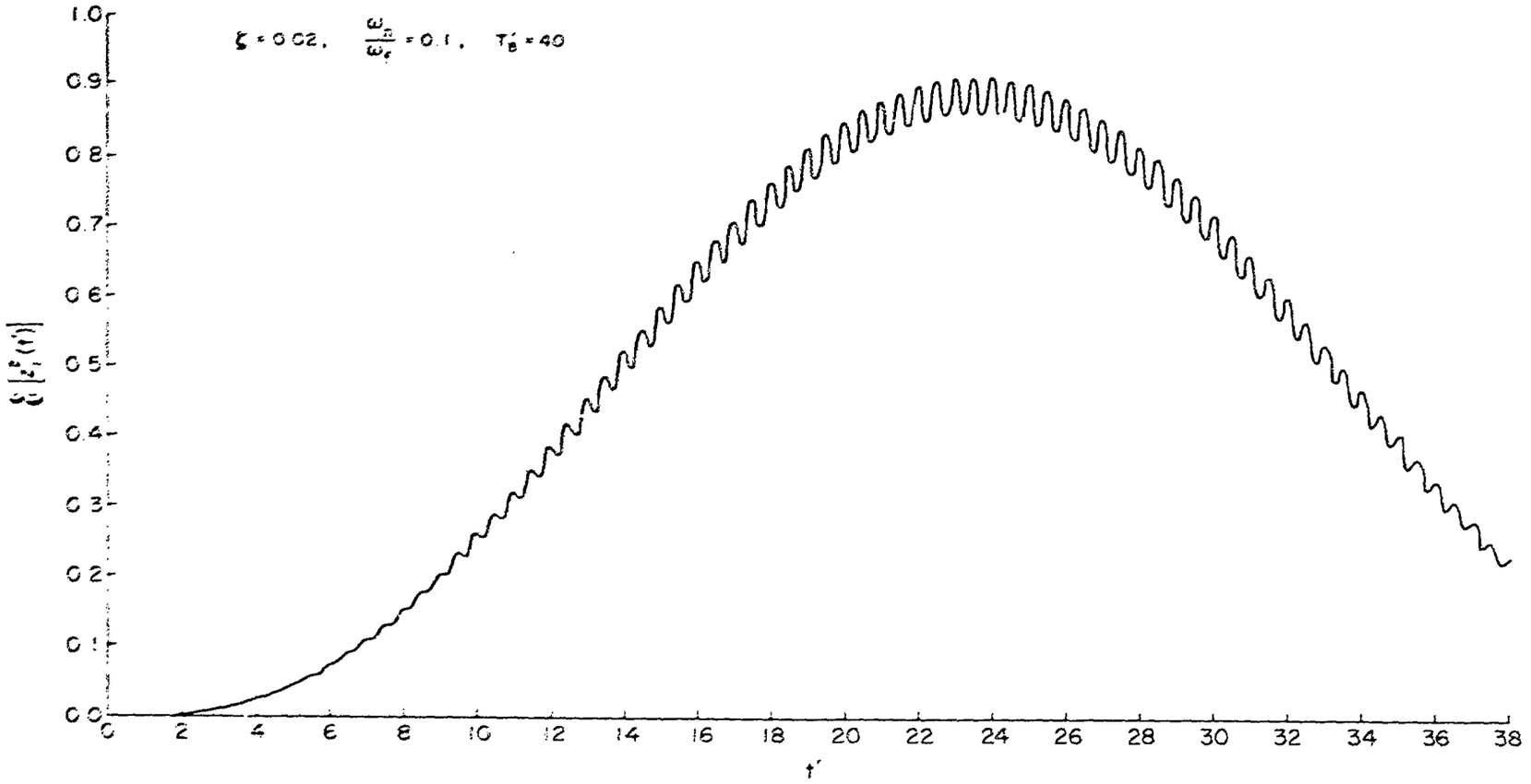

FIG. 28: MEAN SQUARE RESPONSE FOR CASE I: $\zeta = 0.02$, $T'_B = 40$, $\omega_n/\omega_f = 0.1$

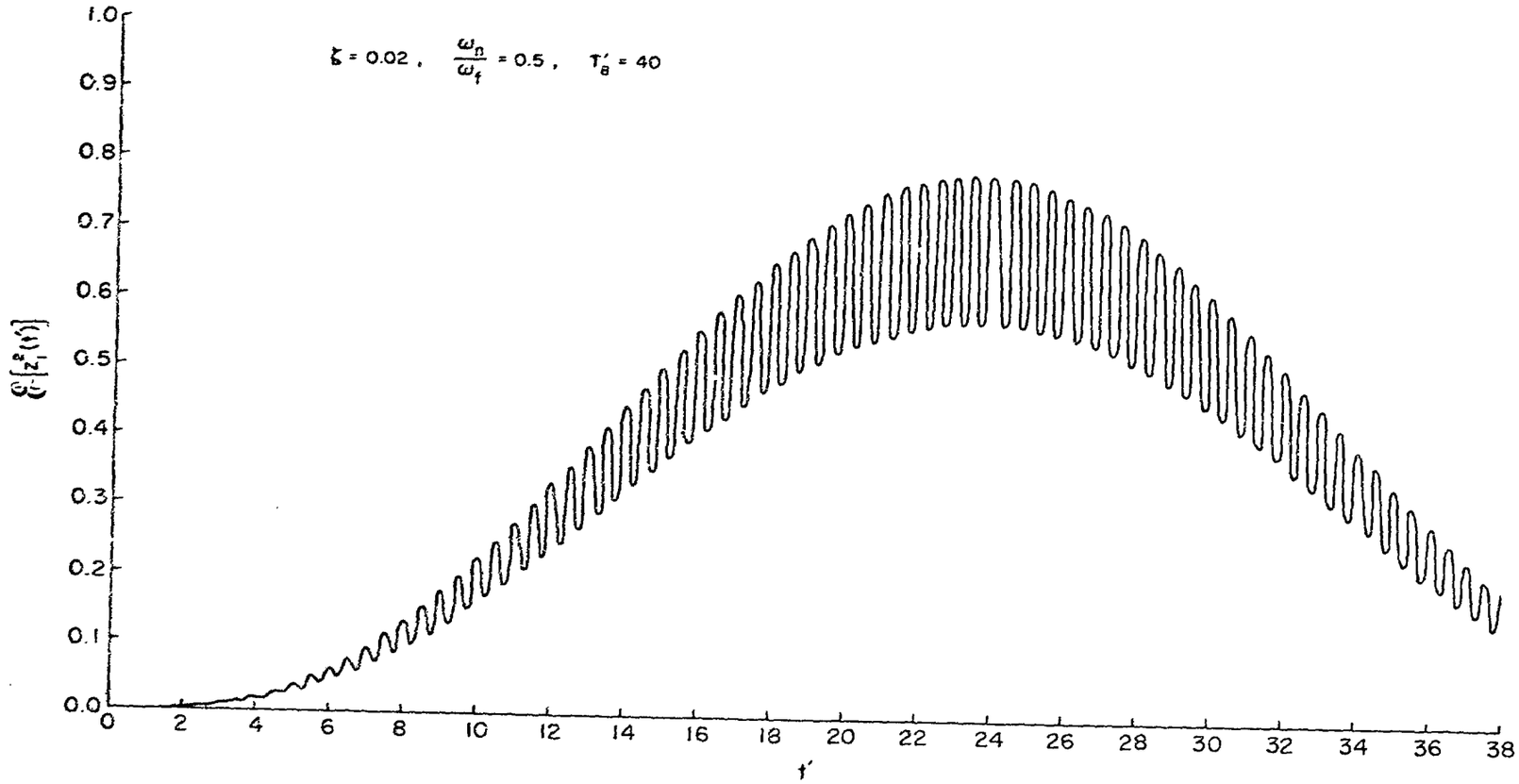

FIG. 29: MEAN SQUARE RESPONSE FOR CASE I: $\zeta = 0.02$, $T_B' = 40$, $\omega_n/\omega_f = 0.5$

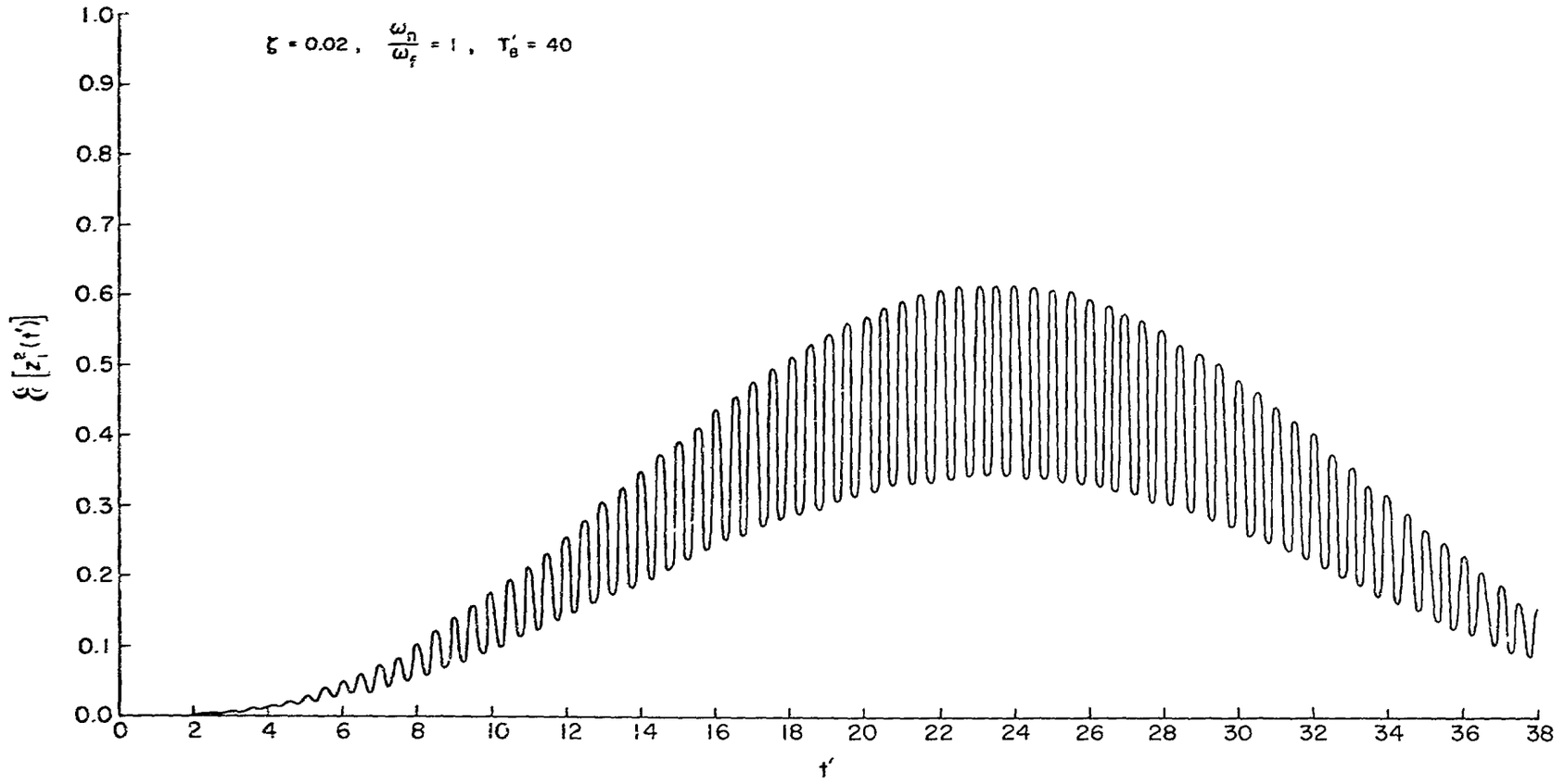

FIG. 30: MEAN SQUARE RESPONSE FOR CASE I: $\zeta = 0.02$, $T'_B = 40$, $\omega_n/\omega_f = 1$

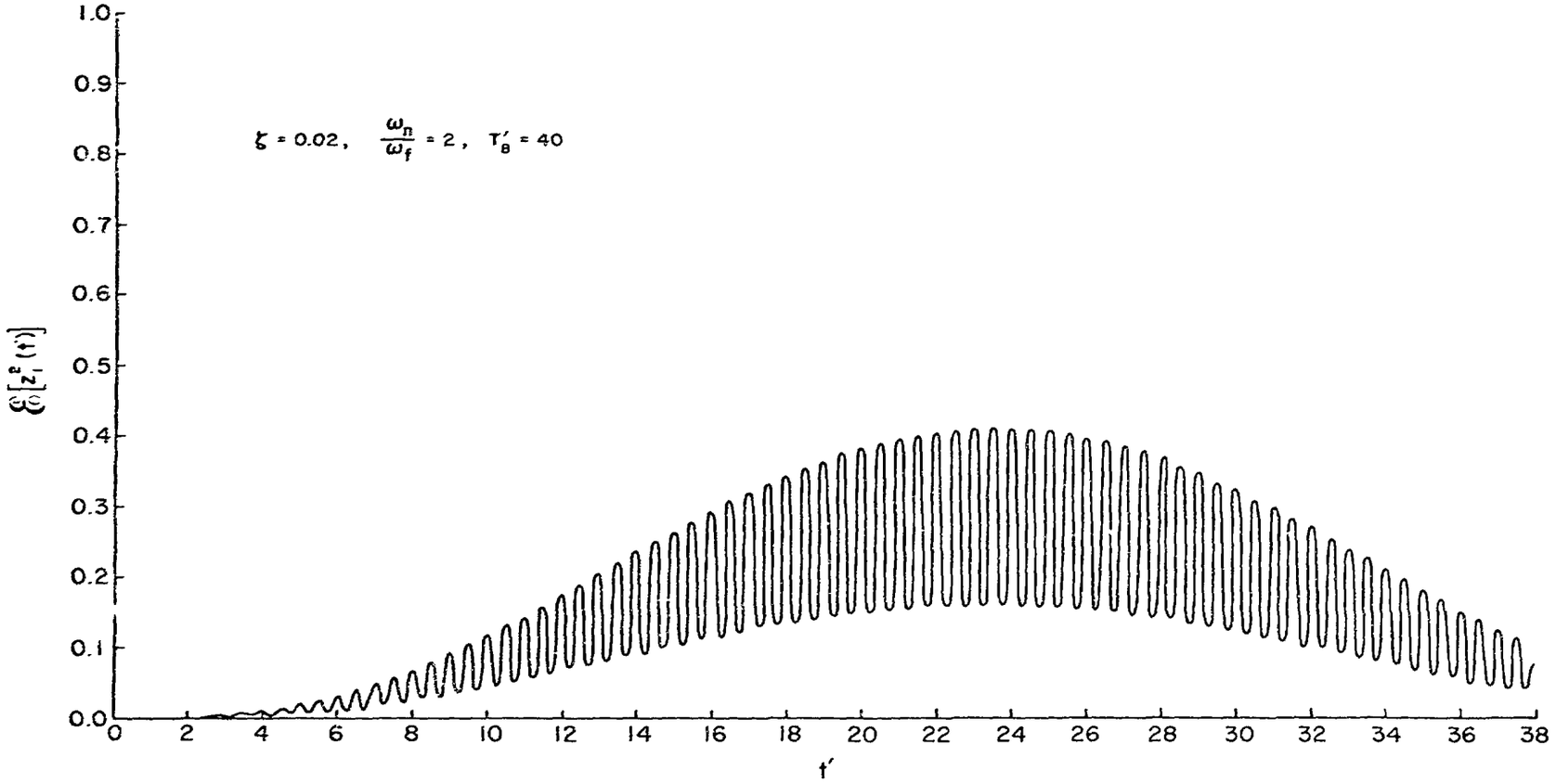

FIG. 31: MEAN SQUARE RESPONSE FOR CASE I: $\zeta = 0.02$, $T'_B = 40$, $\omega_n/\omega_f = 2$

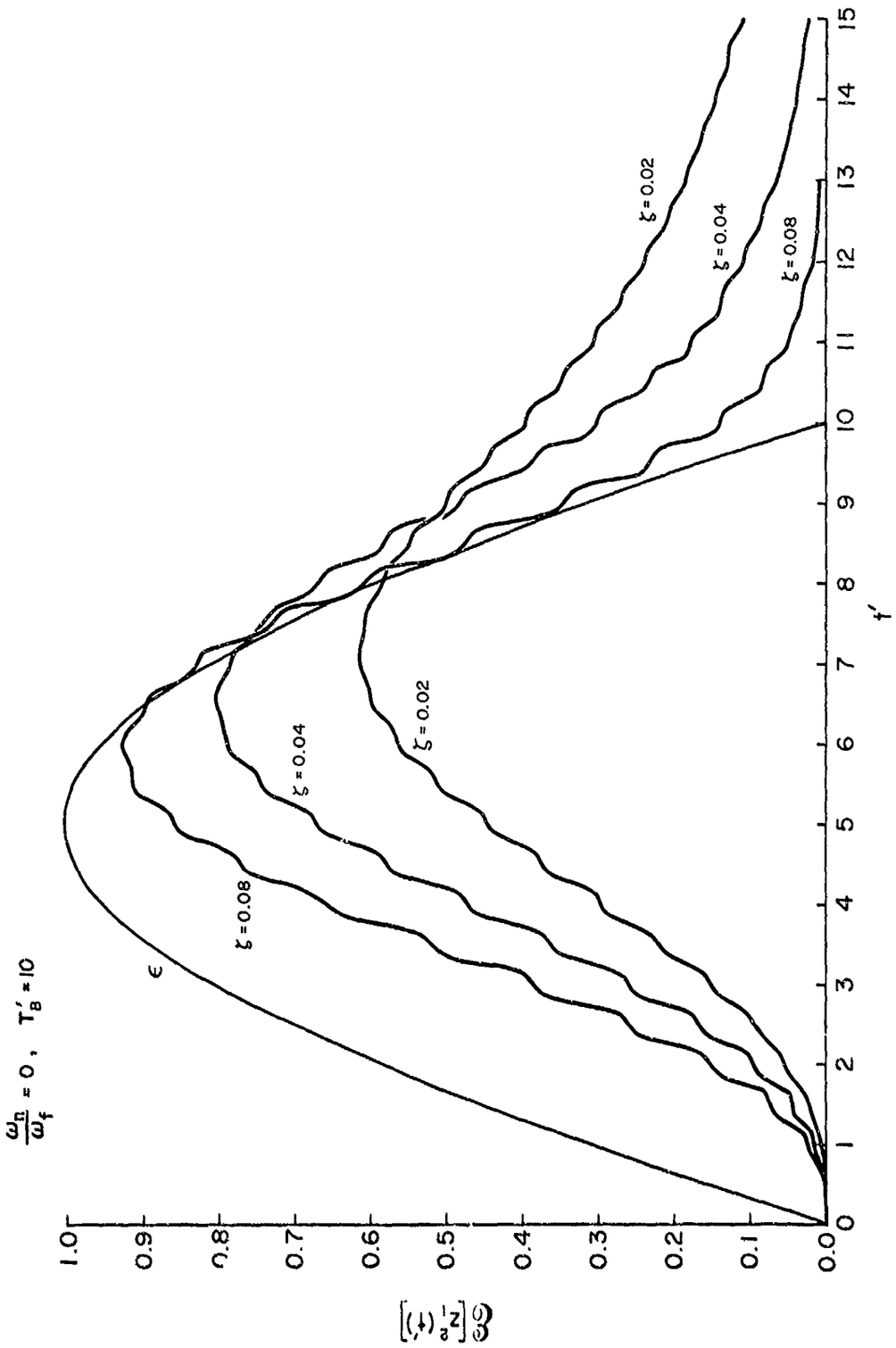

FIG. 32: MEAN SQUARE RESPONSE FOR CASE I: $T'_B = 10$, $\omega_n/\omega_f = 0$

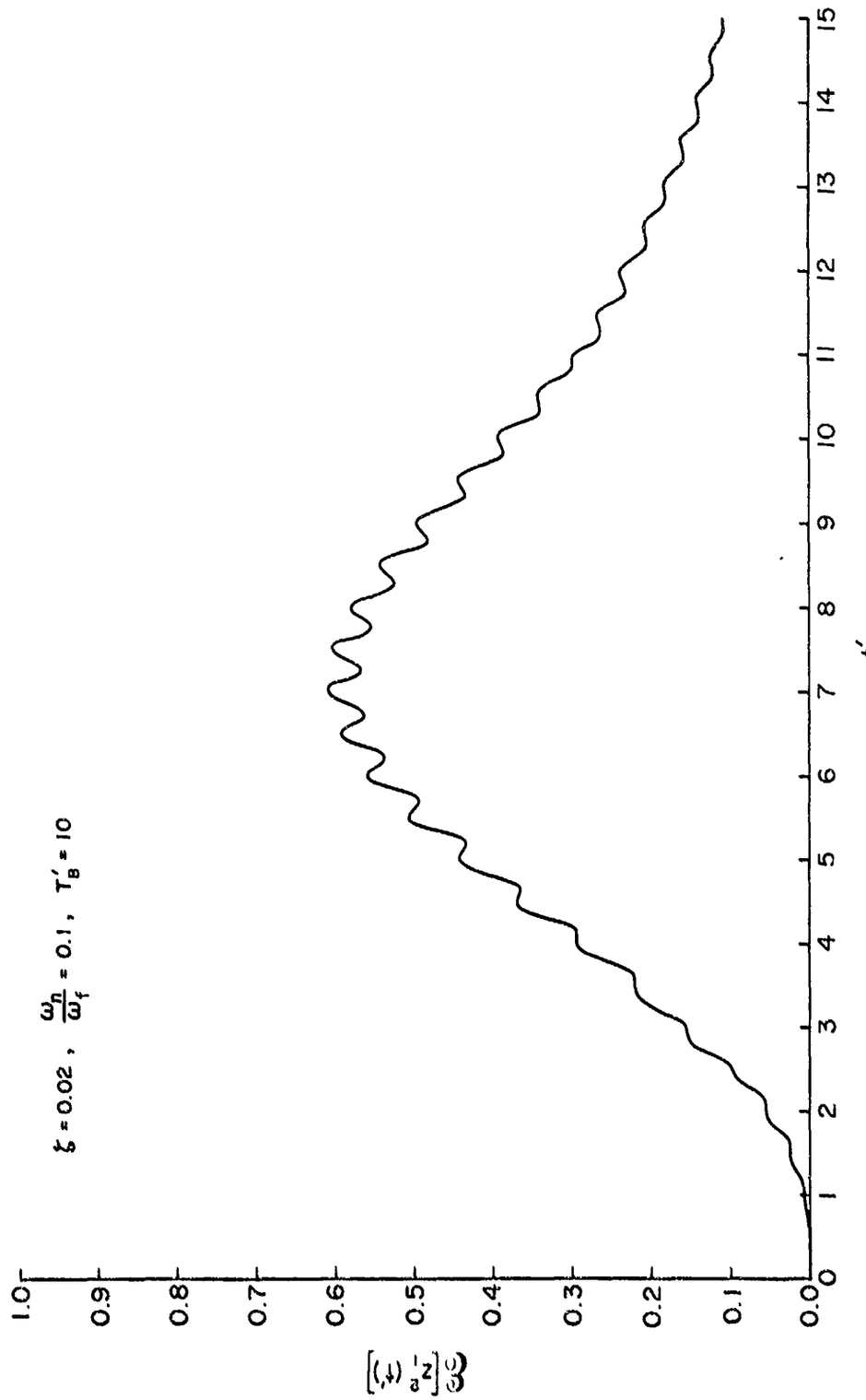

FIG. 33: MEAN SQUARE RESPONSE FOR CASEI: $\zeta = 0.02$, $T_B' = 10$, $\omega_n/\omega_f = 0.1$

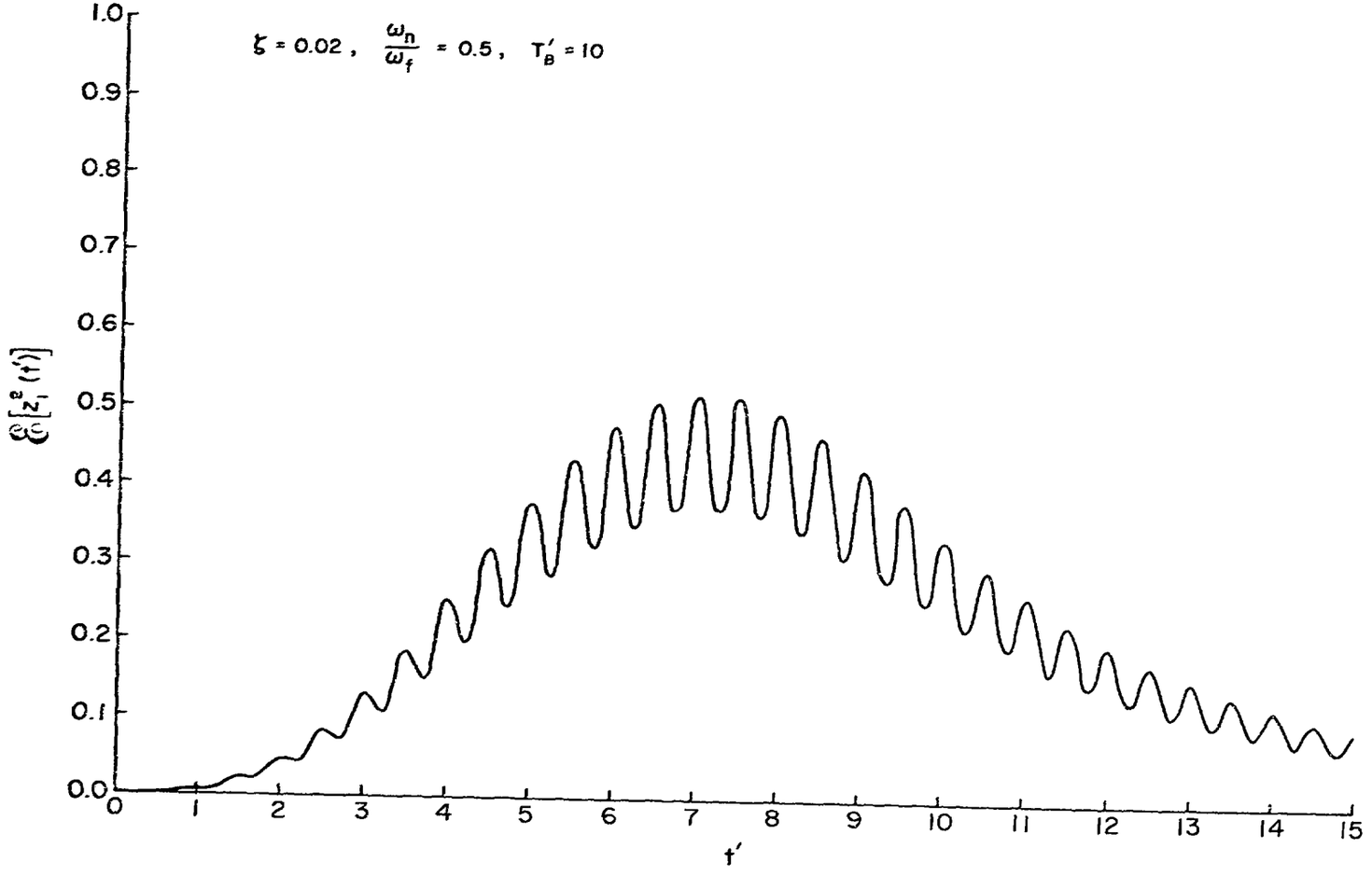

FIG. 34: MEAN SQUARE RESPONSE FOR CASE I: $\zeta = 0.02$, $T_B' = 10$, $\omega_n/\omega_f = 0.5$

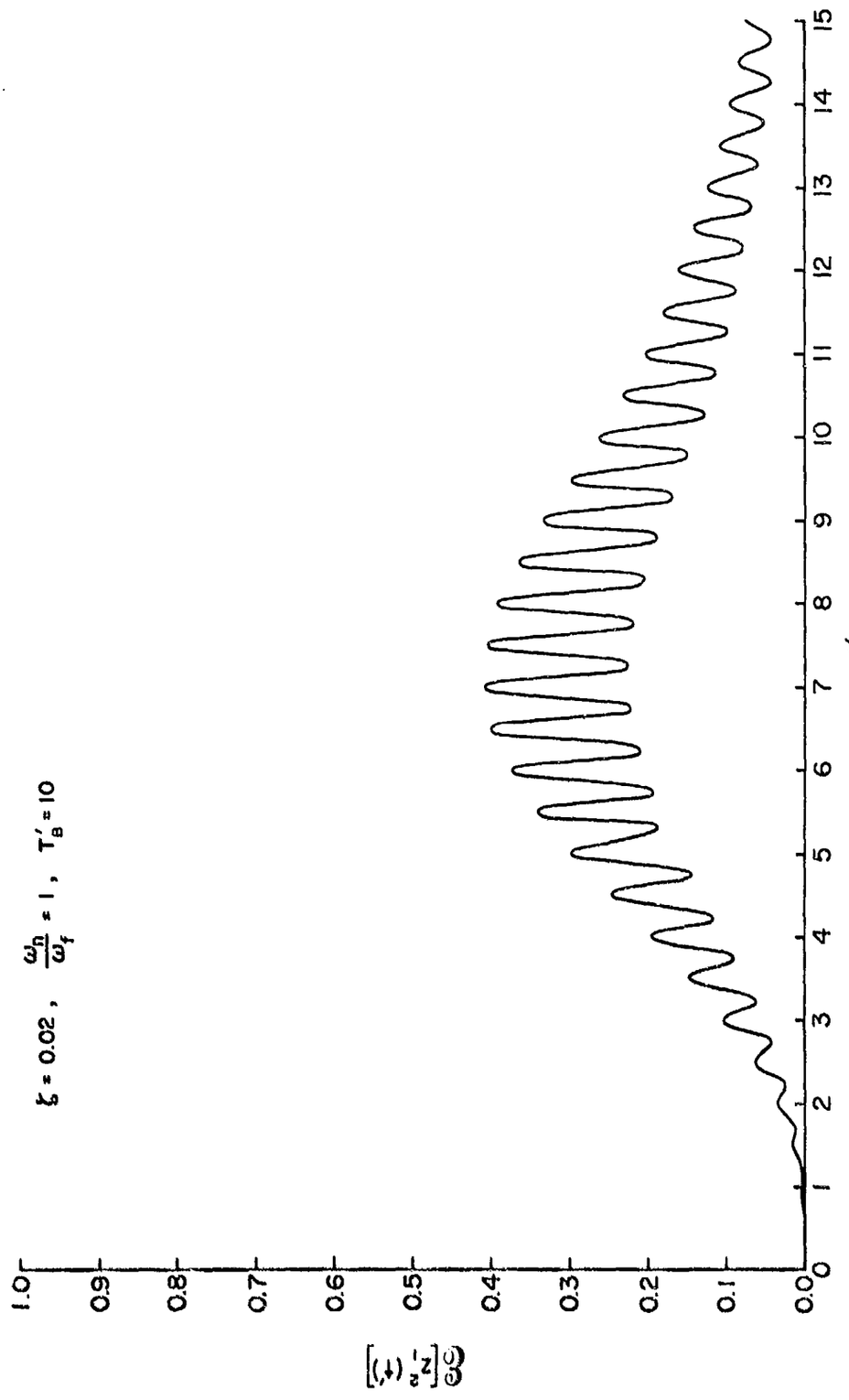

FIG. 35: MEAN SQUARE RESPONSE FOR CASE I: $\zeta = 0.02$, $T'_B = 10$, $\omega_n/\omega_f = 1$

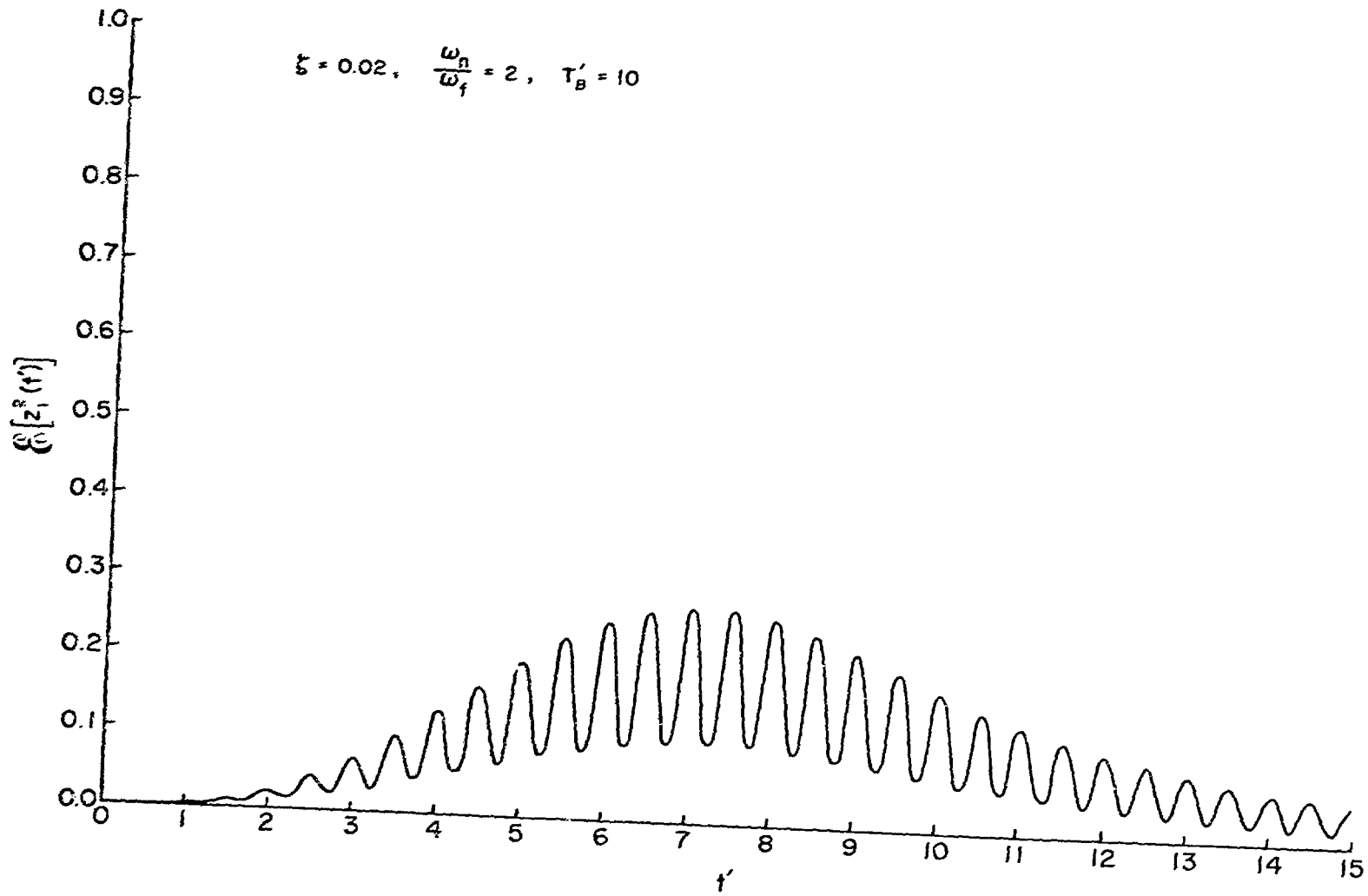

FIG. 36: MEAN SQUARE RESPONSE FOR CASE I: $\zeta = 0.02$, $T_B' = 10$, $\omega_n/\omega_f = 2$

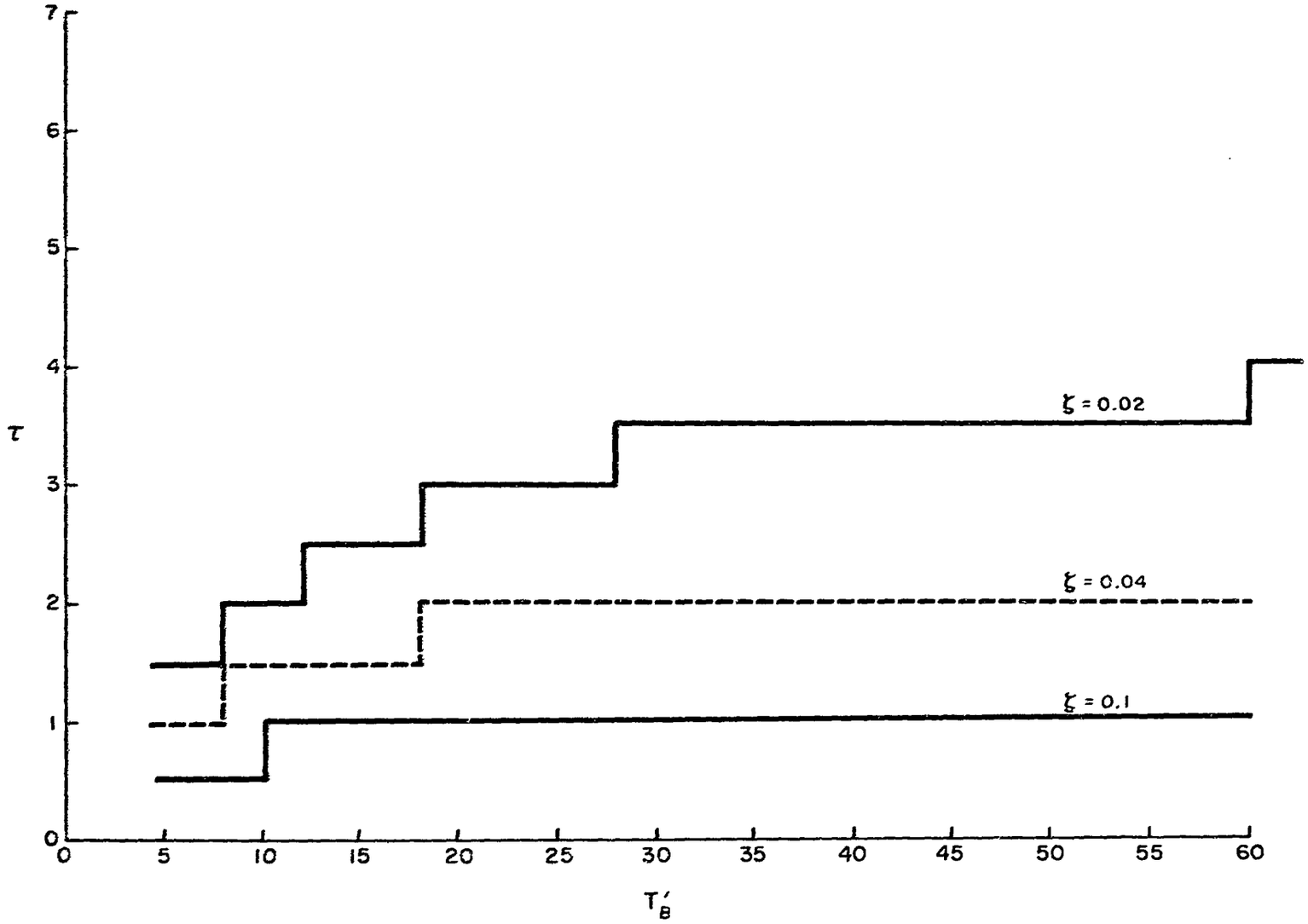

FIG. 37: VARIATION OF DELAY τ WITH DURATION OF APPLIED FORCE T_B'

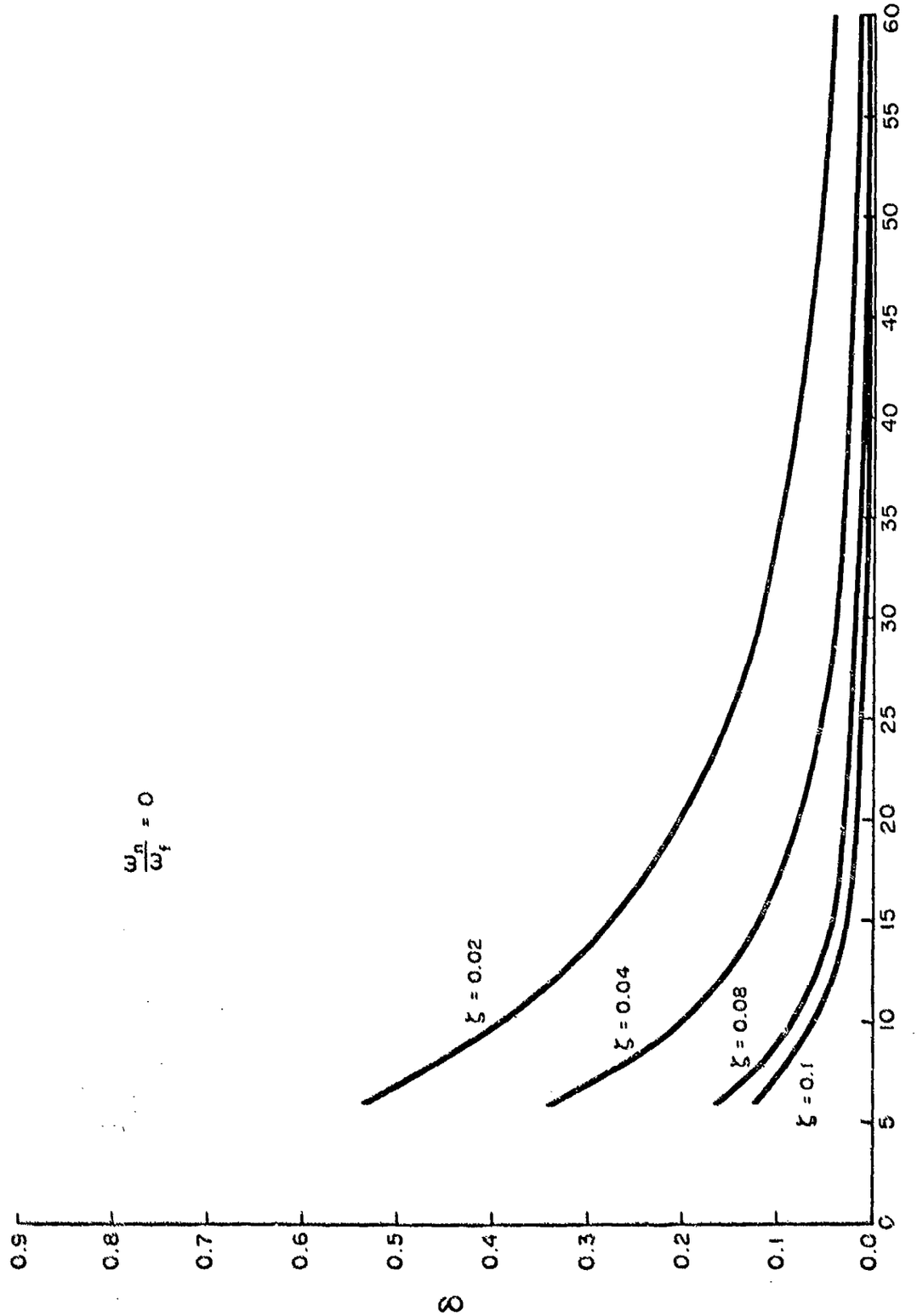

FIG. 38: VARIATION OF AMPLITUDE FUNCTION δ WITH DURATION OF APPLIED FORCE T_B' FOR $\omega_n/\omega_f = 0$

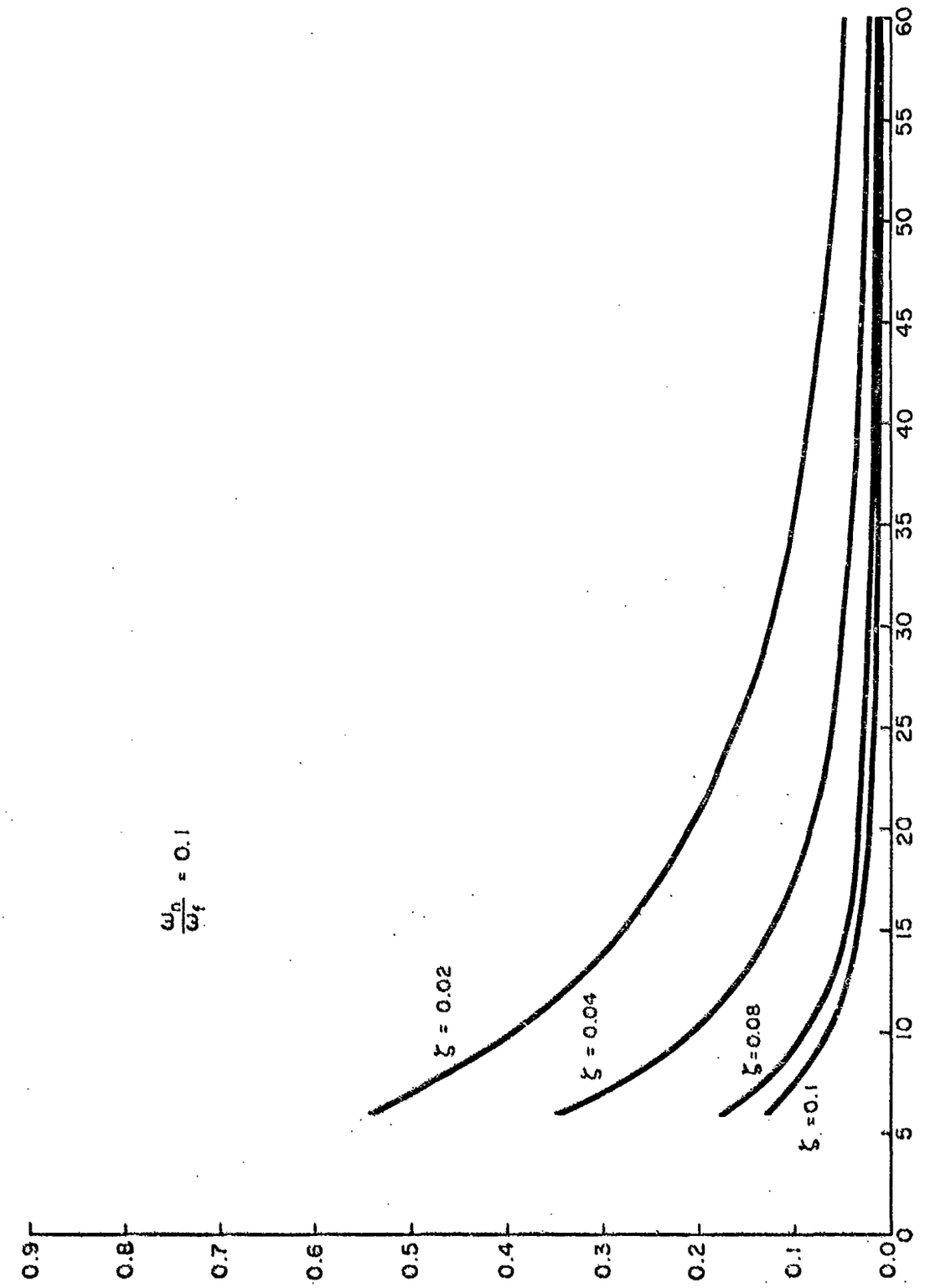

FIG. 39: VARIATION OF AMPLITUDE FUNCTION δ WITH DURATION OF APPLIED FORCE T'_B FOR ω_n/ω_f = 0.1

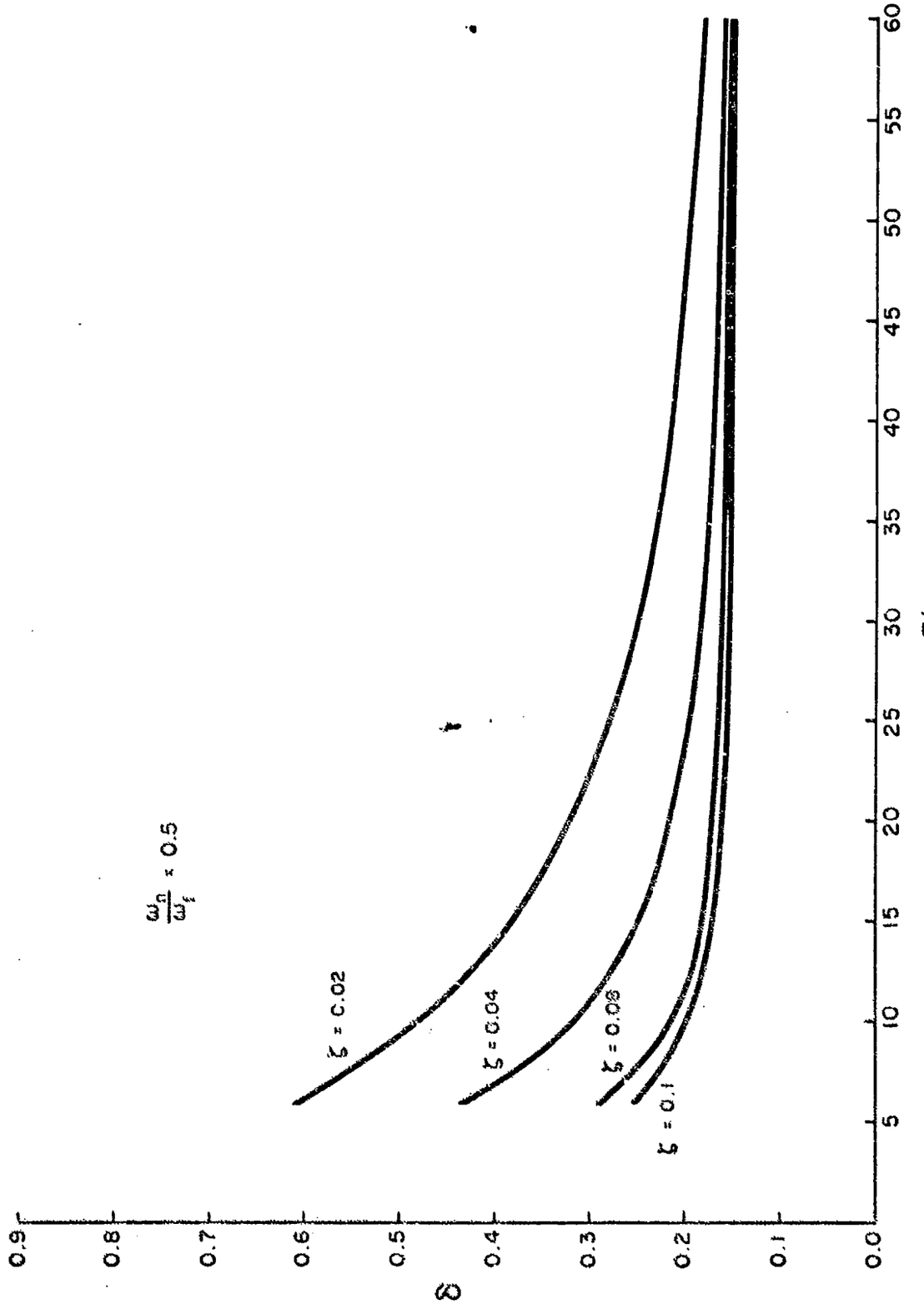

FIG. 40: VARIATION OF AMPLITUDE FUNCTION δ WITH DURATION OF APPLIED FORCE T'_B FOR $\omega_n/\omega_f = 0.5$

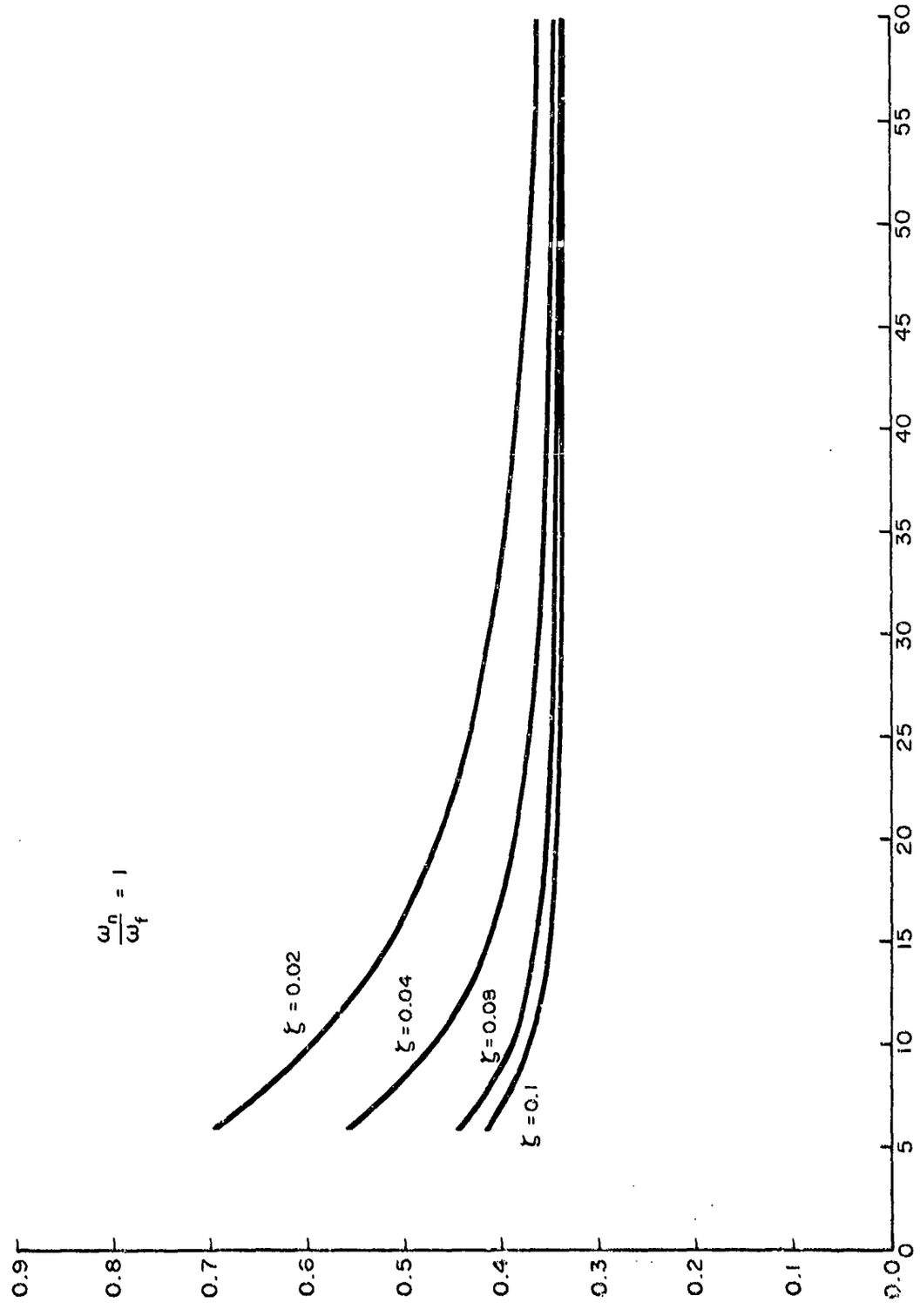

FIG. 41: VARIATION OF AMPLITUDE FUNCTION δ WITH DURATION OF APPLIED FORCE T'_B FOR $\omega_n/\omega_f = 1$

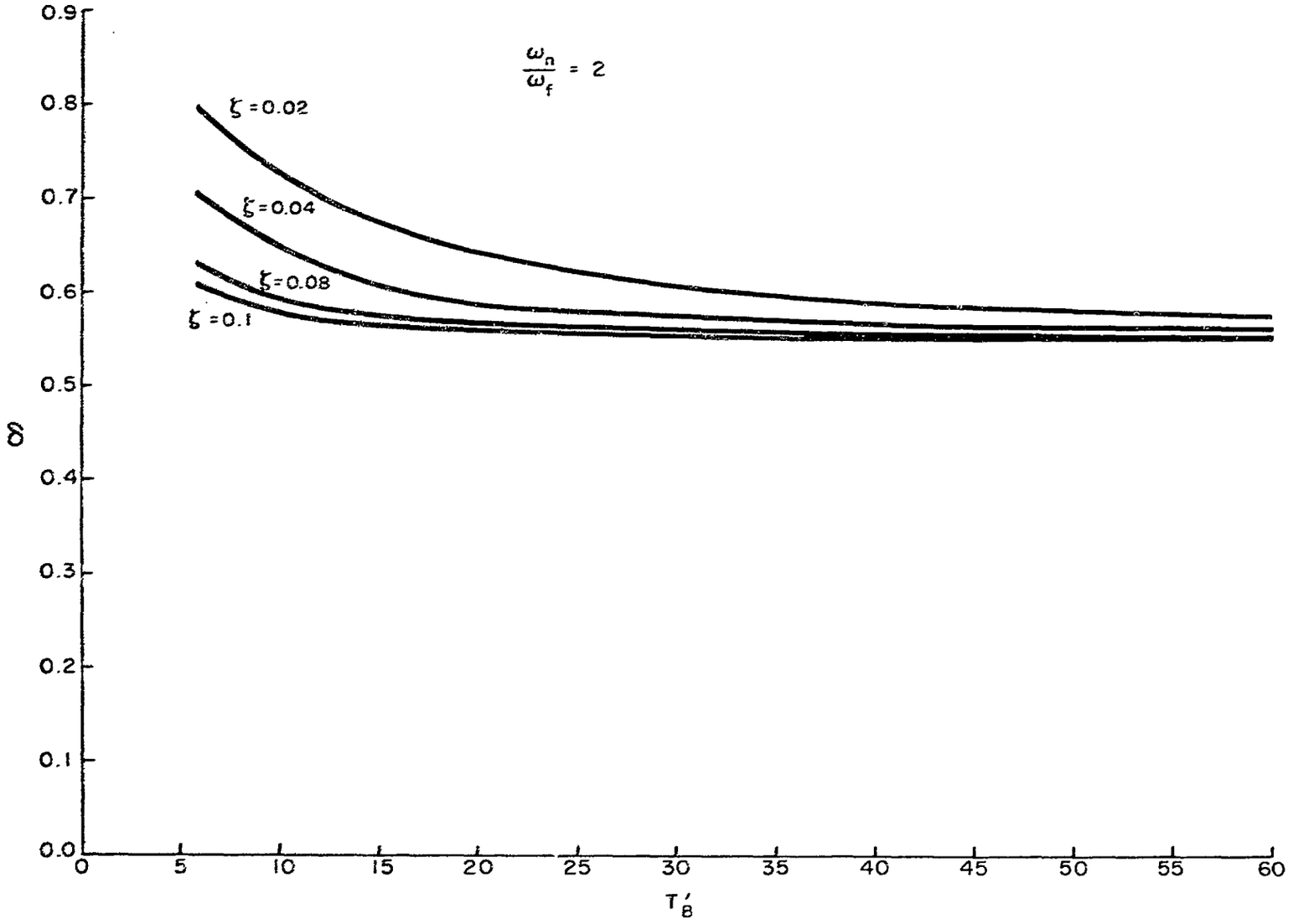

FIG. 42: VARIATION OF AMPLITUDE FUNCTION δ WITH DURATION OF APPLIED FORCE T'_B FOR $\omega_n/\omega_f = 2$

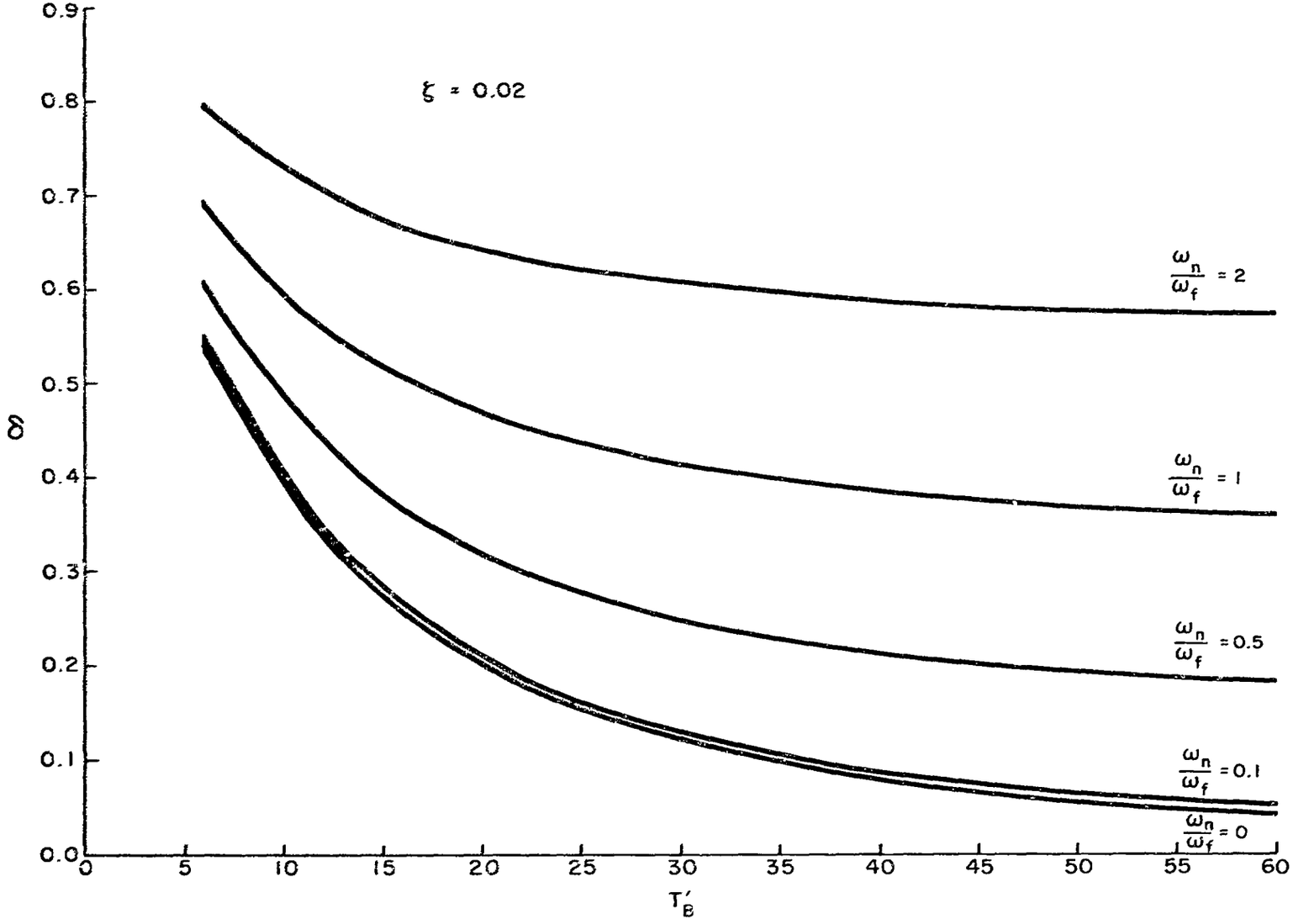

FIG. 43: VARIATION OF AMPLITUDE FUNCTION δ WITH DURATION OF APPLIED FORCE T'_B FOR $\zeta = 0.02$

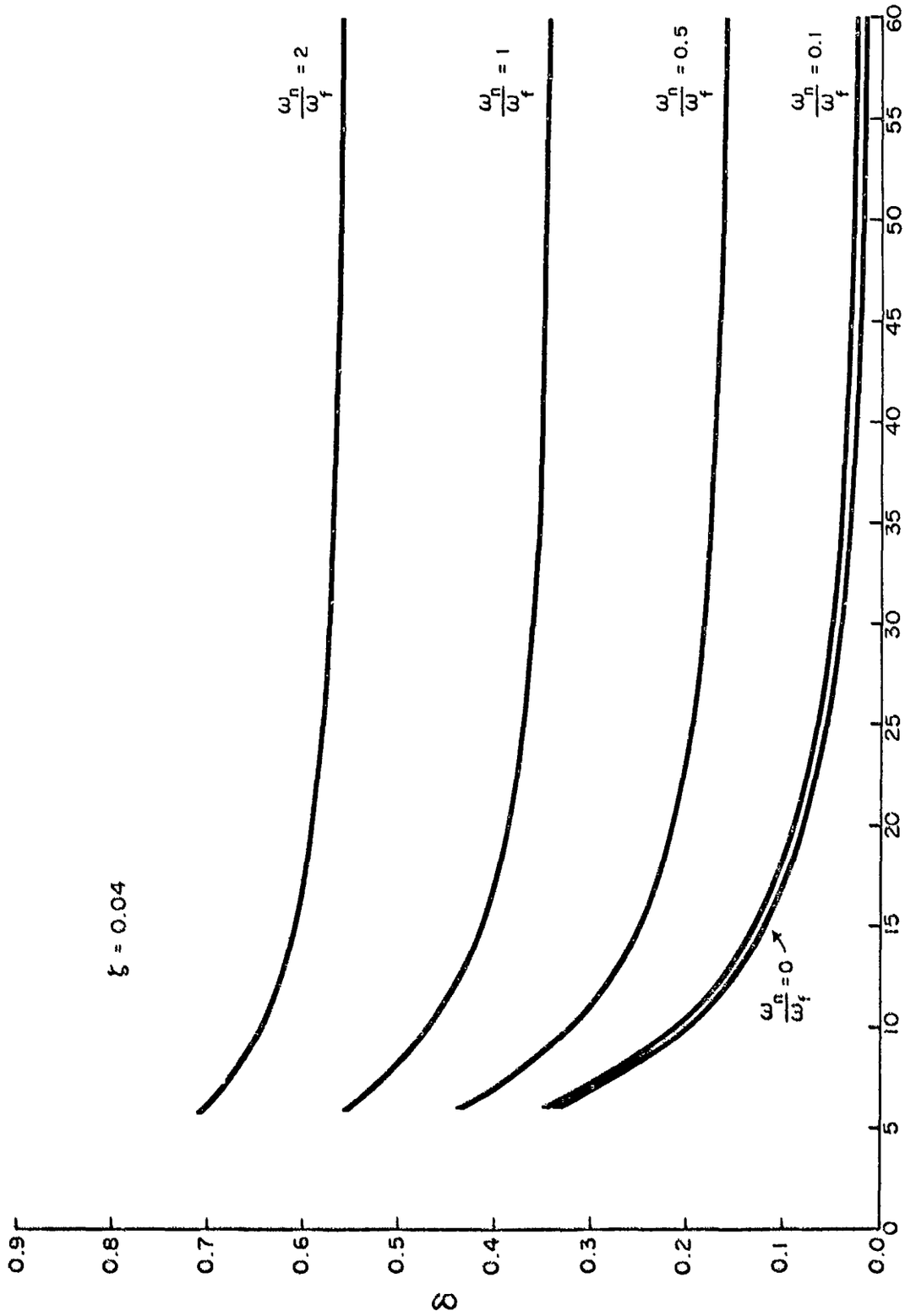

FIG. 44: VARIATION OF AMPLITUDE FUNCTION δ WITH DURATION OF APPLIED FORCE T'_B FOR ζ = 0.04

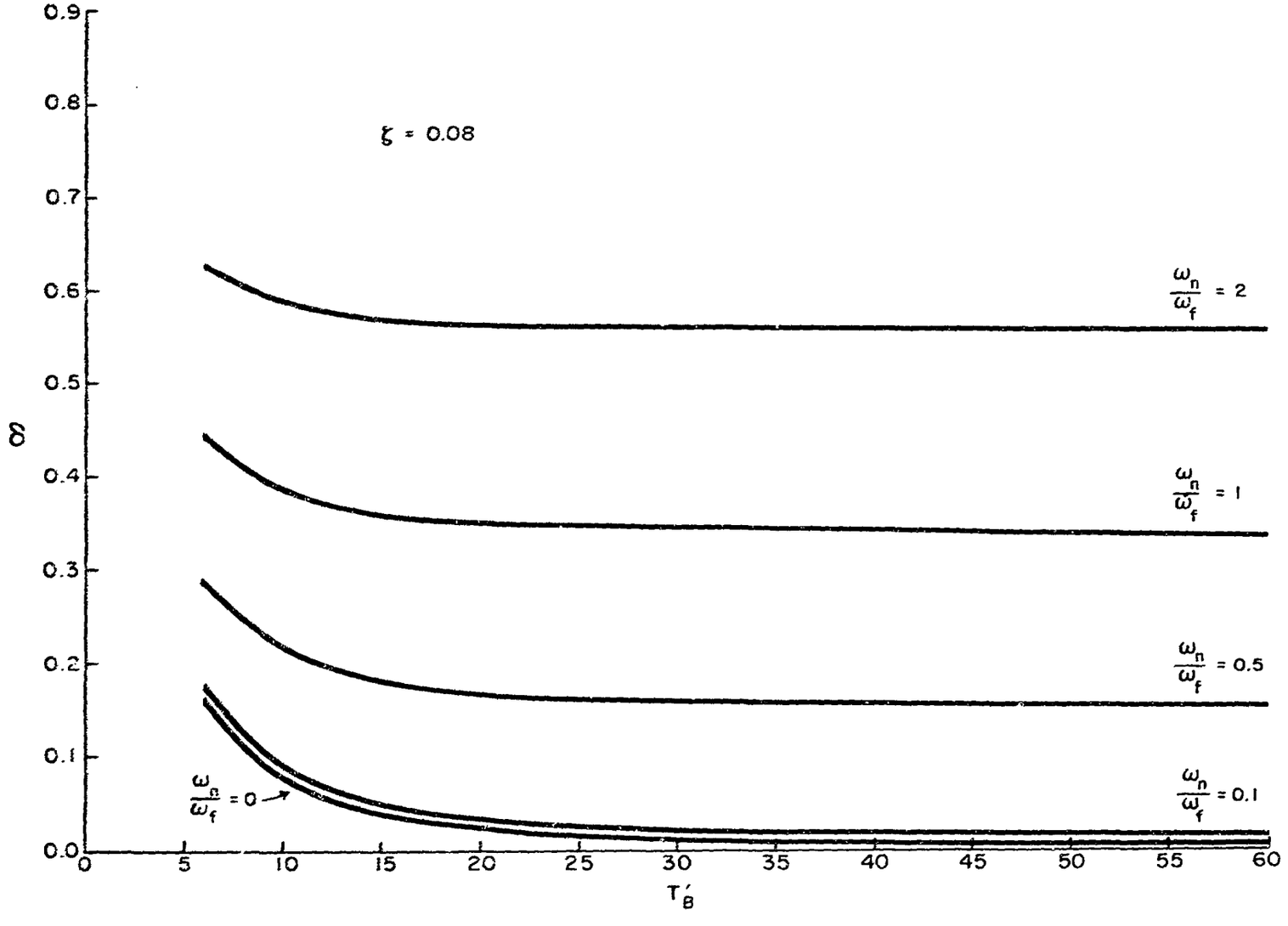

FIG. 45: VARIATION OF AMPLITUDE FUNCTION δ WITH DURATION OF APPLIED FORCE T'_B FOR $\zeta = 0.08$

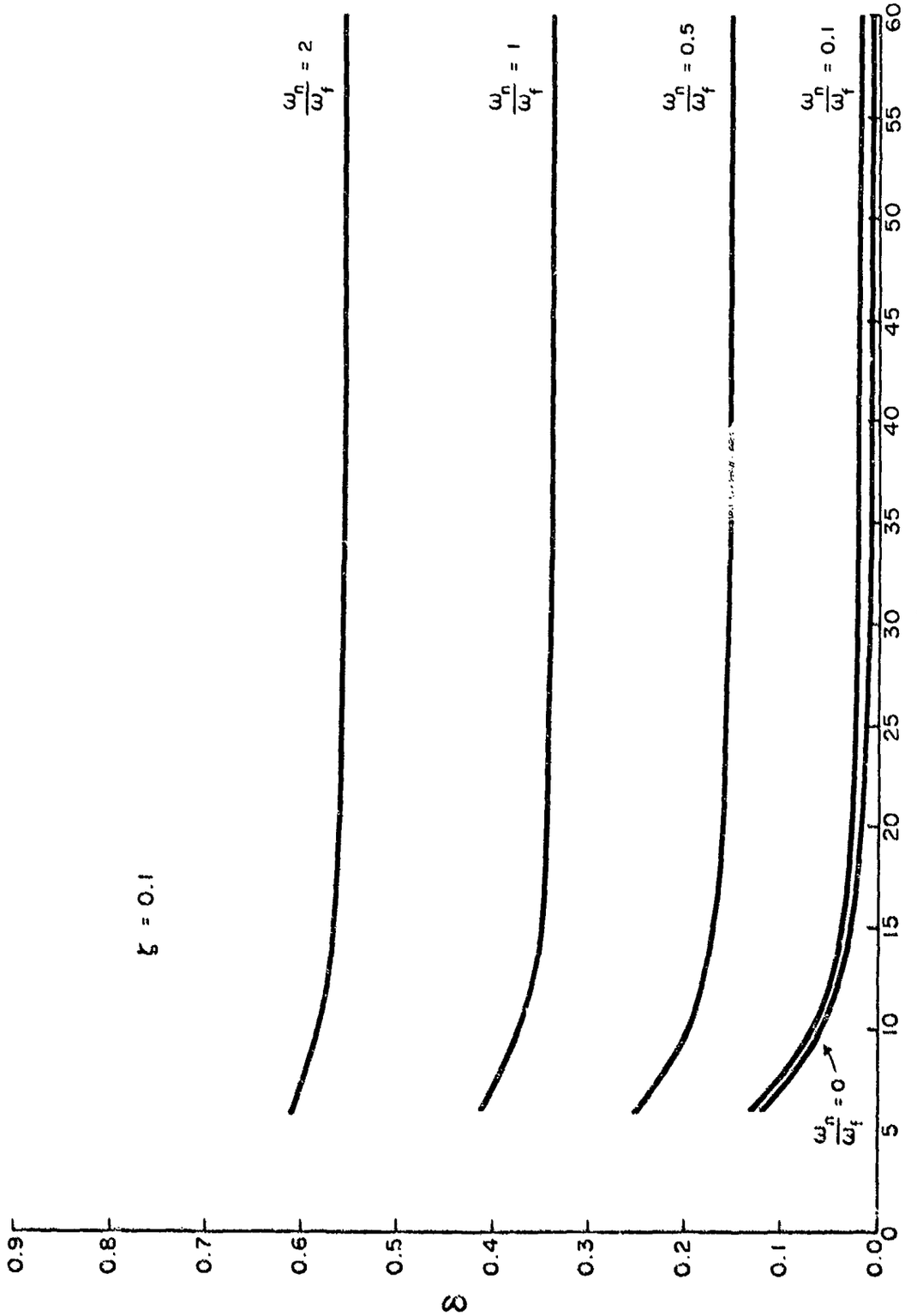

FIG. 46: VARIATION OF AMPLITUDE FUNCTION δ WITH DURATION OF APPLIED FORCE T'_B FOR ζ = 0.1

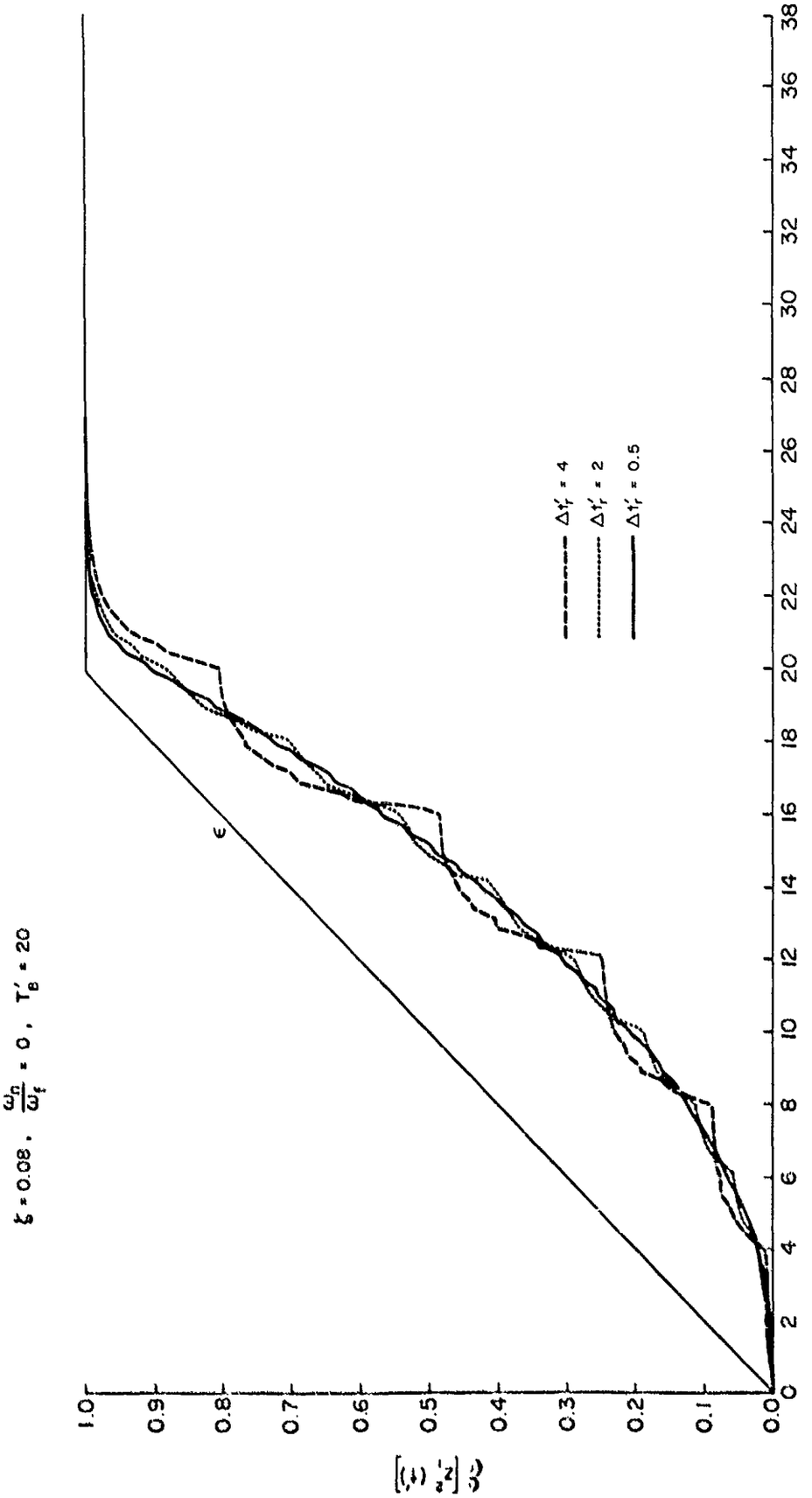

FIG. 47: EFFECT OF $\Delta t_f'$ ON MEAN SQUARE RESPONSE FOR CASE II

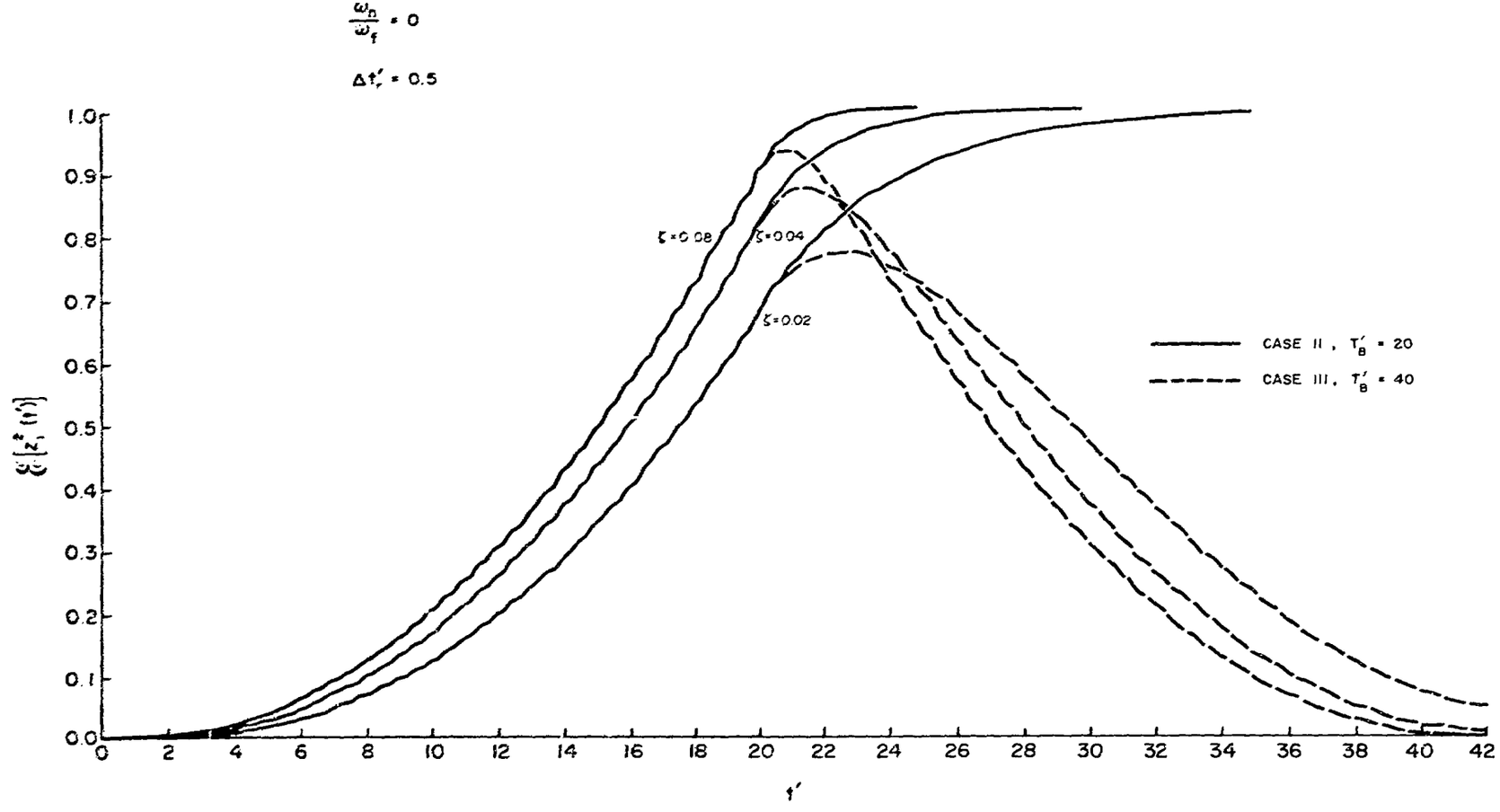

FIG. 48: MEAN SQUARE RESPONSE FOR CASE II AND III: $\omega_n/\omega_f = 0$

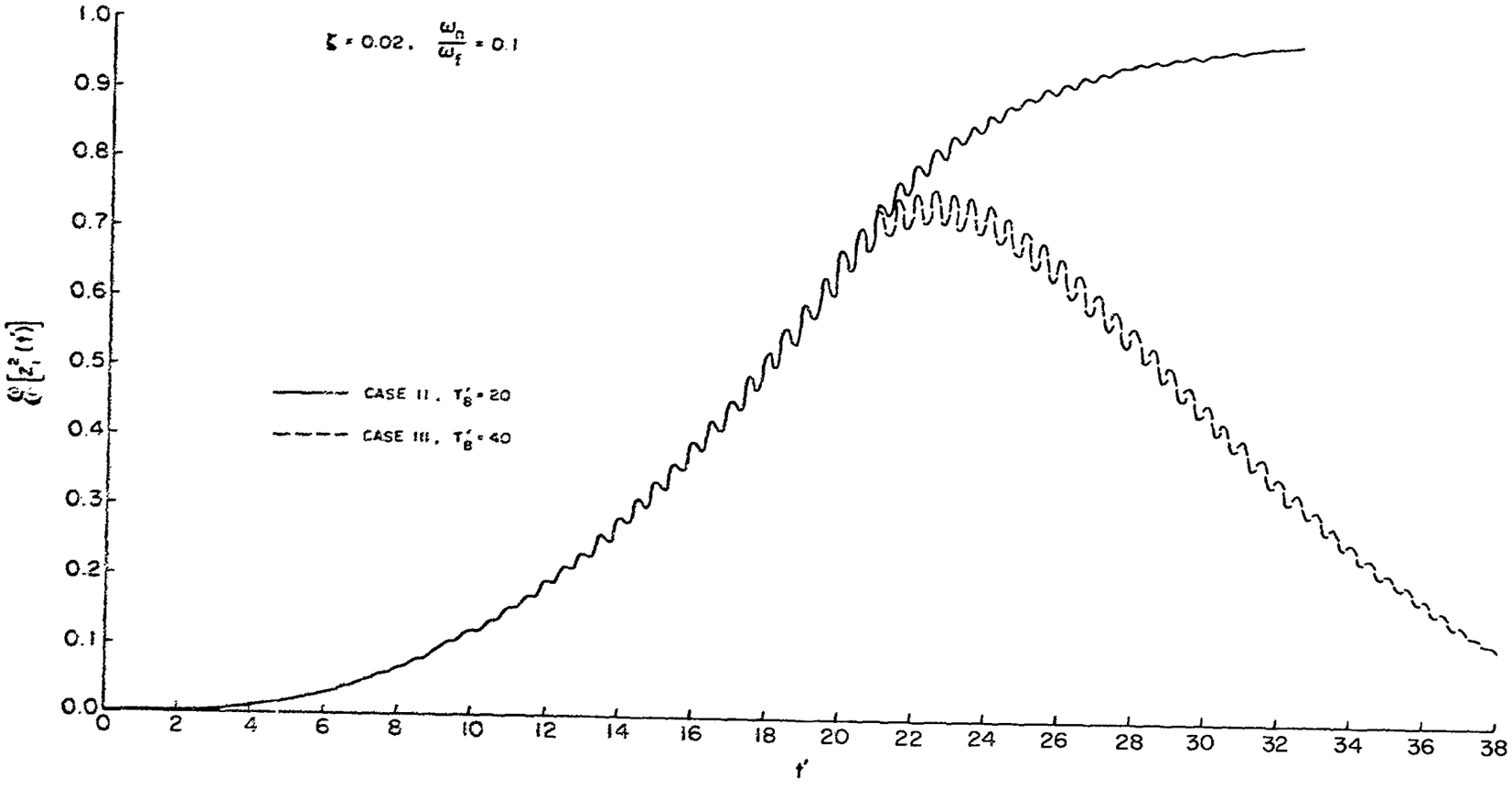

FIG. 49: MEAN SQUARE RESPONSE FOR CASE II AND III: $\zeta = 0.02$, $\omega_n/\omega_f = 0.1$

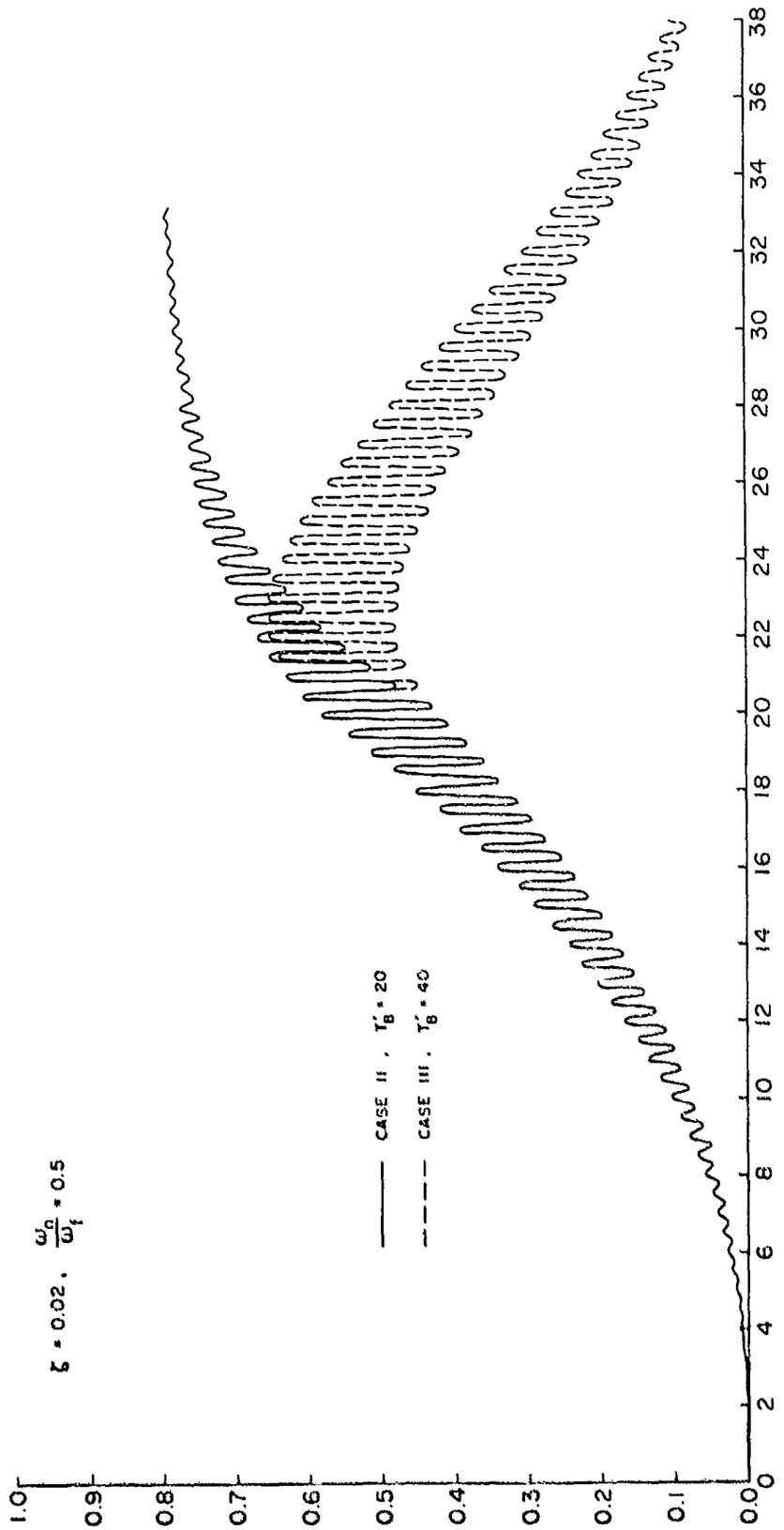

FIG. 50: MEAN SQUARE RESPONSE FOR CASE II AND III: $\zeta = 0.02$, $\omega_n/\omega_f = 0.5$

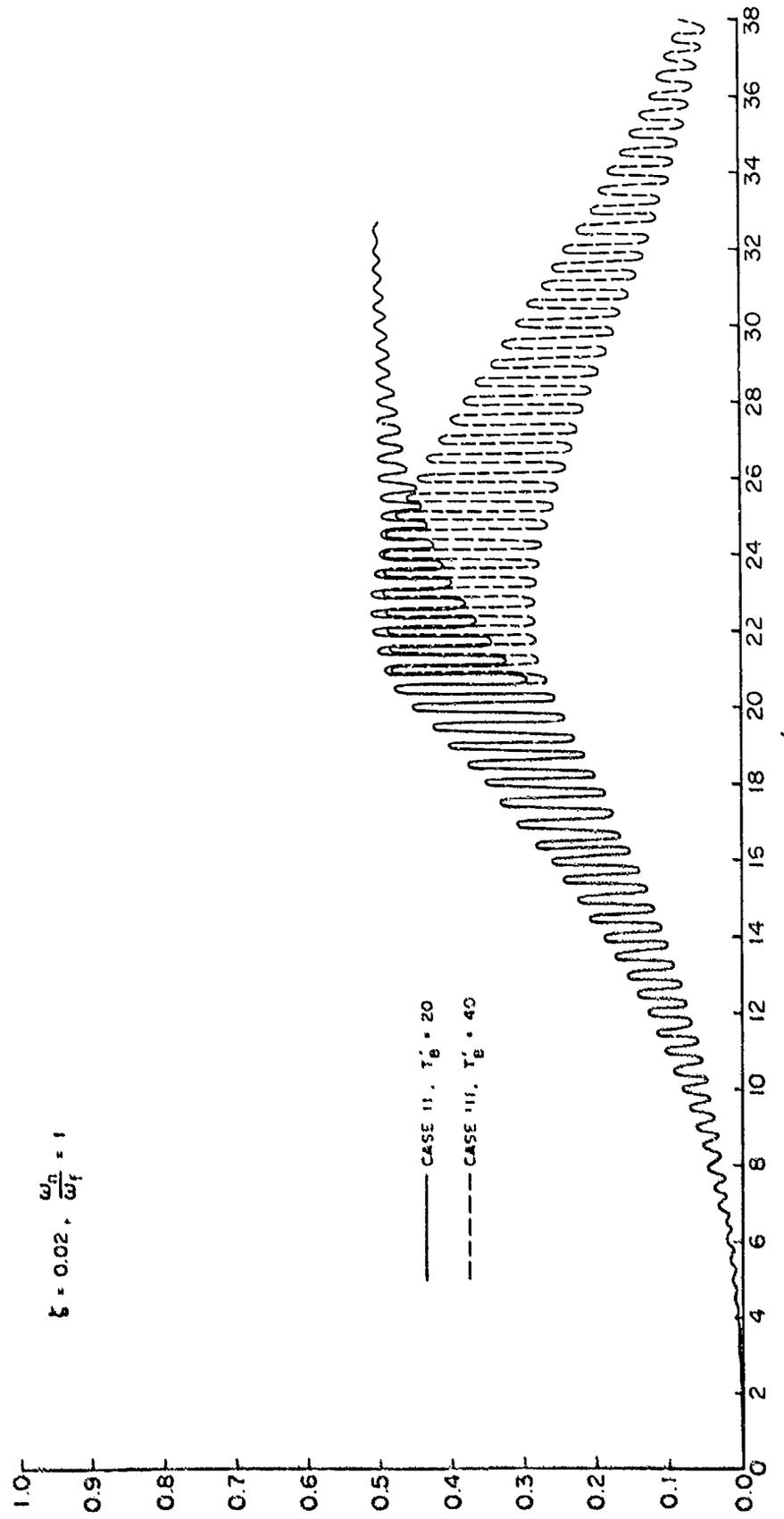

FIG. 51: MEAN SQUARE RESPONSE FOR CASE II AND III: $\zeta = 0.02$, $\omega_n/\omega_f = 1$

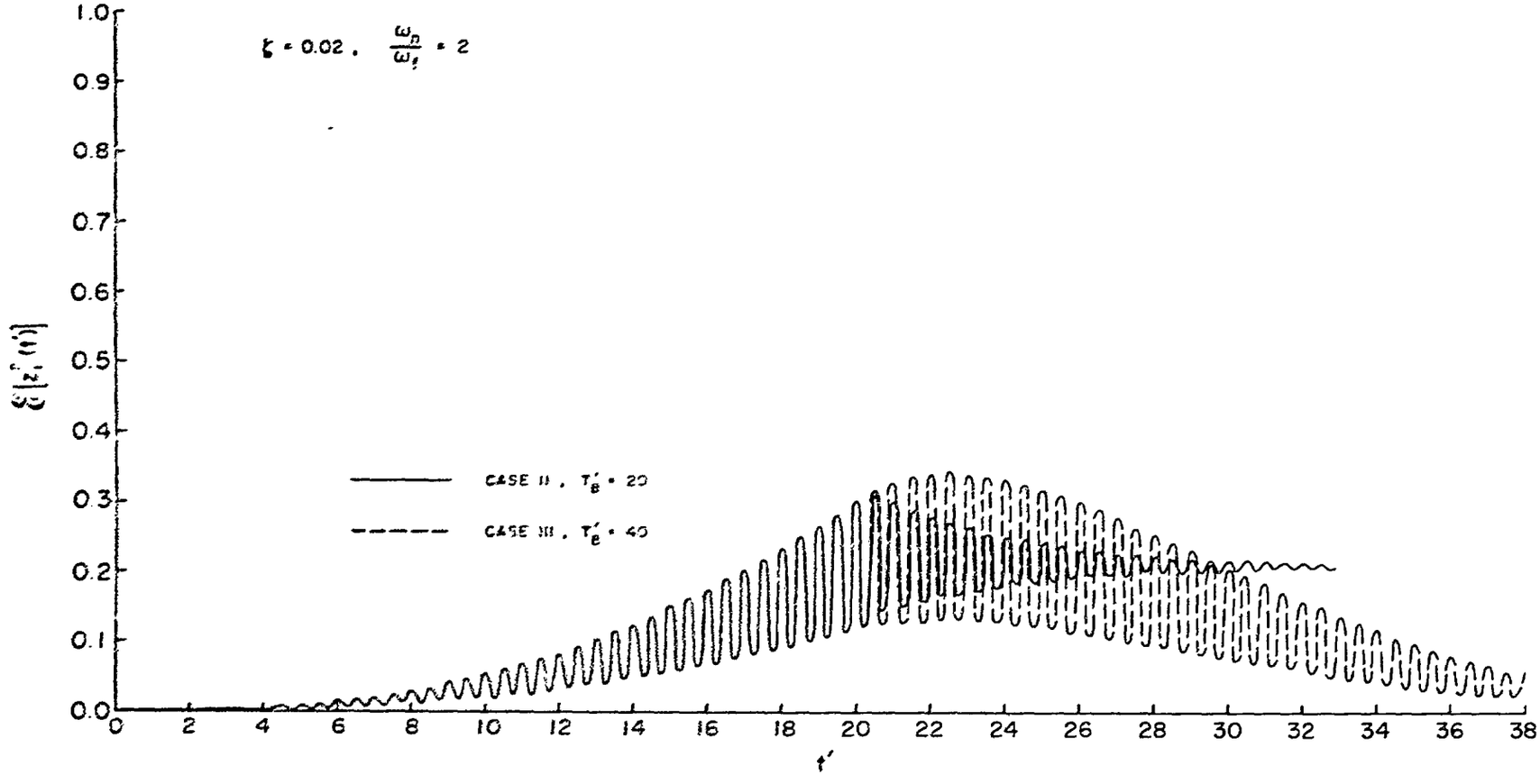

FIG. 52: MEAN SQUARE RESPONSE FOR CASE II AND III: $\zeta = 0.02$, $\omega_n/\omega_f = 2$

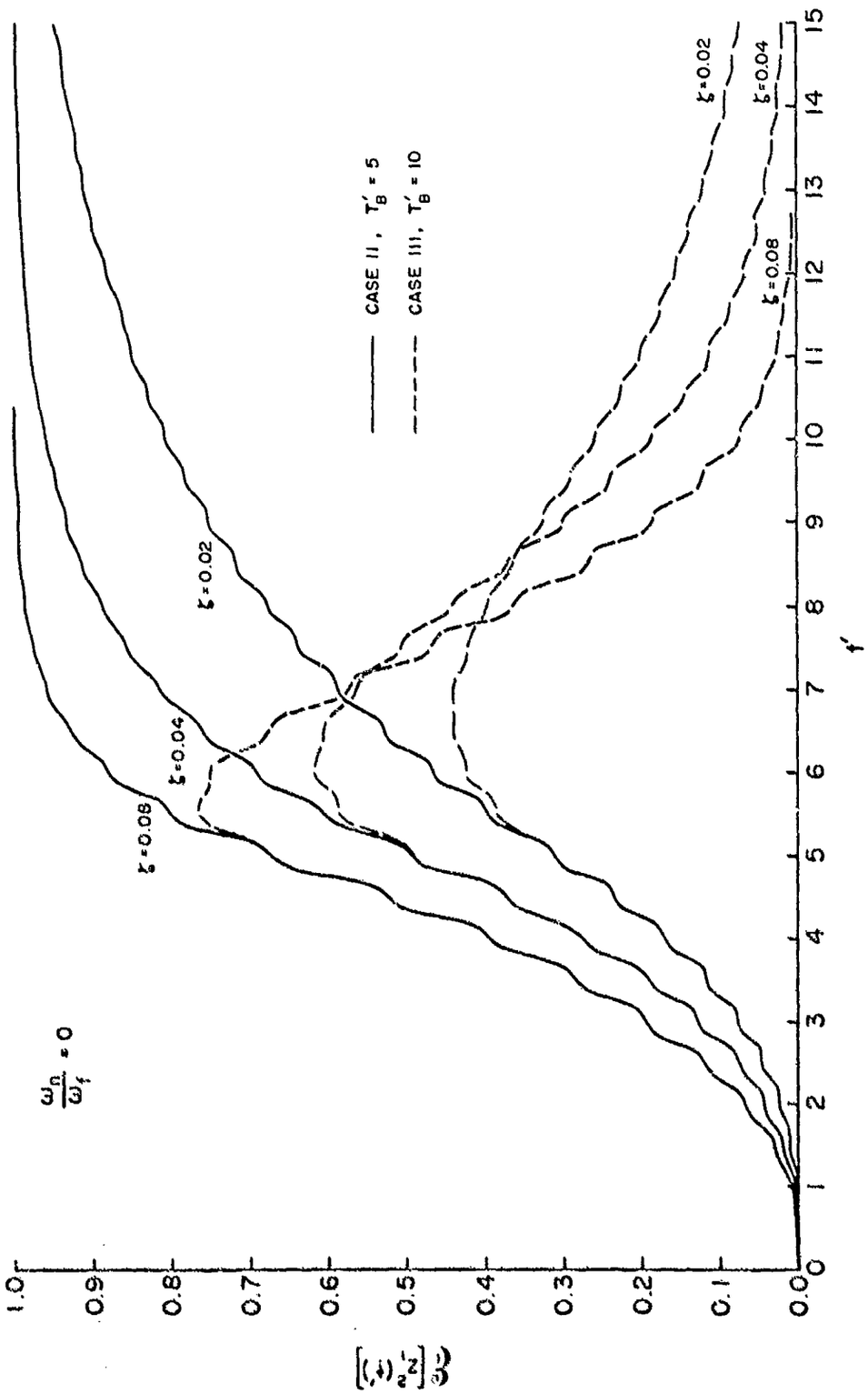

FIG. 53: MEAN SQUARE RESPONSE FOR CASE II AND III: $\omega_n/\omega_f = 0$

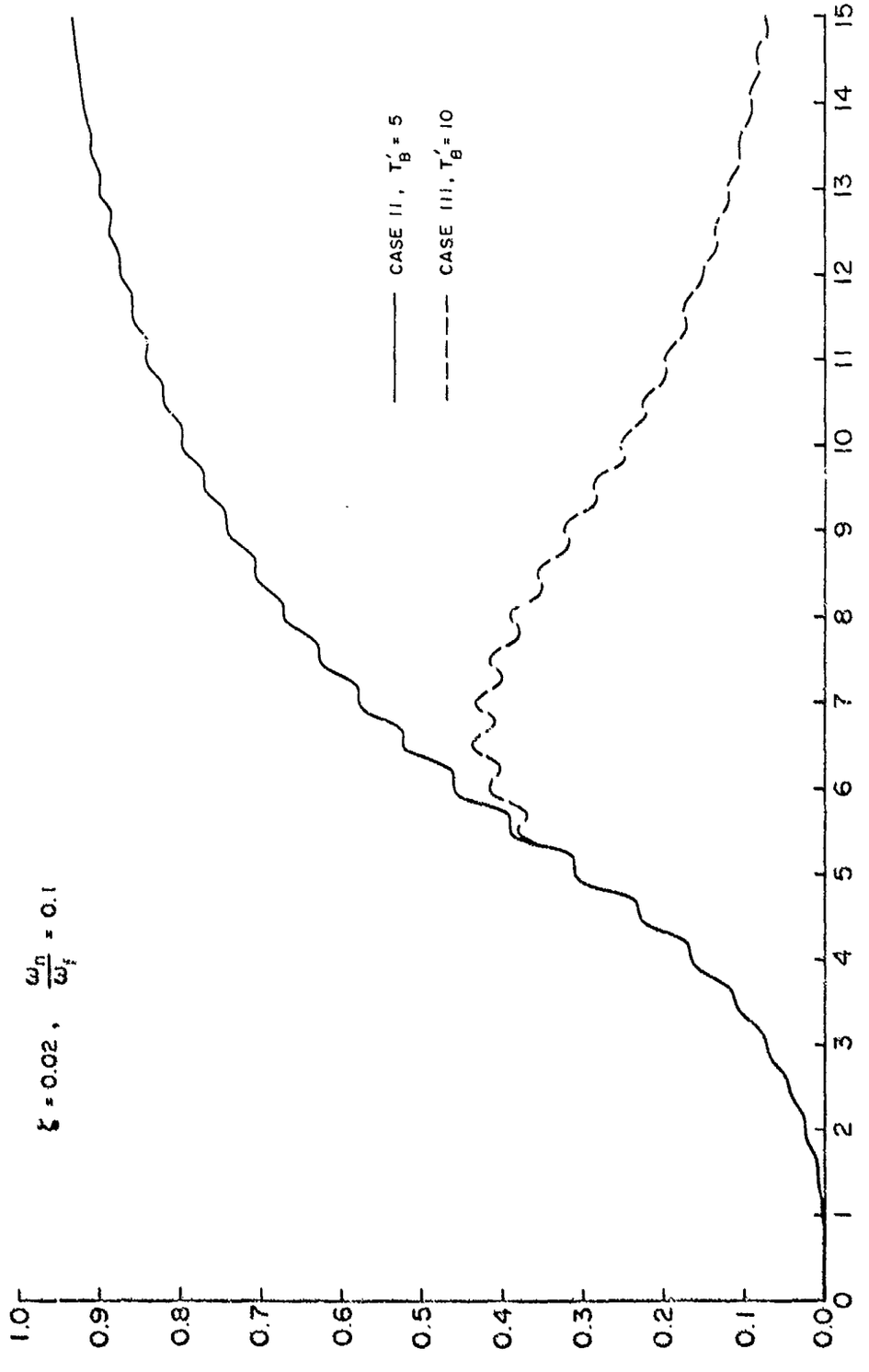

FIG. 54: MEAN SQUARE RESPONSE FOR CASE II AND III: $\zeta = 0.02$, $\omega_n/\omega_f = 0.1$

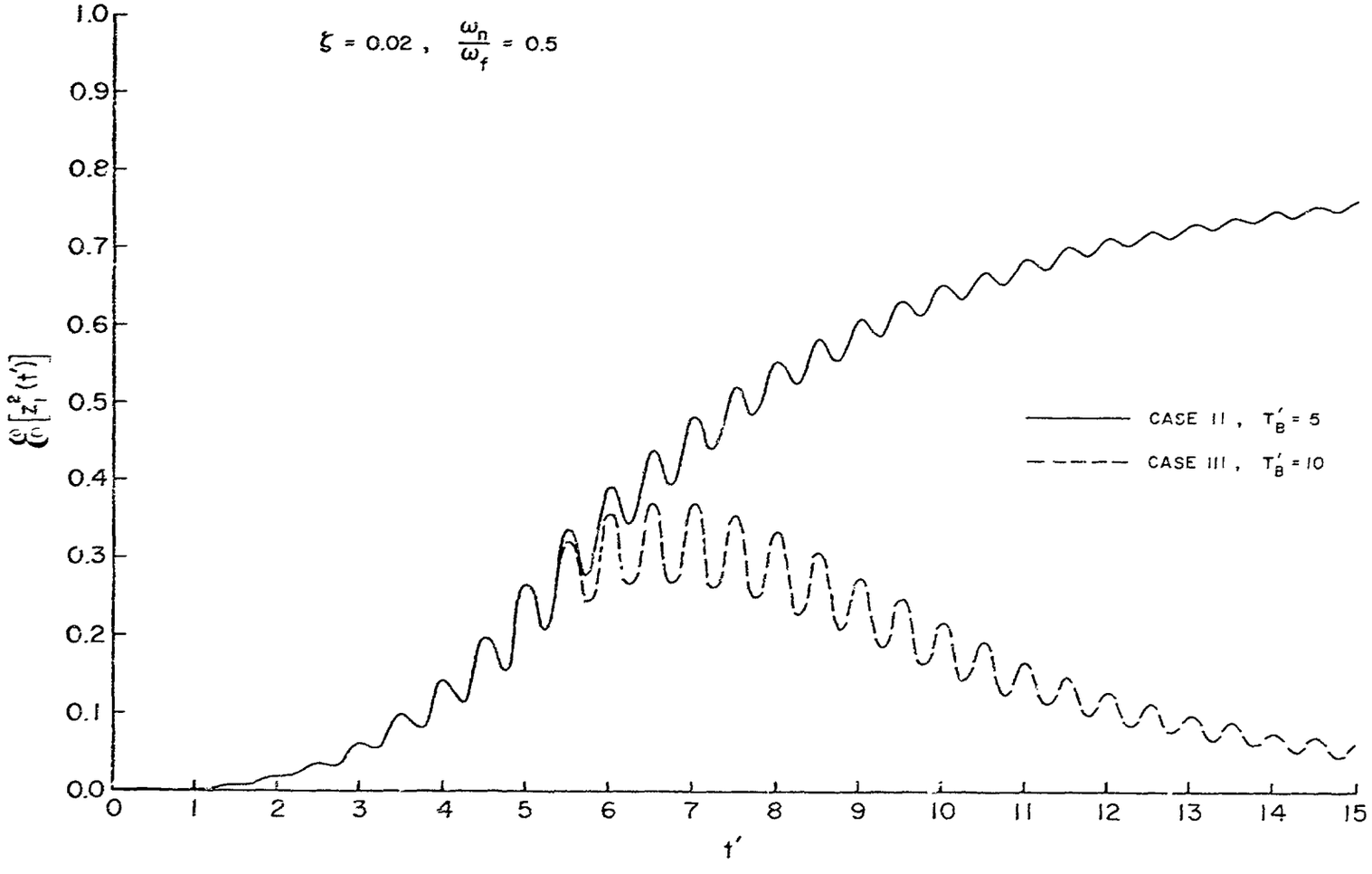

FIG. 55: MEAN SQUARE RESPONSE FOR CASE II AND III: $\zeta = 0.02$, $\omega_n/\omega_f = 0.5$

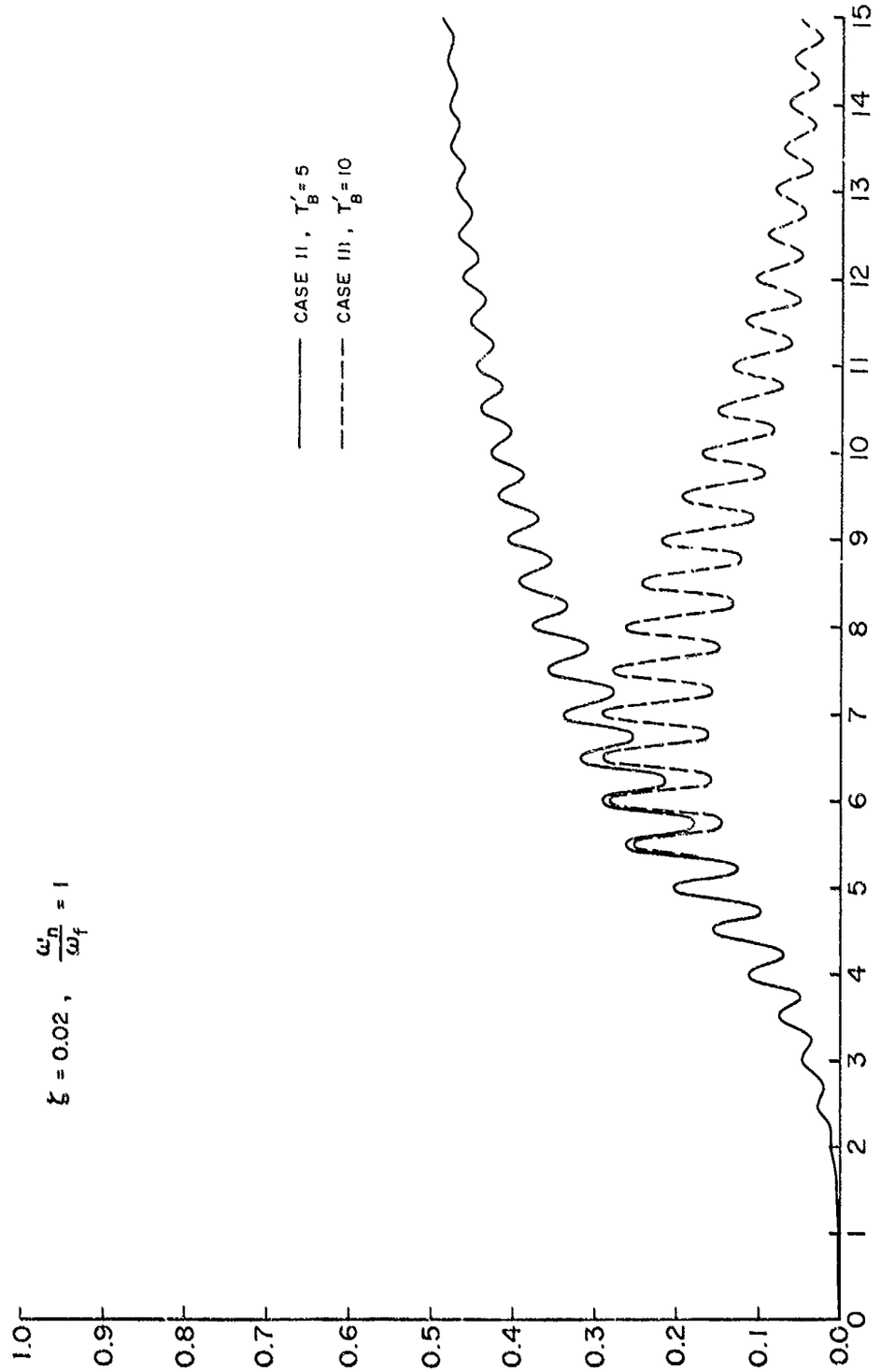

FIG. 56: MEAN SQUARE RESPONSE FOR CASE II AND III: $\zeta = 0.02$, $\omega_n/\omega_f = 1$

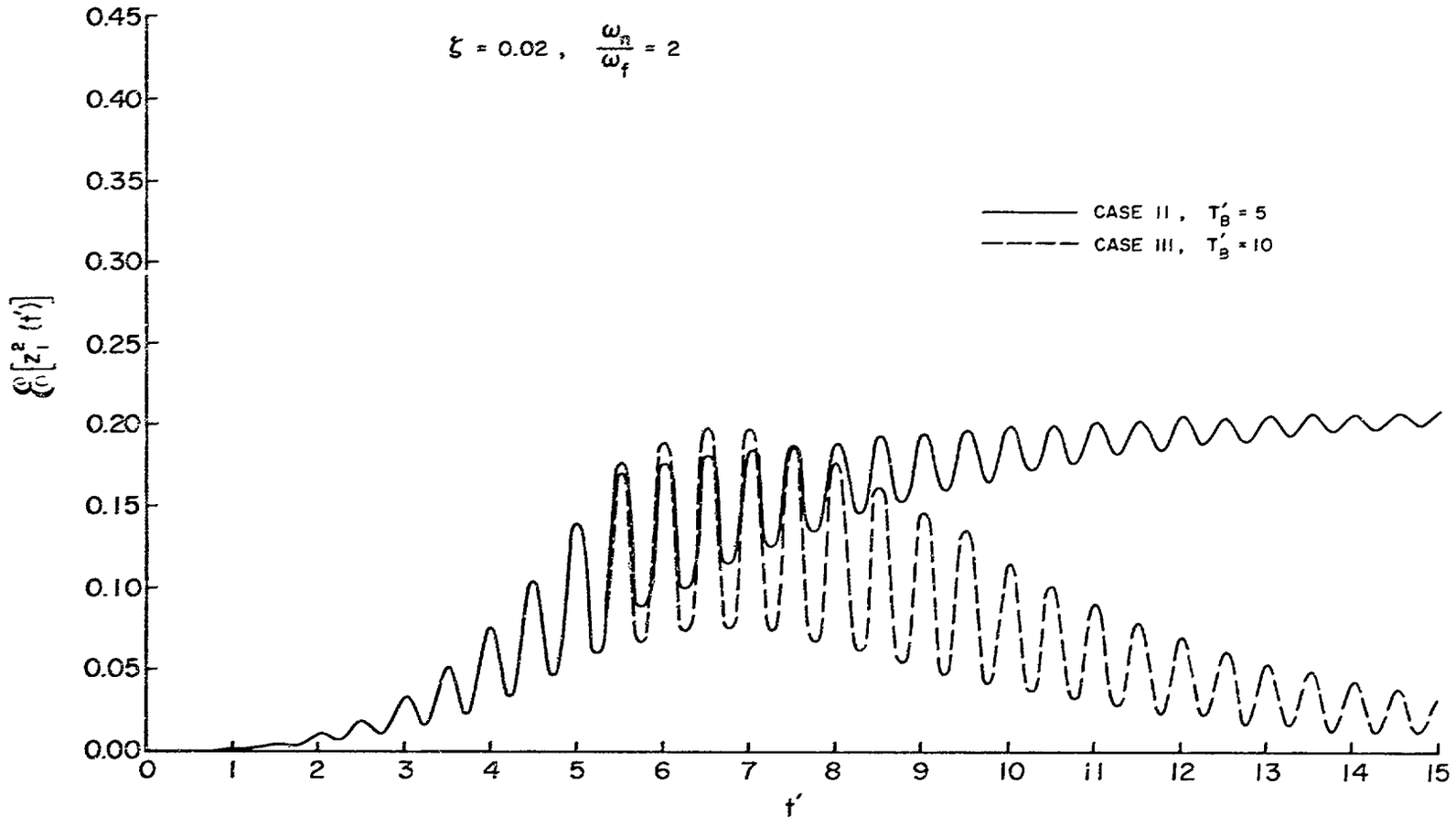

FIG. 57: MEAN SQUARE RESPONSE FOR CASE II AND III: $\zeta = 0.02$, $\omega_n/\omega_f = 2$

NRC, NAE LR-597
National Research Council Canada. National Aeronautical Establishment.

THEORETICAL ANALYSIS OF THE TRANSIENT RESPONSE OF A WING TO NON-STATIONARY BUFFETS LOADS.
Lee, B.H.K. April 1979. 85 pp. (incl. figures).

A method for predicting the response of a wing to non-stationary buffet loads is presented. The wing is treated as a cantilever beam with known mass distribution. Using generalized co-ordinates, the vibration of the wing is governed by the second order mass-spring-damper oscillator equation. The buffet load on the wing is expressed as an integral of the sectional force, which is a function of the spanwise location and time. The non-stationary load is represented by the product of a deterministic time function and a statistically stationary random function. The time history of the applied load is segmented into a number of time intervals. Analytical expressions for the mean square response of the wing displacement are derived using a power spectral density for the random part of the applied load, similar to that used in the theory of isotropic turbulence. The effects of damping, ratio of the undamped natural frequency of the system to the half power frequency of the power spectral density, length of time segment, and duration of applied load on the response of the wing have been investigated for three examples of the load versus time histories.

NRCC No. 17465

UNCLASSIFIED

1. Transient response.
2. Buffeting.

I. Lee, B.H.K.
II. NRC, NAE LR-597

NRC, NAE LR-597
National Research Council Canada. National Aeronautical Establishment.

THEORETICAL ANALYSIS OF THE TRANSIENT RESPONSE OF A WING TO NON-STATIONARY BUFFETS LOADS.
Lee, B.H.K. April 1979. 85 pp. (incl. figures).

A method for predicting the response of a wing to non-stationary buffet loads is presented. The wing is treated as a cantilever beam with known mass distribution. Using generalized co-ordinates, the vibration of the wing is governed by the second order mass-spring-damper oscillator equation. The buffet load on the wing is expressed as an integral of the sectional force, which is a function of the spanwise location and time. The non-stationary load is represented by the product of a deterministic time function and a statistically stationary random function. The time history of the applied load is segmented into a number of time intervals. Analytical expressions for the mean square response of the wing displacement are derived using a power spectral density for the random part of the applied load, similar to that used in the theory of isotropic turbulence. The effects of damping, ratio of the undamped natural frequency of the system to the half power frequency of the power spectral density, length of time segment, and duration of applied load on the response of the wing have been investigated for three examples of the load versus time histories.

NRCC No. 17465

UNCLASSIFIED

1. Transient response.
2. Buffeting.

I. Lee, B.H.K.
II. NRC, NAE LR-597

NRC, NAE LR-597
National Research Council Canada. National Aeronautical Establishment.

THEORETICAL ANALYSIS OF THE TRANSIENT RESPONSE OF A WING TO NON-STATIONARY BUFFETS LOADS.
Lee, B.H.K. April 1979. 85 pp. (incl. figures).

A method for predicting the response of a wing to non-stationary buffet loads is presented. The wing is treated as a cantilever beam with known mass distribution. Using generalized co-ordinates, the vibration of the wing is governed by the second order mass-spring-damper oscillator equation. The buffet load on the wing is expressed as an integral of the sectional force, which is a function of the spanwise location and time. The non-stationary load is represented by the product of a deterministic time function and a statistically stationary random function. The time history of the applied load is segmented into a number of time intervals. Analytical expressions for the mean square response of the wing displacement are derived using a power spectral density for the random part of the applied load, similar to that used in the theory of isotropic turbulence. The effects of damping, ratio of the undamped natural frequency of the system to the half power frequency of the power spectral density, length of time segment, and duration of applied load on the response of the wing have been investigated for three examples of the load versus time histories.

NRCC No. 17465

UNCLASSIFIED

1. Transient response.
2. Buffeting.

I. Lee, B.H.K.
II. NRC, NAE LR-597

NRC, NAE LR-597
National Research Council Canada. National Aeronautical Establishment.

THEORETICAL ANALYSIS OF THE TRANSIENT RESPONSE OF A WING TO NON-STATIONARY BUFFETS LOADS.
Lee, B.H.K. April 1979. 85 pp. (incl. figures).

A method for predicting the response of a wing to non-stationary buffet loads is presented. The wing is treated as a cantilever beam with known mass distribution. Using generalized co-ordinates, the vibration of the wing is governed by the second order mass-spring-damper oscillator equation. The buffet load on the wing is expressed as an integral of the sectional force, which is a function of the spanwise location and time. The non-stationary load is represented by the product of a deterministic time function and a statistically stationary random function. The time history of the applied load is segmented into a number of time intervals. Analytical expressions for the mean square response of the wing displacement are derived using a power spectral density for the random part of the applied load, similar to that used in the theory of isotropic turbulence. The effects of damping, ratio of the undamped natural frequency of the system to the half power frequency of the power spectral density, length of time segment, and duration of applied load on the response of the wing have been investigated for three examples of the load versus time histories.

NRCC No. 17465

UNCLASSIFIED

1. Transient response.
2. Buffeting.

I. Lee, B.H.K.
II. NRC, NAE LR-597